

Contract No. W-7405-eng-26

Health and Safety Research Division

EDISTR — A COMPUTER PROGRAM TO OBTAIN A NUCLEAR
DECAY DATA BASE FOR RADIATION DOSIMETRY

L. T. Dillman*

*Department of Physics, Ohio Wesleyan University, Delaware,
Ohio; Consultant to the Health Studies Section of the
Health and Safety Research Division of Oak Ridge National
Laboratory

Date Published: January 1980

OAK RIDGE NATIONAL LABORATORY
Oak Ridge, Tennessee 37830
operated by
UNION CARBIDE CORPORATION
for the
DEPARTMENT OF ENERGY

DISCLAIMER

This book was prepared as an account of work sponsored by an agency of the United States Government. Neither the United States Government nor any agency thereof, nor any of their employees, makes any warranty, express or implied, or assumes any legal liability or responsibility for the accuracy, completeness, or usefulness of any information, apparatus, product, or process disclosed, or represents that its use would not infringe privately owned rights. Reference herein to any specific commercial product, process, or service by trade name, trademark, manufacturer, or otherwise, does not necessarily constitute or imply its endorsement, recommendation, or favoring by the United States Government or any agency thereof. The views and opinions of authors expressed herein do not necessarily state or reflect those of the United States Government or any agency thereof.

DISTRIBUTION OF THIS DOCUMENT IS UNLIMITED

fay

CONTENTS

	<u>Page</u>
LIST OF FIGURES	v
LIST OF TABLES	vii
ACKNOWLEDGMENTS	ix
ABSTRACT	1
INTRODUCTION	1
1. THEORETICAL AND EMPIRICAL METHODS	4
1.1 Alpha Decay	4
1.2 Beta Decay	5
1.3 Electron-Capture Decay	11
1.4 Internal Conversion of Gamma Rays	14
1.5 X-ray and Auger-Electron Intensities and Energies	21
1.6 Spontaneous Fission	32
1.7 Bremsstrahlung Radiation	33
2. INPUT DATA REQUIREMENTS FOR EDISTR	41
3. DETAILED DESCRIPTION OF SUBROUTINES USED BY EDISTR	51
3.1 Input Phase	51
3.2 Computational Phase	59
3.3 Output Phase	62
REFERENCES	70
Appendix A. FLUORESCENCE AND COSTER-KRONIG YIELDS USED IN THIS WORK	73
Appendix B. K-SERIES RELATIVE X-RAY INTENSITIES USED IN THIS WORK	77
Appendix C. L-SERIES RELATIVE X-RAY INTENSITIES USED IN THIS WORK	80
Appendix D. K-SERIES RELATIVE AUGER-ELECTRON INTENSITIES USED IN THIS WORK	84
Appendix E. KLL AUGER TRANSITION PROBABILITIES USED IN THIS WORK FOR Z < 29	86
Appendix F. L-SERIES RELATIVE AUGER ELECTRON INTENSITIES USED IN THIS WORK	87

	<u>Page</u>
Appendix G. EXAMPLES OF OUTPUT FROM SUBROUTINE BALAN	89
Appendix H. EXAMPLES OF THE OUTPUT FROM SUBROUTINE TABIPU	91
Appendix I. EXAMPLES OF THE OUTPUT DECAY SCHEME DATA	95
Appendix J. EXAMPLES OF BETA SPECTRA GENERATED BY PROGRAM EDISTR .	101
Appendix K. EXAMPLES OF DECAY SCHEME DATA OUTPUT IN COMPUTER RETRIEVABLE FORMAT	105
Appendix L. EXAMPLES OF INPUT DECAY SCHEME DATA FOR EDISTR FORMATTED ACCORDING TO THE ENSDF SYSTEM	108
Appendix M. EXAMPLE OF BREMSSTRAHLUNG DATA GENERATED BY EDISTR .	110

LIST OF FIGURES

	<u>Figure</u>	<u>Page</u>
1	Beta spectrum shape for the β^- decay of ^{14}C	103
2	Beta spectrum shape for the β^+ decay of ^{15}O	104
3	Bremsstrahlung spectrum in a tissue medium for the β^- decay of ^{85}Kr	112

LIST OF TABLES

<u>Table</u>	<u>Page</u>
1 Rules to determine forbiddenness of beta spectra	6
2 Values of total angular momentum quantum numbers for various atomic subshells	12
3 Ratios of electron-capture probabilities for outer orbital electrons	14
4 Calculated $N+M$ capture ratios	15
5 Multipole classification of gamma-ray transitions	18
6 Designation of x-ray transitions used in this work	23
7 Relative intensities of L_3MM Auger transition components	30
8 Expressions for computation of intensities and average energies of spontaneous fission	33
9 Compositions of media used in bremsstrahlung calculations . .	39
10 Input-output (I/O) channels and associated disk files used by EDISTR	50
11 Absolute intensities for L -series x rays for selected radionuclides	69

ACKNOWLEDGMENTS

I am grateful to the Nuclear Data Project of the Oak Ridge National Laboratory for supplying data tapes of the Evaluated Nuclear Structure Data File (ENSDF) decay data sets and internal conversion coefficient data. Over the past several years I have had useful discussions with Murray J. Martin and W. Bruce Ewbank of the Nuclear Data Project concerning the use of ENSDF and related matters. Discussions with Norwood B. Gove, Computer Sciences Division, concerning aspects of the computer code related to beta decay and to bremsstrahlung have been most helpful. The tireless efforts of Sarah B. Watson, Computer Sciences Division, and Mary Rose Ford, Health and Safety Research Division, in helping to implement, maintain, update, modify, and improve the computer code and the data bank generated by it are appreciated greatly. Finally, I acknowledge the guidance of the late Dr. Walter S. Snyder, of the former Health Physics Division. His interest and support motivated much of this research.

EDISTR — A COMPUTER PROGRAM TO OBTAIN A NUCLEAR
DECAY DATA BASE FOR RADIATION DOSIMETRY

L. T. Dillman

ABSTRACT

This report provides documentation for the computer program EDISTR. EDISTR uses basic radioactive decay data from the Evaluated Nuclear Structure Data File developed and maintained by the Nuclear Data Project at the Oak Ridge National Laboratory as input and calculates the mean energies and absolute intensities of all principal radiations associated with the radioactive decay of a nuclide. The program is intended to provide a physical data base for internal dosimetry calculations. The principal calculations performed by EDISTR are the determination of (1) the average energy of beta particles in a beta transition, (2) the beta spectrum as a function of energy, (3) the energies and intensities of x rays and Auger electrons generated by radioactive decay processes, (4) the bremsstrahlung spectra accompanying beta decay and monoenergetic Auger and internal conversion electrons, and (5) the radiations accompanying spontaneous fission. This report discusses the theoretical and empirical methods used in EDISTR and also practical aspects of the computer implementation of the theory. Detailed instructions for preparing input data for the computer program are included, along with examples and discussion of the output data generated by EDISTR.

INTRODUCTION

The Biomedical Effects and Instrumentation Section of the Health and Safety Research Division of the Oak Ridge National Laboratory (ORNL) has collected and analyzed radioactive decay scheme data for a number of years. Although several other sources of radioactive decay scheme data are available — for example, *Nuclear Data Sheets*¹ and *Table of Isotopes*² — we have chosen to maintain an independent capability for several reasons. Both *Nuclear Data Sheets* and *Table of Isotopes* are weighted heavily toward the needs of the basic research scientist in the field of nuclear

structures studies and often lack information needed by users in applied fields. As an example, for medical and health physics dosimetry calculations, the mean energies and absolute intensities of all the radiations emitted in the radioactive decay process must be known. Radioactive decay of a nucleus is nearly always accompanied by subsequent atomic transitions, including x-ray and Auger-electron emission, which may be important in dosimetry calculations. Information on these atomic processes is not available in *Nuclear Data Sheets* or *Table of Isotopes*. For dosimetry calculations one must also know the average energy of the β^+ or β^- particles and the energies and intensities of radiations concomitant with spontaneous fission; again, this information is not available from *Nuclear Data Sheets* or *Table of Isotopes*. Furthermore, in a few instances, bremsstrahlung radiation may contribute appreciably to radiation dose. Bremsstrahlung yield and spectral shape information are also not available in the standard nuclear data tables.

The Nuclear Data Project group at ORNL and others have attempted to remedy some of the above-mentioned problems by means of special publications³⁻⁵ for applied workers in dosimetry. These publications give average energies of beta particles and intensities and energies of x rays and Auger electrons, in addition to the standard nuclear parameters. They do not, however, provide data on spontaneous fission radiations or bremsstrahlung radiation and supply data for only a limited number of radionuclides. Furthermore, for beta depth-dose calculations it is useful to know the spectral shapes of the continuous beta distributions. Again, this information is not provided in these or other publications.

We have developed a computer program, EDISTR, that takes basic radioactive decay information as input and calculates intensities and mean energies of alpha, beta, gamma, internal-conversion-electron, x-ray, Auger-electron, and bremsstrahlung radiations emitted as a result of nuclear decay. In the few cases in which spontaneous fission occurs, the yields of radiations concomitant with spontaneous fission are computed. Furthermore, beta spectral shapes may also be calculated. This computer program has undergone many improvements and refinements

over the past several years. Some of these recent changes have not been described previously in the open literature, and much of the program has lacked careful documentation. Provided here is a detailed documentation of the entire computer program EDISTR.

This report is divided into three sections. In the first one, we discuss the theory and methods associated with each of the basic types of calculations performed by the program. In Sect. 2, we discuss the input data required. Then, in Sect. 3, we describe in detail the various subroutines that implement the theory and empirical methods, examine sample output data, and discuss comparisons of our results with experimental information.

1. THEORETICAL AND EMPIRICAL METHODS

1.1 Alpha Decay

In the case of alpha decay, the computations made by the computer are trivial. Input data consist of the ground-state Q value (total energy available for a ground-state to ground-state transition), the various excitation energies of the levels in the daughter nuclide at which the alpha transitions end, and the corresponding alpha intensities. From these data the kinetic energies of the alpha particles and the associated recoil nuclei are computed using conservation of energy and momentum principles. The resulting equations are

$$E_\alpha = E/(1 + 4.0026/A) , \quad (1)$$

$$E_r = 4.0026E_\alpha/A , \quad (2)$$

and

$$E = Q + E_p - E_L , \quad (3)$$

where E , E_α , and E_r are transition, alpha, and recoil-nucleus energies, respectively, Q is the ground-state energy available, E_p is the excitation energy of the parent ($E_p = 0.0$ except for isomeric-level parents), E_L is the energy of the level in the daughter at which the transition ends, 4.0026 is the atomic mass of an alpha particle, and A is the mass number of the daughter nuclide. If the alpha particle is not known to be associated with a specific level in the daughter nuclide, the alpha-particle kinetic energy may be input directly. In such a case, the recoil-nucleus energy is computed using conservation of energy and momentum.

1.2 Beta Decay

Beta decay is a three-body process and therefore gives rise to a continuous spectrum of beta kinetic energies even when a transition to a single-daughter level is involved. Because of this, beta decay requires many more computations than does alpha decay. For dosimetry work, calculation of the average energy of the beta particles in the emitted continuous spectrum is desirable. This requires the use of the Fermi theory of beta decay and the input of additional data to determine the forbiddenness of the beta spectrum, as we shall describe.

First, equations similar to Eq. (3) are used to determine the end-point kinetic energy of the beta particles, namely,

$$E_0(\beta^-) = Q + E_p - E_L , \quad (4)$$

$$E_0(\beta^+) = Q + E_p - E_L - 2m_0c^2 . \quad (5)$$

In Eq. (4), $E_0(\beta^-)$ is the end-point kinetic energy for β^- particles. Similarly, in Eq. (5), $E_0(\beta^+)$ is the end-point kinetic energy for β^+ particles, and m_0c^2 is the rest-mass energy equivalent of an electron. The other symbols are defined in Eq. (3). As in the case of alpha decay, the end-point kinetic energy of the beta transition may be entered directly for those cases in which the transition is not known to be associated with a particular level of the daughter nuclide.

Beta spectra are classified into various degrees of forbiddenness depending on the spin and parity changes that occur between the parent and daughter nuclear levels. The forbiddenness classifications are illustrated in Table 1. As suggested by the terminology of Table 1, the spectral shapes (i.e., the probability of emission as a function of beta energy) of first, second, and third forbidden nonunique transitions are not unique. However, empirical evidence indicates that most first and second forbidden nonunique transitions are similar in shape to allowed and first forbidden unique transitions respectively. In our work we have assumed that first, second, and third forbidden nonunique transitions

Table 1. Rules to determine the
forbiddenness of beta spectra

Classification of beta spectrum	Nuclear spin change	Parity change
Allowed	0, ± 1 (but not $0 \rightarrow 0$)	No
First forbidden nonunique	0, ± 1	Yes
First forbidden unique	± 2	Yes
Second forbidden nonunique	± 2	No
Second forbidden unique	± 3	No
Third forbidden nonunique	± 3	Yes
Third forbidden unique	± 4	Yes

have allowed, first forbidden unique, and second forbidden unique spectral shapes respectively. Input data on the spin and parity of the parent and daughter nuclear levels are used to determine the forbiddenness of the beta transition. If spin or parity information is lacking for parent or daughter nuclear level, then the $\log(ft)$ input data are examined in an attempt to determine the most probable forbiddenness of the transition.

The following rules, derived from studies of the systematics of $\log(ft)$ values, are applied:

Range of value	Forbiddenness assumed
$\log(ft) < 9$	Allowed
$9 < \log(ft) \leq 13$	First forbidden unique
$\log(ft) > 13$	Second forbidden unique

It has recently been pointed out to the author that there are numerous allowed transitions with $\log(ft) > 9$. The above rules apply only if a majority of all known transitions with $9 < \log(ft) \leq 13$ are of the unique first forbiddenness classification and a majority of all known transitions with $\log(ft) > 13$ are of the unique second forbidden classification. The $\log(ft)$ ranges for the three types of transitions are currently under study, and the outcome of these studies may result in the decision to modify the computer program, assuming an allowed transition for all cases in which the forbiddenness is not uniquely determined from known spin and parity information. If a $\log(ft)$ value is not available and spin or parity change information is lacking, then a transition is assumed to be allowed because a preponderance of known transitions are classified as allowed.

The average kinetic energy, \bar{E} , of the beta particles is determined from

$$\bar{E} = \frac{\int_0^{E_0} P(E) E dE}{\int_0^{E_0} P(E) dE} = \frac{\int_1^W P(W) W dW}{\int_1^W P(W) dW}, \quad (6)$$

where $P(E) dE$ is proportional to the probability that the beta particle will be emitted with kinetic energy between E and $E + dE$. In Eq. (6), W and W_0 are the total beta energy (rest-mass energy equivalent + kinetic energy) in units of $m_0 c^2$ and the total end-point energy in units of $m_0 c^2$ respectively. These are introduced because they are convenient parameters to use in discussing beta-decay theory. According to the theory of beta decay as summarized by Gove and Martin,⁶ $P(W)$ is given by

$$P(W) = pW(W_0 - W)^2 S_n(Z, W), \quad (7)$$

where $p = (W^2 - 1)^{1/2}$ = the momentum of the beta particle, $S_n(Z, W)$ is a shape factor for the n th forbidden beta decay, and Z is the atomic number of the daughter nucleus. The energy dependence of the shape factor is unique for allowed ($n = 0$) and unique forbidden beta spectra and may be written as

$$S_n(Z, W) \propto \sum_{k=1}^{m+1} \frac{\lambda_k(Z, W)p^{2(k-1)}(W_0 - W)^{2(n-k+1)}}{(2k-1)![2(n-k+1)+1]!}, \quad (8)$$

where,

$$\lambda_k(Z, W) = \frac{(g_{-k}^2 + f_k^2)}{2p^2} \left[\frac{(2k-1)!!}{(pR)^{k-1}} \right]^2, \quad (9)$$

$$\begin{Bmatrix} f_k \\ g_k \end{Bmatrix} = (1 \mp W)^{1/2} Q_k \left[S_k {}_1F_1(a; b; z) \mp \text{c.c.} \right], \quad (10)$$

$$Q_k = \frac{(2pR)^{\gamma_k} \exp(\pi y/2) |\Gamma(\gamma_k + iy)|}{2RW^{1/2} \Gamma(2\gamma_k + 1)}, \quad (11)$$

$$S_k = \exp(-ipR + i\eta)(\gamma_k + iy), \quad (12)$$

$$a = \gamma_k + 1 + iy, \quad (13)$$

$$b = 2\gamma_k + 1, \quad (14)$$

$$z = 2ipR, \quad (15)$$

$$\gamma_k = (k^2 - \alpha^2 Z^2)^{1/2}, \quad (16)$$

$$\exp(2i\eta) = (-k + iy/W)/(\gamma_k + iy), \quad (17)$$

$$y = \pm dZW/p \quad \begin{aligned} &> 0 \text{ for negatron emission} \\ &< 0 \text{ for positron emission} \end{aligned}, \quad (18)$$

$$R = 0.002908A^{1/3} - 0.002437A^{-1/3}, \quad (19)$$

= nuclear radius in h/mc units

α = fine structure constant = $1/137.036$,

Γ = gamma function,

A = mass number of nuclide,

${}_1F_1$ = confluent hypergeometric function,

c.c. = complex conjugate.

For β^+ decay, $P(W) \rightarrow 0$ as $p \rightarrow 0$ (or $W \rightarrow 1$); however, for β^- decay, $P(W)$ remains finite as $p \rightarrow 0$. In this case an asymptotic expression for $P_n(W)$ is

$$P_n(W) = 2\pi W \sum_{k=1}^{n+1} \left\{ \frac{[(2k-1)!!]^2 (2\alpha ZR)^{2\gamma_k-1} (W_0 - W)^{2(n-k+2)}}{(2k-1)![2(n-k+1)+1]! R^{2k-1} |\Gamma(2\gamma_k + 1)|^2} \times (\gamma_k + k) \left(k - \frac{(2k+1)(2\alpha ZR)}{2\gamma_k + 1} \right) \right\}. \quad (20)$$

In this expression for $P_n(W)$, the subscript n stands for an n th forbidden transition; $n = 0$ for an allowed transition.

The above theory was corrected for screening of the nuclear Coulomb field by the electron cloud. An appropriate method of taking screening into account is to introduce the new parameters $W' = W \mp V_o$ and $p' = (W'^2 - 1)^{1/2}$ into Eqs. (7) through (20) in place of W and p , respectively, except that $W_0 - W$ is not replaced by $W_0 - W'$.⁶ In the first of these replacement equations, the minus sign applies to β^- decay, the plus sign applies to β^+ decay, and V_o is a screening potential in units of $m_0 c^2$. The screening potential used in this work for β^- decay is given by

$$V_o(\beta^-) = -9.45 \times 10^{-9} Z^3 + 3.014 \times 10^{-6} Z^2 + 1.881 \times 10^{-4} Z - 5.116 \times 10^{-4}. \quad (21)$$

For β^+ decay, the screening correction used is

$$V_o(\beta^+) = V_o(\beta^-)(\alpha_1/p + \alpha_2/p^2), \quad (22)$$

where

$$\alpha_1 = 1.11 \times 10^{-7} Z^3 - 1.01 \times 10^{-5} Z^2 - 2.38 \times 10^{-3} Z + 0.102,$$

$$\alpha_2 = -2.42 \times 10^{-8} Z^3 + 3.83 \times 10^{-6} Z^2 + 3.60 \times 10^{-5} Z - 0.0156 .$$

In the case of β^- decay and in the region $W < 1 + V_0$ where p' is imaginary, Eq. (20) is used, although strictly speaking, the substitution $W' = W - V_0$ is only valid if $W > 1 + V_0$. The justification for this is that Eq. (20) shows $P(W)$ to be independent of p at low energies.

The above theory was also corrected for finite nuclear size. This correction is negligibly small for $Z \leq 50$ in β^- decay or for $Z \leq 80$ in β^+ decay. For high Z , finite-nuclear-size effects can be accounted for by a correction factor,⁶ which multiplies the expression in Eq. (9) for $\lambda_1(Z, W)$. The correction factors used in this work are

$$\Delta\lambda_1(Z, W)(\beta^-) = (Z - 50)[-25 \times 10^{-4} - 4 \times 10^{-6} W(Z - 50)]$$

and

$$\Delta\lambda_1(Z, W)(\beta^+) = (Z - 80)[-17 \times 10^{-5} W + 6.3 \times 10^{-4}/W - 8.8 \times 10^{-3}/W^2] .$$

It is often necessary in beta dosimetry calculations to know the spectral shape of the emitted beta particles in addition to the average energy of the beta particles. Hence, we have an option in our computer program to obtain data on the value of $P(E)$ as a function of the beta kinetic energy E . The spectral shape may be obtained for each individual beta transition or for the composite of all beta transitions associated with the decay. In either case, $P(E)$ in units of betas per million electron volts per disintegration of the parent is printed on an approximately logarithmic energy scale. These data are convenient to use directly in beta depth-dose calculations.

Last, in the case of β^+ decay, our computer program computes an intensity of annihilation quanta that is twice the intensity of all the β^+ branches combined, assigning an energy of 0.511 MeV to all annihilation quanta. This procedure ignores the small probability of annihilation in flight.

1.3 Electron-Capture Decay

Electron capture results in vacancies in the atomic subshells of the daughter nuclide. Vacancies are most likely to be created in the K shell; if energetically possible, vacancies may also be created in the higher shells. The distribution of primary vacancies created in the various atomic shells and subshells as a result of the electron-capture process must be calculated because this distribution affects the relative intensities of the x rays and Auger electrons that result from the initial vacancies. Given a specific electron-capture transition, the basic computations required are the $K/L/M$ capture ratios. The theoretical aspects of electron-capture ratios were first reviewed by Brysk and Rose,⁷ but for our work we have used the theoretical results presented in a more recent and comprehensive review by Behrens and Janecke.⁸ Using a modified version of their notation, we note that the probability of electron capture in subshell X for an n th unique forbidden transition of transition energy E is proportional to λ_X where λ_X is compactly given by

$$\lambda_X = \sum_{k=1}^{n+1} C(k, n) (E - E_X)^{2(n-k+2)} \beta_X^2 N_X B_X \times \left([1 - (1 - E_X/m_0 c^2)^2] (m_0 c^2)^2 \right)^{k-1} \delta[2(j_X - k) + 1] , \quad (23)$$

for $E > E_X$ and by $\lambda_X = 0$ for $E \leq E_X$, where

$$C(k, n) = \frac{n! (2k - 1)!! (k - 1)! [2(n - k) + 3]!! (n - k + 1)!}{(2n + 1)!!} ,$$

E_X = binding energy of an electron in subshell X ,

β_X = Coulomb amplitude for the bound-electron wave function for subshell X ,

N_X = the occupation factor for subshell X ($N_X = 1$, filled shell; $N_X = 0$, empty subshell),

B_X = an electron-exchange and imperfect-atomic-overlap correction factor for subshell X ,

m_0c^2 = rest-mass energy equivalent of an electron,

$$\delta[2(j_X - k) + 1] = \text{Kronecker delta of argument } 2(j_X - k) + 1$$

in which j_X is the total angular momentum quantum number associated with subshell X .

Values of j_X for the various subshells are given in Table 2.

Table 2. Values of total angular momentum quantum numbers for various atomic subshells

Subshell	Total angular momentum quantum number
K, L_1, L_2, M_1, M_2	1/2
L_3, M_3, M_4	3/2
M_5	5/2

We used the binding energy values, E_X , given by Bearden and Burr.⁹ The values of β_X were taken from the numerical tables given by Behrens and Janecke.⁸ We determined occupation factors for partially filled shells from the ground-state electronic structure of atoms given by Richtmyer, Kennard, and Cooper.¹⁰ The occupation factor is linearly proportional to the fraction of electrons occupying the subshell and equals 0 for an empty subshell and 1 for a completely filled subshell. The exchange and overlap correction-factor values, B_X , are from the numerical calculations of Gove and Martin as reported by Martin and Blichert-Toft.³ Martin and Blichert-Toft give values of B_X for the K, L_1, L_2, L_3 , and M_1 subshells. $B_{L_3} = B_{L_2}$ within the accuracy of their calculations. One expects the ratio B_{M_2}/B_{L_2} to be similar to the ratios B_{L_1}/B_K and B_{M_1}/B_{L_1} . Hence, we have estimated values of B_{M_2} through B_{M_5} using the equation

$$B_{M_2} = B_{M_3} = B_{M_4} = B_{M_5} = 0.5B_{L_2}(B_{L_1}/B_K + B_{M_1}/B_{L_1}) . \quad (24)$$

The values of B_{M_2} through B_{M_5} estimated in this way are close to 1, ranging from 1.083 at $Z = 19$ to 1.008 at $Z = 100$.

The necessary numerical data to implement Eq. (23) directly are not available for shells higher than the M subshells. For estimating the additional contribution from capture in N and higher shells (designated $N+$), we used the results of Robinson¹¹ given in Table 3. For allowed transitions ($n = 0$), Eq. (23) implies

$$\frac{\lambda_{N+}}{\lambda_M} = \frac{R_0\lambda_{M_1} + R_1\lambda_{M_2}}{\lambda_{M_1} + \lambda_{M_2}} \approx \frac{R_0\beta_{M_1}^2 + R_1\beta_{M_2}^2}{\beta_{M_1}^2 + \beta_{M_2}^2} , \quad (25)$$

where R_0 and R_1 are the electron-capture ratios given by Robinson. We have used the fact that $E - E_X \approx E$ for all M subshells, except in the rare case of an extremely low-energy electron-capture transition. Hence, for all practical purposes, as indicated by Eq. (25), λ_{N+}/λ_M is independent of transition energy. Using the Coulomb amplitude factors, β , computed by Behrens and Janecke⁸ and the electron-capture ratios given by Robinson, we used Eq. (25) to obtain $N+/M$ capture ratios. To obtain $N+/M$ capture ratios for atomic numbers other than those given by Robinson, linear interpolations were used for $40 < Z < 80$. For $18 < Z < 40$, we weight the value at $Z = 40$ according to the number of electrons in the N shell. For $Z > 80$, we made a crude extrapolation based on a graph of our calculated results using Eq. (25). Table 4 gives the final results obtained by these procedures.

To determine corresponding values of $N+/M$ capture ratios for unique forbidden transitions, we note that the term $[1 - (1 - E_X/m_0c^2)^2]$ of Eq. (23) is equal to $2E_X/m_0c^2 - (E_X/m_0c^2)^2 \approx 2E_X/m_0c^2$ because $E_X \ll m_0c^2$ for the M or higher shells. The net result of this is that $N+/M$ capture ratios for unique forbidden transitions reduce approximately to Eq. (25) for allowed transitions. Hence, the $N+/M$ capture ratio is nearly independent of both energy and forbiddenness and is a function only of atomic number.

Calculation of f_X , the fraction per decay of primary vacancies created in subshell X , is made using

Table 3. Ratios of electron-capture probabilities for outer orbital electrons^a

Atomic number	Electron-capture ratios (states designated by standard spectroscopic notation)		
	$R_0 = \frac{4s + 5s + \dots}{3s}$	$R_1 = \frac{4p + 5p + \dots}{3p}$	$R_2 = \frac{4d + 5d + \dots}{3d}$
40	0.16	0.14	
42	0.17	0.15	
55	0.25	0.23	0.19
59	0.27	0.24	0.21
69	0.27	0.25	0.23
80	0.30	0.29	0.28

^aData from B. L. Robinson, *Nucl. Phys.* 64: 197-208 (1965).

$$f_X = I\lambda_X / \sum \lambda_X , \quad (26)$$

where $\sum \lambda_X$ is the sum of λ_X over all subshells in the K , L , M , and N^+ shells, and I is the intensity of the electron-capture transition in fraction per decay of the parent. In our work, the individual λ_X values for the M subshells are not used directly; rather, a sum over the five subshells is calculated and used, that is, $\lambda_M = \lambda_{M_1} + \lambda_{M_2} + \lambda_{M_3} + \lambda_{M_4} + \lambda_{M_5}$. As discussed in Sect. 1.5, the current state of theory and the experimental results concerning the production of x rays and Auger electrons from a vacancy in the M shell indicate that separating data for the M subshells is not warranted. Using the fact that λ_{N^+} is equal to λ_M multiplied by the N^+/M ratio given in Table 4, λ_{N^+} is calculated.

The procedure by which the f_X values calculated from Eq. (25) are used to determine intensities of x rays and Auger electrons will be discussed in detail in Sect. 1.5.

1.4 Internal Conversion of Gamma Rays

Internal conversion is a process by which the energy of a transition between two states of a nucleus is transferred to an orbital electron. The orbital electron is ejected from the atom with an energy equal to the transition energy minus the binding energy of the shell from which the

Table 4. Calculated N^+/M capture ratios^a

Z	N^+/M	Z	N^+/M	Z	N^+/M
0-18	0.0	49	0.213	82	0.305
19	0.016	50	0.219	83	0.307
20-23	0.032	51	0.225	84	0.308
24	0.016	52	0.232	85	0.309
25-28	0.032	53	0.238	86	0.311
29	0.016	54	0.244	87	0.313
30	0.032	55	0.250	88	0.314
31	0.048	56	0.255	89	0.315
32	0.064	57	0.260	90	0.316
33	0.080	58	0.264	91	0.317
34	0.096	59-69	0.269	92	0.318
35	0.112	70	0.272	93	0.319
36-38	0.128	71	0.274	94	0.321
39	0.144	72	0.277	95	0.322
40	0.160	73	0.280	96	0.323
41	0.165	74	0.283	97	0.324
42	0.170	75	0.285	98	0.325
43	0.176	76	0.288	99	0.326
44	0.182	77	0.291	100	0.327
45	0.188	78	0.294	101	0.328
46	0.195	79	0.296	102	0.329
47	0.201	80	0.299	103	0.330
48	0.207	81	0.302	104	0.331

^aThese results are approximately correct regardless of the forbiddenness of the transition.

electron is ejected. This process competes with gamma-ray emission. Internal conversion in the *K* shell is usually the most probable, if energetically possible, although it also occurs in varying degrees in higher shells. The problem is essentially the same as that in the case of electron capture; namely, internal conversion leads to primary vacancies in the various atomic shells, and one must calculate the distribution of these vacancies before calculation of x-ray and Auger-electron intensities can be done.

The internal conversion process is conveniently discussed in terms of internal conversion coefficients, α_X . For a given nuclear transition, α_X is defined as the ratio of the number of internal conversion electrons ejected per unit time from atomic subshell *X* to the number of gamma rays ejected per unit time. If the internal conversion coefficients are known, f_X , the fraction per decay of primary vacancies created in subshell *X*, can be calculated readily using the equation

$$f_X = I\alpha_X / (1 + \sum \alpha_X) , \quad (27)$$

where $\sum \alpha_X$ is the sum of α_X over all subshells in the *K*, *L*, *M*, and *N* shells, and *I* is the total transition intensity (gamma rays plus internal conversion electrons) in fraction per decay of the parent. The fraction per decay of emitted gamma rays, f_g , is correspondingly given by

$$f_g = I / (1 + \sum \alpha_X) . \quad (28)$$

Experimental measurements of α_X are difficult to make with precision, particularly for the higher subshells. Even for the *K* shell, experimental measurements may be subject to large errors if α_X is quite small or quite large. Fortunately, however, theoretical computations of α_X have been made and tabulated.¹² In cases in which precise experimental measurements were made, the agreement between theory and experiment usually was excellent. In our computer program we use theoretical conversion coefficients almost exclusively. The only exception is when

the experimental total conversion coefficient, $\alpha = \sum \alpha_X$, is known and the theoretical value of α differs from the experimental value by more than 10%. In this case, the theoretical values of α_X are scaled to give the experimental value of α while maintaining the theoretical conversion coefficient ratios. This procedure is useful for transitions that appear to be of mixed multipolarity but for which a mixing ratio is not known.

The use of theoretical internal conversion coefficients requires an extensive table because α_X varies rapidly with gamma-ray multipolarity and gamma-ray energy, as well as with the atomic number of the nuclide in which the transition occurs. The gamma-ray multipolarity is determined by the nuclear spin quantum number and parity changes that occur during the transition. Both magnetic (*M*) and electric (*E*) multipoles are possible; for the time being we confine ourselves to radiative multipoles. The special case of the nonradiative electric monopole (*E0*) multipole will be discussed later in this section. The various classifications of radiative multipoles are presented in Table 5.

An examination of Table 5 indicates that mixed multipole radiation is possible. If, for example, the nuclear spins and parities of the initial and final levels are 3+ and 1+, respectively, then *E2*, *M3*, and *E4* multipole radiations are all possible. Experimentally, it is observed that the lowest multipole order possible usually predominates. Hence, in the example, we expect the radiation to be of type *E2*. We assumed in our computer program, except for two cases to be discussed, that the lowest-order multipole possible predominates, and we used theoretical conversion coefficients associated with the lowest-order multipole.

Experimentally, there are two major exceptions to the rule that the lowest-order multipole possible predominates. When *M1* and *E2* or *E1* and *M2* multipoles are both possible, mixing of the two multipoles often occurs. In such a case, a mixing ratio parameter, δ , is measured. The quantity δ^2 gives the ratio of intensity of the higher to lower multipole radiations in the multipole mixture. This data is used to determine α_X values for the multipole mixture according to the equations

$$\alpha_X(M1 + E2) = \alpha_X(M1) + \delta^2 \alpha_X(E2) / (1 + \delta^2) , \quad (29)$$

Table 5. Multipole classification of gamma-ray transitions^a

Multipole ^b	Absolute value of nuclear spin quantum number change	Parity change
E1	≤ 1	Yes
E2	≤ 2	No
E3	≤ 3	Yes
E4	≤ 4	No
M1	≤ 1	No
M2	≤ 2	Yes
M3	≤ 3	No
M4	≤ 4	Yes

^aThe table gives conditions that are necessary but not sufficient for radiative transitions. The relation $|J' - J''| \leq l \leq J' + J''$ for the l th multipole, where J' and J'' are the nuclear spin quantum numbers of the initial and final states, respectively, must be obeyed. Thus, for example, transitions from $J' = 0$ to $J'' = 0$ are strictly forbidden. Such transitions occur entirely by emission of conversion electrons or by formation of electron-positron pairs.

^bIn this column, E = electric multipole and M = magnetic multipole. The number following the E or M is the value of l , the multipole order.

and

$$\alpha_X(E1 + M2) = \alpha_X(E1) + \delta^2 \alpha_X(M2)/(1 + \delta^2) . \quad (30)$$

In many cases, δ^2 is determined by least-squares fitting of experimental α_X values to Eq. (29) or Eq. (30). The parameter δ may also be determined in some cases through angular correlation measurements.

If both $M1$ and $E2$ or $E1$ and $M2$ multipoles are possible and δ is not available, our computer program assumes that the lower-order multipole predominates. If spin change information is available but parity change information is lacking, our program makes an arbitrary multipole assignment assuming no parity change. If parity is known to change but spin change information is lacking, an $E1$ multipole is assumed; if parity does not change and spin change information is lacking, an $M1$ multipole is assumed. If no information concerning spin or parity changes is available, an $M1$ multipole is assumed if $Z \leq 50$; if $Z > 50$, an $E2$ multipole is assumed. These rules can, of course, lead to significant errors in some cases, but they are not completely arbitrary.

From a purely statistical point of view, most gamma transitions are of low multipolarity and more transitions are of $E1$, $M1$, or $E2$ types than of any other multipole type. Of the $E1$, $M1$, and $E2$ multipoles, $M1$ usually has the intermediate K -shell conversion coefficient for $Z < 50$ and hence is a representative compromise. For $Z > 50$, the $E2$ multipole usually has the intermediate K -shell conversion coefficient. In many cases in which information is insufficient to uniquely assign a multipole type to the transition, the internal conversion coefficients are expected, on the basis of energy considerations, to be quite small. We feel that the above rules represent the best compromise possible for instances in which needed information is lacking.

The theoretical internal conversion coefficient data bank we use is a combination of the data computed by Hager and Seltzer,¹² Dragoun, Plajner, and Schmutzler,¹³ and Band, Trzhaskovskaya, and Listengarten.¹⁴ For K , L , and M shells, Hager and Seltzer tabulate data for each atomic number in the range $30 \leq Z \leq 103$. Dragoun, Plajner, and Schmutzler

provide additional data for the N^+ shells for each atomic number in the range $37 < Z < 100$, whereas Band, Trzhaskovskaya, and Listengarten give K- and L-shell conversion coefficient data for atomic numbers 3, 6, and 10 and for each atomic number in the range $14 \leq Z \leq 29$. For atomic numbers 3 and 6, the L-shell data of Band, Trzhaskovskaya, and Listengarten are limited to the L_1 subshell. We used a spline-curve-fitting program to obtain corresponding data for atomic numbers 4, 5, 7, 8, 9, 11, 12, and 13. These data were integrated into our overall data bank so that interpolations on atomic number are never required when running the computer program.

We have not yet considered the possibility of an $E0$ transition. In an $E0$ transition, there is no spin or parity change in the transition, and the emission of single quantum electromagnetic radiation is strictly forbidden. The transition occurs entirely by means of emission of internal conversion electrons and, if energetically possible, by emission of electron-positron pairs. Emission of two photons is also possible but usually negligible. Although $E0$ transitions can occur when the initial and final spin quantum number is greater than 0, such transitions are rarely observed because competing radiative multipoles usually predominate. Most $E0$ transitions that have been experimentally observed are of the $0 + 0$ type; that is, both the initial and final spin quantum numbers are 0. Church and Weneser¹⁵ have noted that the K/L ratio for $E0$ multipoles is almost identical to that for $M1$ multipoles. We use the $K/L/M/N^+$ conversion ratios of an $M1$ transition whenever an $E0$ multipole occurs. Thus, using the $M1$ conversion coefficients, the equation corresponding to Eq. (27) is

$$f_X = I\alpha_X(M1)/\sum \alpha_X(M1) \quad (\text{for } E0 \text{ multipole}) . \quad (31)$$

We close this section by noting that if the transition energy exceeds $2m_0c^2$ (i.e., $E > 1.022$ MeV), an excited nucleus may emit a positron-electron pair as an alternative to gamma-ray emission. The theory of this process, which is an electromagnetic process in that it takes place in the Coulomb field of the excited nucleus, shows that the

probability of pair internal conversion increases with transition energy, is greatest for small multipolarities, and is almost independent of atomic number. However, even at a transition energy of 10 MeV and for an $E1$ multipole, the number of pairs created per gamma ray emitted is only about 0.003. In this work we have neglected internal-pair emission and other extremely low-intensity phenomena such as emission of two photons or of one photon and one conversion electron.

1.5 X-ray and Auger-Electron Intensities and Energies

In this section we show how the numbers of primary vacancies in the various subshells, f_X , as given by Eq. (26) for electron capture or Eqs. (27) and (31) for internal conversion of electrons, are used to obtain intensities of x rays and Auger electrons. We begin by briefly discussing the atomic processes that result when a vacancy occurs in an inner atomic shell.

An atom excited by an atomic vacancy in one of its inner shells decays by x-ray or Auger-electron emission or, in some cases, by Coster-Kronig transitions. In the x-ray emission process, an electron in an outer shell, Y , makes a transition to the vacancy in an inner shell, X , and an x-ray quantum is emitted. The energy of the emitted x ray is equal to E_X , the binding energy of an electron in the shell X , minus E_Y , the binding energy of an electron in shell Y . The original vacancy in shell X is transferred to shell Y .

In an Auger-electron emission process, an electron in an outer shell, Y , makes a transition to the vacancy in the inner shell, X , and an electron in another shell, Y' (Y' may be the same as Y but is not necessarily so), is ejected from the atom. The emitted electron is called an Auger electron. The energy of the emitted Auger electron is approximately equal to $E_X - E_Y - E_{Y'}$. The Auger-electron emission process results in vacancies in both the Y and Y' shells where there was originally a single vacancy in the X shell. If X is the K shell, Y the L_1 subshell, and Y' the L_2 subshell, then the Auger electron is designated as a KL_1L_2 Auger electron. A KLL Auger electron would be one in which shells Y and Y' could each be any one of the three L subshells.

A Coster-Kronig transition is a nonradiative process involving an electron transition between two subshells of the same major shell. For example, if a vacancy is transferred from the L_1 subshell to the L_2 subshell and the small energy difference between the subshells is transferred to one of the outermost electrons, ejecting it from the atom, the transition is said to be a Coster-Kronig transition. The essential difference between Coster-Kronig transitions and Auger emission processes is that in the case of Coster-Kronig transitions, one of the final vacancies is in the same major shell as the initial vacancy; in Auger-electron emission, both the final vacancies are in a major shell different from that of the initial vacancy.

A useful parameter for our discussion is the fluorescence yield. For any shell or subshell X , the fluorescence yield, ω_X , is defined as the number of radiative (x-ray) transitions per vacancy in the shell or subshell. An expression for the intensity of the various K -series x rays can be easily written in terms of the fluorescence yield in the K shell, ω_K . We have

$$I_{KX_i} = f_K \omega_K N_{KX_i}, \quad (32)$$

where I_{KX_i} is the intensity in fraction per decay of K -series x rays of type i , f_K is the number of primary vacancies in the K shell as given by Eqs. (26), (27), and (31), and N_{KX_i} is the relative number of K -series x rays of type i normalized to $\sum_i N_{KX_i} = 1$. In this work we considered the seven most prominent x rays of the K series, as given in Table 6.

The values of ω_K used in this work are given in Appendix A, and the values of N_{KX_i} , normalized to $N_{K\alpha_1} = 1$, are given in Appendix B.

The energies of the K -series x rays are obtained from the binding energy data of Bearden and Burr.⁹ For example, according to Table 6, the K_{α_1} x ray involves an $L_3 \rightarrow K$ electron transition; thus, the K_{α_1} x-ray energy is the binding energy of the K shell, E_K , minus the binding energy of the L_3 subshell, E_{L_3} . The K_{β_2} and K_{β_5} x rays are mixtures of two or more quantum transitions. In each of these cases we obtained a weighted

Table 6. Designation of x-ray transitions used in this work
(For each series the x rays are listed in approximate order of decreasing relative intensity)

Siegbahn notation	Associated electron transition	Siegbahn notation	Associated electron transition
K_{α_1}	$L_3 \rightarrow K$	L_{β_1}	$M_4 \rightarrow L_2$
K_{α_2}	$L_2 \rightarrow K$	L_{γ_1}	$N_4 \rightarrow L_2$
K_{β_1}	$M_3 \rightarrow K$	L_{η}	$M_1 \rightarrow L_2$
K_{β_3}	$M_2 \rightarrow K$	L_{γ_6}	$O_4 \rightarrow L_2$
K_{β_2}	$N+ \rightarrow K$		
K_{β_5}	$M_4 + M_5 \rightarrow K$	L_{α_1}	$M_5 \rightarrow L_3$
K_{α_3}	$L_1 \rightarrow K$	L_{β_2}	$N_4 + N_5 \rightarrow L_3$
		L_{α_2}	$M_4 \rightarrow L_3$
		L_{β_3}	$O_4 + O_5 \rightarrow L_3$
		L_{β_4}	$N_1 \rightarrow L_3$
		L_{γ_3}	L_7
		L_{γ_2}	$M_1 \rightarrow L_3$

average energy using the theoretical x-ray emission rates presented by Scofield.¹⁶ For example, the weighted average energy associated with the K_{β_5} transition, $\bar{E}_{K_{\beta_5}}$, is obtained from

$$\bar{E}_{K_{\beta_5}} = \frac{(E_K - E_{M_4})R_{M_4} + (E_K - E_{M_5})R_{M_5}}{R_{M_4} + R_{M_5}}, \quad (33)$$

where R_{M_4} and R_{M_5} are the theoretical M_4 - and M_5 -subshell emission rates computed by Scofield.¹⁶

For Auger electrons arising from vacancies in the K shell, we have

$$I_{KA_i} = f_K(1 - \omega_K)N_{KA_i}, \quad (34)$$

where I_{KA_i} is the intensity in fraction per decay of K -series Auger electrons of type i and N_{KA_i} is the relative number of K -series Auger electrons of type i , normalized to $\sum_i N_{KA_i} = 1$. In this work the K -series Auger transitions considered are the six components of the KLL transitions, KL_1L_1 , KL_1L_2 , KL_1L_3 , KL_2L_2 , KL_2L_3 , and KL_3L_3 , and the four transitions KL_1X , KL_2X , KL_3X , and KXY . The intensities of the latter four transitions relative to the KLL transitions used in this work are presented in Appendix D. The relative intensities of the six major components of the KLL Auger electrons were obtained from the polynomial fits of Babenkov, Bobykin, and Petukhov.¹⁷ Their polynomials are

$$R_{11} = KL_1L_1(^1S_0)/\Sigma KLL = -0.006 + 0.00210Z, \quad (35)$$

$$R_{12} = KL_1L_2(^1P_1 + ^3P_0)/\Sigma KLL = 0.312 - 0.00751Z + 8.49 \times 10^{-5}Z^2, \quad (36)$$

$$R_{13} = KL_1L_3(^3P_1 + ^3P_2)/\Sigma KLL = -0.125 + 0.00803Z - 5.85 \times 10^{-5}Z^2, \quad (37)$$

$$R_{22} = KL_2L_2(^1S_0)/\Sigma KLL = 0.037 - 0.00011Z, \quad (38)$$

$$R_{23} = KL_2L_3(^1D_2)/\Sigma KLL = 0.625 - 0.00430Z, \quad (39)$$

$$R_{33} = KL_3L_3(^3P_2 + ^3P_0)/\Sigma KLL = -1.078 + 0.07583Z - 1.6707 \times 10^{-3}Z^2 + 1.5940 \times 10^{-5}Z^3 - 5.695 \times 10^{-8}Z^4, \quad (40)$$

where Z is the atomic number. In Eqs. (35) through (40), the quantities in parentheses are standard spectroscopic notation for the quantum states giving rise to the transitions. That is, KL_1L_2 , KL_1L_3 , and KL_3L_3 transitions are each a composite of two quantum transitions, one of which is called a satellite transition. Babenkov, Bobykin, and Petukhov¹⁷ give the following polynomials for the satellite transitions:

$$S_{12} = KL_1L_2(^3P_0)/\Sigma KLL = 0.039 - 0.00108Z + 1.54 \times 10^{-5}Z^2, \quad (41)$$

$$S_{13} = KL_1L_3(^3P_2)/\Sigma KLL = 0.046 - 0.00081Z + 9.1 \times 10^{-6}Z^2, \quad (42)$$

and

$$S_{33} = KL_3L_3(^3P_0)/\Sigma KLL = -0.010 + 0.00146Z - 1.52 \times 10^{-5}Z^2. \quad (43)$$

Babenkov, Bobykin, and Petukhov state that the polynomials given in Eqs. (35) through (43) are valid for $29 \leq Z \leq 94$.¹⁷ This is the range of Z values for which experimental data are available for comparison purposes. Graphs of these polynomials reveal that they vary slowly and smoothly if $Z > 94$, and we have assumed that the same curves hold for $Z > 94$. For $Z < 29$, we used the theoretical Auger transition probabilities calculated in intermediate coupling by Chen and Crasemann¹⁸ to obtain relative intensities of the KLL Auger components. Chen and Crasemann calculated results at $Z = 13, 15, 18, 20, 23$, and 28 ; we obtained data for other atomic numbers by interpolation and extrapolation. The transition probabilities we used for $Z < 29$ are shown in Appendix E. The polynomial equations of Babenkov, Bobykin, and Petukhov are in good

agreement with the experimental and theoretical values reported by Rao, Chen, and Crasemann¹⁹ and by Bambynek et al.²⁰

The energies of the six major KLL Auger components were calculated using the data presented by Sevier.²¹ Sevier reports data on each of the nine energy states associated with the six KLL Auger components (as indicated above, the KL_1L_2 , KL_1L_3 , and KL_3L_3 components are each doublets) for atomic numbers $6 \leq Z \leq 100$. A weighted average energy was computed for each of the doublets. For example, for the KL_1L_2 average energy, $\bar{E}(KL_1L_2)$, we have

$$\bar{E}(KL_1L_2) = \{E[KL_1L_2(^1P_1)](R_{12} - S_{12}) + E[KL_1L_2(^3P_0)]S_{12}\}/R_{12}, \quad (44)$$

where $E[KL_1L_2(^1P_1)]$ and $E[KL_1L_2(^3P_0)]$ are the energy values given by Sevier, and R_{12} and S_{12} are from Eqs. (36) and (41) respectively.

The average energy values of the KL_1X , KL_2X , KL_3X , and KXY Auger transitions were estimated using the empirical equations

$$\bar{E}(KL_iX) = E_K - E_{L_i} - E_{M_3} - 0.75(E_{M_3+} - E_{M_3}) \quad (45)$$

and

$$\bar{E}(KXY) = E_K - 2E_{M_3} - 0.75(E_{M_3+} - E_{M_3}), \quad (46)$$

where E_K , E_{L_i} , and E_{M_3} are binding energies given by Bearden and Burr.⁹ The binding energy of the M_3 subshell for the next higher atomic number is E_{M_3+} . In this work we used the M_3 -subshell binding energy to represent an X or Y shell because the M shell will give rise to the dominant components of the Auger transitions involved.

The calculation of intensities of L -series x rays and Auger electrons is considerably more complex than the corresponding equations for the K series. This is because K -series x rays and Auger electrons lead to an altered distribution of vacancies in the various L subshells. The problem is further complicated by the presence of Coster-Kronig

transitions, which further alter the distribution of vacancies in the L subshells. For the L_1 subshell, one obtains

$$I_{L_1X_i} = \omega_1 f_{L_1} N_{L_1X_i} \quad (47)$$

and

$$I_{L_1A_i} = (1 - \omega_1 - f_{12} - f_{13}) f'_{L_1} N_{L_1A_i}, \quad (48)$$

where

$$f'_{L_1} = f_{L_1} + I_{K_{\alpha_3}} + 2I_{KL_1L_1} + I_{KL_1L_2} + I_{KL_1L_3} + I_{KL_1X}, \quad (49)$$

and where ω_1 is the L_1 -subshell fluorescence yield, f_{12} and f_{13} are L_1-L_2X and L_1-L_3X Coster-Kronig yields, respectively; $I_{L_1X_i}$ and $I_{L_1A_i}$ are intensities in fraction per decay of L_1 -series x rays and Auger electrons of type i ; and $N_{L_1X_i}$ and $N_{L_1A_i}$ are the relative number of L_1 -series x rays and Auger electrons of type i , normalized to $\sum_i N_{L_1X_i} = 1$ and $\sum_i N_{L_1A_i} = 1$ respectively. In Eq. (49), the value of f_{L_1} comes from Eqs. (26) and (27) or Eq. (31), the value of $I_{K_{\alpha_3}}$ comes from Eq. (32), and the values of $I_{KL_1L_1}$, $I_{KL_1L_2}$, $I_{KL_1L_3}$, and I_{KL_1X} come from Eq. (34).

Using analogous notation, one obtains the following equations for the L_2 and L_3 subshells:

$$I_{L_2X_i} = \omega_2 (f_{12} f'_{L_1} + f'_{L_2}) N_{L_2X_i}, \quad (50)$$

$$I_{L_2A_i} = (1 - f_{23} - \omega_2) (f_{12} f'_{L_1} + f'_{L_2}) N_{L_2A_i}, \quad (51)$$

$$I_{L_3X_i} = \omega_3 [(f_{12} f_{23} + f_{13}) f'_{L_1} + f_{23} f'_{L_2} + f'_{L_3}] N_{L_3X_i}, \quad (52)$$

$$I_{L_3A_i} = (1 - \omega_3)[(f_{12}f_{23} + f_{13})f'_{L_1} + f_{23}f'_{L_2} + f'_{L_3}]N_{L_3A_i}, \quad (53)$$

where

$$f'_{L_2} = f_{L_2} + I_{K_{\alpha_2}} + 2I_{KL_2L_2} + I_{KL_2L_3} + I_{KL_1L_2} + I_{KL_2X}, \quad (54)$$

$$f'_{L_3} = f_{L_3} + I_{K_{\alpha_1}} + I_{KL_1L_3} + I_{KL_2L_3} + 2I_{KL_3L_3} + I_{KL_3X}. \quad (55)$$

To implement Eqs. (47) through (55), we used the values of ω_1 , ω_2 , ω_3 , f_{12} , f_{13} , and f_{23} given in Appendix A. The values of the L -series relative x-ray intensities, $N_{L_1X_i}$, $N_{L_2X_i}$, and $N_{L_3X_i}$, used in this work are given in Appendix C, and the designation of the L -series x rays considered are listed in Table 6. Appendix F includes the values of the L -series relative Auger-electron intensities, $N_{L_1A_i}$, $N_{L_2A_i}$, and $N_{L_3A_i}$. The energies of the L -series x rays are obtained in a manner analogous to that discussed for the K -series x rays.

Accurate values for the energies of the L -series Auger electrons are difficult to obtain partly because of the complexity of the structure of L -series Auger transitions and partly because of the fact that experimental information is meager. Haynes,²² who has made a comprehensive study of the systematics of L - and M -series Auger spectra, gives the following expression for the energy of the L_iMX and L_iXY Auger transitions:

$$\bar{E}(L_iMX) = E_{L_i} - E_M - E_{X+} \quad (56)$$

and

$$\bar{E}(L_iXY) = E_{L_i} - E_X - E_{Y+}, \quad (57)$$

where E_{L_i} , E_M , and E_X are binding energies in the L_i , M , and X shells,

respectively, and E_{X+} and E_{Y+} are the binding energies in the X and Y shells, respectively, for an atomic number increased by 1. In our work we have used $E_M = E_{M_5}$, $E_{X+} = E_{N_4+}$, $E_X = E_{N_4}$, and $E_{Y+} = E_{N_5+}$.

The assignment of an energy value to the L_iMM Auger-electron group is not as simple. Haynes notes that the relative intensities of the various components of the L_3MM transitions do not change very much with atomic number, except for low Z in which shells are incompletely filled.²² This same statement is expected to be true for the components of the L_1MM and L_2MM Auger transitions. From graphs developed by Haynes, we have estimated the relative intensities of the more intense L_3MM components (Table 7). For a transition $L_iM_jM_k$, we calculate an energy according to the equation given by Haynes:

$$\bar{E}(L_iM_jM_k) = E_i - E_j - E_k - \Delta E_{jk}, \quad (58)$$

where

$$\Delta E_{jk} = \Delta E_{45} + m(E_4 + E_5 - E_j - E_k),$$

$$\Delta E_{45} = (E_{5+} - E_5)\Delta Z,$$

$$\Delta Z = 0.69 + 0.85(71 - Z)/35 \quad 36 < Z < 71,$$

$$= 0.69 \quad Z \geq 71,$$

$$m = -0.011 + 0.024(71 - Z)/35 \quad 36 < Z < 71,$$

$$= -0.011 \quad Z \geq 71.$$

In Eq. (58) and its associated equations, the subscripts j , k , 4, and 5 refer to M subshells and the subscript 5+ refers to the M_5 subshell for an atomic number increased by 1. Equation (58) has been used for each of the Auger components given in Table 7 and a weighted average energy

Table 7. Relative intensities of L_3MM Auger transition components

Auger component	Relative intensity ^a
$L_3M_4M_5$	1.0
$L_3M_5M_5$	0.7
$L_3M_3M_5$	0.55
$L_3M_3M_4$	0.35
$L_3M_3M_3$	0.25
$L_3M_2M_3$	0.25
$L_3M_2M_5$	0.16
$L_3M_1M_3$	0.15
$L_3M_4M_4$	0.05
$L_3M_2M_4$	0.025

^aThese data are from graphs given by Haynes.²² The relative intensities are fairly independent of Z except for incompletely filled shells.

determined on the basis of the relative intensities. We have used the same procedure for all three L subshells, changing the value of E_i to the value appropriate for the L_i subshell. This procedure overestimates the average energy of the L_1MM and L_2MM Auger transitions; the relative intensities given in Table 7 apply only to the L_3MM transitions. However, although the errors may be quite significant to an Auger spectroscopist, they will be quite small for internal dosimetry purposes because the variation of M -subshell binding energies is small compared with the L -subshell binding energies.

For shells higher than the L shell, in most cases experimental data on fluorescence yields and Coster-Kronig transitions are not available. We have assumed that Auger processes completely dominate x-ray transitions. We estimate an intensity for MXY Auger transitions without breaking it down into the multitude of components that the MXY transitions encompass by adding to the initial M -shell vacancy per decay the additional vacancies created by the K and L x-ray and Auger-electron series. For this purpose we assume that KXY Auger transitions lead to two vacancies in the M shell. We have

$$I_{MXY} = f_M + I_{K\beta_1} + I_{K\beta_3} + I_{K\beta_5} + \sum_i I_{KL_iX} + 2I_{KXY} + I_{L\beta_1}$$

$$+ I_{L\beta_3} + I_{L\beta_4} + I_{L\eta} + I_{L\zeta} + I_{L\alpha_1} + I_{L\alpha_2}$$

$$+ 2\sum_i I_{L_i^{MM}} + \sum_i I_{L_i^{MX}} .$$

(59)

A weighted average energy is associated with the MXY Auger electron according to the equation

$$\bar{E}_{MXY} = \sum_j \bar{E}_j I_j / \sum I_j ,$$

where \bar{E}_j is the average energy associated with the vacancy created in the M shell because of the radiation of intensity I_j . The index j ranges over the radiation components listed in Eq. (59). With the exception of the $K\beta_5$ x ray, all the x-ray transitions in Eq. (59) result in a single vacancy in a particular M subshell; the value of \bar{E}_j in these cases is simply the binding energy of the associated N subshell. For the $K\beta_5$ x ray and for the Auger transitions of Eq. (59) in which the final M -shell vacancy may occur in one of several M subshells, we estimate \bar{E}_j as follows:

Process causing M -subshell vacancy	\bar{E}_j
Primary vacancy from nuclear process	E_{M_3}
$K\beta_5$ x ray	$E_K - \bar{E}_{L\beta_5}$
KL_i Auger electron	$E_K - E_{Li} - \bar{E}_{KL_iX}$
KXY Auger electron	$E_K - \bar{E}_{KXY}$
L_i^{MM} Auger electron	$E_{Li} - \bar{E}_{L_i^{MM}}$
L_i^{MX} Auger electron	E_{M_5}

Equation (60) will slightly overestimate the average energy because it neglects binding in the high-order X and Y shells, and because the effects of multiple ionization of the atom are not completely taken into account.

Finally, we estimate an intensity for residual low-energy radiations from vacancies created in the N and higher shells in a manner analogous to that used in Eq. (59) for the MXY Auger transitions. We have

$$\begin{aligned} I(\text{residual}) = & f_{N+} + I_{L_{\gamma_1}} + I_{L_{\gamma_2}} + I_{L_{\gamma_3}} + I_{L_{\gamma_6}} + I_{L_{\beta_2}} + I_{L_{\beta_5}} \\ & + I_{L_{\beta_6}} + \sum_i I_{L_i^{MX}} + \sum_i I_{L_i^{XY}}. \end{aligned} \quad (61)$$

We compute an average energy associated with this residual low energy in a manner exactly analogous to Eq. (60) and the discussion related to Eq. (60).

Although Eqs. (59) through (61) involve many assumptions that may or may not be valid, note that these equations correctly account for the total energy being emitted as x rays or Auger electrons in this low-energy region. From a dosimetry point of view, all the radiations arising from vacancies in the M or higher shells will be nonpenetrating and may be lumped together as a single group.

1.6 Spontaneous Fission

Spontaneous fission gives rise to a variety of radiations. These include spontaneous fission fragments, neutrons, beta particles, prompt gamma rays, and delayed gamma rays. Dillman and Jones²³ comprehensively reviewed the internal dosimetry of spontaneously fissioning radionuclides. Their results indicate that the fission decay fraction, f_{SF} , the number of neutrons emitted per fission, \bar{v} , the mass number of the parent nuclide, A , and the atomic number of the parent nuclide, Z , are sufficient data to compute intensity and energy values for all the radiations emitted. Table 8 summarizes the pertinent results of the work of Dillman and Jones.

For some dosimetry applications, the spectral distribution of the neutrons, prompt and delayed gamma rays, and beta particles must be known, in addition to the average energies of these respective radiations. Spectral distributions were calculated by Dillman and Jones,²³ but we have not incorporated them directly into the decay-scheme computer program.

Table 8. Expressions for computation of intensities and average energies of radiations accompanying spontaneous fission^a

Radiation type	Average energy (MeV)	Intensity in fraction per decay
Neutrons	$0.75 + 0.65 (\bar{v} + 1)^{1/2}$	$\bar{v} f_{SF}$
Fission fragments	$0.0698Z^2/A^{1/3} - 10.988$	$2f_{SF}$
Prompt gamma rays	0.8847	$8.636f_{SF}$
Delayed gamma rays	0.9578	$0.2102m^2 f_{SF}$
Beta particles	0.2058m	mf_{SF}

^aIn this table, \bar{v} = neutrons per fission, f_{SF} = spontaneous fissions per decay, Z = atomic number of parent, A = mass number of parent, and $m = 5.98 + 92A/236 - Z$.

1.7 Bremsstrahlung Radiation

Bremsstrahlung radiation is the continuous spectrum of electromagnetic radiation generated when charged particles are slowed down by matter. The energy of the electromagnetic quantum generated is statistically variable and may range from zero up to the kinetic energy of the particle giving rise to it. Theory indicates that bremsstrahlung radiation intensity associated with alpha and other heavy charged particles is exceedingly small. In this work we confine our attention to bremsstrahlung associated with beta particles and monoenergetic conversion and Auger electrons. Even for beta particles, the bremsstrahlung radiation usually accounts for only a very small fraction of the total emitted energy. Bremsstrahlung radiation will be of importance in dosimetry in cases of high-end-point-energy beta decay or in cases in which the bremsstrahlung radiation accounts for a significant fraction of penetrating radiations. For example, a large fraction of the genetic dose is often from penetrating radiations; in such a case, the bremsstrahlung radiation will be of importance for a pure beta emitter.

There are two basic types of bremsstrahlung radiation — internal and external. Internal bremsstrahlung occurs as the beta particle is

being ejected from the nucleus and may be considered an inherent radiation component resulting from the radioactive decay process. External bremsstrahlung results from interaction of the beta particle with external atoms subsequent to its emission from the nucleus. Thus the spectrum of external bremsstrahlung generated depends on the atomic composition of the external medium and therefore is not an inherent unvarying component of the radioactive decay process. In dosimetry work, the important external media to be considered are air, muscle tissue, adipose tissue (fat), and bone. We compute the external bremsstrahlung radiation generated in each of these four media.

Our calculation of bremsstrahlung radiation is patterned after a computer code developed by Van Tuyl.²⁴ However, we have made a number of significant improvements in the methods used by Van Tuyl, which we shall point out as we proceed with the discussion of the theory used. We first consider external bremsstrahlung.

According to Liden and Starfelt,²⁵ the spectral distribution of external bremsstrahlung photons, $S(k)$ is given by

$$S(k) dk = \int_{1+k}^{E_m} P(E_i) \int_{1+k}^{E_i} \frac{N\phi}{(-dE_0/dx)_{\text{total}}} dE_i / \int_1^{E_m} P(E_i) dE_i , \quad (62)$$

where

$S(k) dk$ = number of photons emitted with energy between k and $k + dk$ per incident beta,

E_m = end-point total energy of the beta spectrum,

E_i = total energy with which beta particle is emitted,

E_0 = total energy of beta particle during absorption,

E = total energy of beta particle after radiation,

$k = E_0 - E$ = bremsstrahlung photon energy,

N = number of atoms per cubic centimeter of absorber,

$P(E_i) dE_i$ = a function proportional to the probability of beta emission with energy between E_i and $E_i + dE_i$,

ϕ = differential bremsstrahlung cross section for emitting a photon of energy k to $k + dk$ in units of square centimeter per atom per incident electron,

$-(dE_0/dx)$ = total energy loss (radiative + ionization) of electron per centimeter of path length.

In Eq. (62), all energies are in units of $m_0 c^2$, the energy equivalent of the rest mass of an electron.

We improved the methods of Van Tuyl²⁴ to implement Eq. (62) in three important ways. First, we used the value of $P(E_i)$ given by Eq. (7) derived from an exact expression of beta-decay theory. Van Tuyl used an approximate formula for $P(E_i)$ that was rather crude in the case of unique forbidden beta decay and, furthermore, he considered only the first forbidden unique beta-decay case in addition to allowed transitions.²⁴ Second, we used a more accurate and elaborate expression for the bremsstrahlung cross section than that which was used by Van Tuyl. Third, we used an expression for the ionization energy loss per centimeter, $(-dE_0/dx)_{\text{ion}}$, that takes into account differences between electrons and positrons in their interaction with matter.

The various theoretical calculations of bremsstrahlung cross sections were reviewed by Koch and Motz²⁶ and compared with experimental results. Their review indicates that in the energy region of interest for this study, beta energies of several million electron volts end point or lower, the cross-section formula from Bethe and Heitler²⁷ is in fairly good agreement with experiment if a multiplicative Coulomb correction factor, from Elwert,²⁸ is applied. In the energy region from roughly 0.1 to 2.0 MeV, Coulomb corrections to the Born-approximation formula of Bethe and Heitler are not available in analytical form, and the Elwert correction factor is rather crude in this energy region. However, an additional multiplicative empirical correction factor is

expected to be close to 1 for the low-atomic-number absorbers of primary interest in this study.

The Bethe-Heitler²⁷ cross-section formula is expected to break down near the high-frequency limit (i.e., when the bremsstrahlung photon energy is near the beta end-point energy). In the high-frequency limit, the Bethe-Heitler cross section goes to 0, whereas the theoretical results of Fano, Koch, and Motz²⁹ and limited experimental evidence indicate a finite value for the cross section at the high-frequency limit. We have not attempted to correct the Bethe-Heitler cross section in the high-frequency limit because the number of photons present near the high-frequency limit is very small.

The cross section from Bethe and Heitler that we used is given by

$$\phi = \alpha Z_\alpha (Z_\alpha + 1) r_0^2 \frac{dk}{k} \frac{p}{p_0} \left[\frac{4}{3} + F_1 + L \left(F_2 + \frac{k}{2p_0 p} F_3 \right) \right], \quad (63)$$

where

$$F_1 = -2E_0 E \left(\frac{p^2 + p_0^2}{p^2 p_0^2} \right) + \frac{\epsilon_0 E}{p_0^3} + \frac{\epsilon E_0}{p^3} - \frac{\epsilon \epsilon_0}{p_0 p},$$

$$L = 2 \ln[(E_0 E + p_0 p - 1)/k],$$

$$F_2 = \frac{8E_0 E}{3p_0 p} + \frac{k^2(E_0^2 E^2 + p_0^2 p^2)}{p_0^3 p^3},$$

$$F_3 = \left(\frac{E_0 E + p_0^2}{p_0^3} \right) \epsilon_0 - \left(\frac{E_0 E + p^2}{p^3} \right) \epsilon + \frac{2kE_0 E}{p^2 p_0^2},$$

$$\epsilon_0 = \ln[(E_0 + p_0)/(E_0 - p_0)],$$

$$\epsilon = \ln[(E + p)/(E - p)],$$

$$p_0 = (E_0^2 - 1)^{1/2},$$

$$p = (E^2 - 1)^{1/2},$$

$$\alpha = \text{fine structure constant} = 1/137.036,$$

$$r_0 = \text{classical radius of electron} = 2.8175 \times 10^{-13} \text{ cm},$$

$$Z_\alpha = \text{atomic number of absorber.}$$

In Eq. (63), the term $(Z_\alpha + 1)$ was substituted for Z_α as an approximate correction for the effects of the absorber electrons. As stated previously, this cross-section expression was corrected by Elwert's multiplicative correction factor C_E , where

$$C_E = \frac{E p_0 [1 - \exp(-2\pi\alpha Z_\alpha E_0 / p_0)]}{E_0 p [1 - \exp(-2\pi\alpha Z_\alpha E / p)]}. \quad (64)$$

To obtain the total energy loss of electrons per centimeter, $(-dE_0/dx)_{\text{total}}$, we first calculate the ionization energy loss per centimeter, $(-dE_0/dx)_{\text{ion}}$. According to Berger and Seltzer,³⁰ the ionization energy loss per centimeter is given by

$$(-dE_0/dx)_{\text{ion}} = \frac{2\pi N r_0^2 Z_\alpha E_0^2 \mu}{E_0^2 - 1} \left\{ \ln \left[\frac{(E_0 - 1)^2 (E_0 + 1)}{(2I/\mu)^2} \right] + F^\pm(E_0) - \delta \right\}, \quad (65)$$

where

$$F^\pm(E_0) = \frac{1}{E_0^2} + \left[\frac{(E_0 - 1)^2}{8} - (2E_0 - 1)\ln 2 \right] / E_0^2 \quad \text{for electrons,} \quad (66)$$

$$F^+(E_0) = 2 \ln 2 - \frac{(E_0^2 - 1)}{12E_0^2} \left[23 + \frac{14}{E_0 + 1} + \frac{10}{(E_0 + 1)^2} + \frac{4}{(E_0 + 1)^3} \right]$$

for positrons, (67)

$\mu = m_0 c^2 = 0.510976$ MeV, the electron rest energy,
 I = mean excitation energy of absorber,
 δ = density-effect correction.

The density-effect correction, δ , which takes into account the reduction of the collision loss from the polarization of the medium, is usually quite small and has been neglected in this work. The mean excitation energy, I , is a function of absorber atomic number. We have used the values recommended by Berger and Seltzer in implementing Eq. (65).

The ratio of energy loss by radiation to energy loss by ionization per unit path length is given by Bethe and Heitler²⁷ as

$$\frac{(dE_0/dx)_{\text{rad}}}{(dE_0/dx)_{\text{ion}}} = \frac{Z E_0}{1600} . \quad (68)$$

Equating the total energy loss per unit path length to the sum of the losses by radiation and ionization gives

$$(dE_0/dx)_{\text{total}} = \frac{Z E_0 + 1600\mu}{1600\mu} (dE_0/dx)_{\text{ion}} . \quad (69)$$

Equation (69) is used to obtain $(dE_0/dx)_{\text{total}}$ needed in Eq. (62).

Equation (62) was used to obtain the spectral distribution of external bremsstrahlung photons for monoenergetic electrons as well as for beta spectra. For monoenergetic electrons, $P(E_i) = 0$ except for $E_i = E_m$, where E_m , in this case, is the monoenergetic electron energy. Thus, for the monoenergetic electron case, $S(k)$ is simply given by the value of the inner integral of Eq. (62), where the upper limit of the

inner integral, E_i , is replaced by E_m , the monoenergetic electron total energy.

As mentioned above, we used Eq. (62) to calculate external bremsstrahlung spectral data for four media - air, muscle tissue, adipose tissue (fat), and bone. For each of the media, an appropriate cross section is obtained by computing the cross section for each atomic number composing the medium, weighting the result according to the fraction by weight of that atomic number, and adding the weighted cross sections. Table 9 lists the compositions of the four media used in this work.

Table 9. Compositions of media used in bremsstrahlung calculations

Atomic number	Fraction by Weight			
	Air	Muscle tissue	Adipose tissue	Bone
1	0.0	0.1048	0.1197	0.07039
6	0.0	0.2303	0.6382	0.2279
7	0.7551	0.02339	0.007977	0.03865
8	0.2317	0.6322	0.2313	0.4856
11	0.0	0.001288	0.0005025	0.003172
12	0.0	0.0001511	0.00001995	0.001090
15	0.0	0.002357	0.00001595	0.06938
16	0.0	0.002213	0.0007340	0.001685
17	0.0	0.001409	0.001197	0.001388
18	0.012877	0.0	0.0	0.0
19	0.0	0.002082	0.0003191	0.001487
20	0.0	0.0	0.00002234	0.09913

According to the formula of Knipp and Uhlenbeck³¹ as extended by Chang and Falkoff,³² the spectral distribution of internal bremsstrahlung for beta emitters is

$$S(k) dk = \frac{\alpha}{\pi} \int_{1+k}^{E_m} P(E_i) \frac{p}{p_i k} \left[\frac{E_i^2 + E^2}{E_i} \frac{\ln(E+p)}{p} - 2 \right] dE_i dk / \int_1^{E_m} P(E_i) dE_i , \quad (70)$$

in which all symbols have been defined previously. Again, in this case, we used the value of $P(E_i)$ given by Eq. (7) rather than the approximation used by Van Tuyl.²⁴

For both the external and internal bremsstrahlung, we calculated $S(k) dk$ for a series of photon energy values, k , ranging from 0.0045 MeV up to the end-point energy of the beta particles. The photon energy values are distributed approximately evenly on a logarithmic scale, with the value of dk increasing as the energy k increases so that the entire energy range is covered without overlapping or skipped energy bands.

2. INPUT DATA REQUIREMENTS FOR EDISTR

The input data for EDISTR consists of two parts. First there are two data cards that assign values to parameters and thus determine the various options to be used. These two data cards are followed by one or more data sets prepared in the format of the Evaluated Nuclear Structure Data File (ENSDF) sets. Each of these two parts is described in detail below.

The first data card contains the input data for the variables IOP, IOP6, IOPTIO, and JAM (in the order shown and with 4I3 format). The second data card contains input data for the variables CUTOFF and CCCUT (in the order indicated and with 2F10.0 format). These variables are defined below.

<u>Variable</u>	<u>Value</u>	
IOP	1	Output decay scheme data in the special format needed for dosimetry codes in use at the Oak Ridge National Laboratory (ORNL) are computed and put in the disk file SEEINP
	0	Output decay scheme data in the special format needed for dosimetry codes in use at ORNL are not computed
IOP6	0	Beta spectrum-shape data are not computed
	1	Beta spectrum-shape data for composite of all beta branches are calculated and printed
	2	Beta spectrum-shape data for each individual beta branch and for the composite of all beta branches are calculated and printed
IOPTIO	0	Bremsstrahlung data are not calculated
	1	Bremsstrahlung data are calculated and printed. The data are also put in disk file BREMST in the special format needed for dosimetry codes in use at ORNL
JAM	0	X rays of similar energy are grouped together in a single composite group; for example, L_{α_1} , L_{α_2} , and L_{α_3} x rays are combined as a single L_{α} entry, with a weighted average energy, in the printed decay

Variable Value

scheme output. Likewise, Auger electrons of similar energy are grouped together; for example, the six *KLL* Auger components are grouped together as a single *KLL* Auger electron with a weighted average energy. This procedure significantly shortens the output decay scheme tables.

- 1 There are no groupings of any x rays or Auger electrons. Every individual component is given in the printed output.

CUTOFF Percentage contribution of a radiation to the total energy release, below which the radiation is neglected in the printed output. CUTOFF is applied separately to (1) gamma rays, x rays, and annihilation radiation, (2) beta particles and internal conversion and Auger electrons, and (3) alpha particles and recoil atoms. A typical value of CUTOFF is 0.01. Its value will significantly affect the length of the output data table generated. CUTOFF has no effect on the data sent to the SEEINP disk file.

CCCUT The value of a theoretical internal conversion coefficient for a particular shell or subshell, below which the internal conversion coefficient is not printed in the listing of the input data used to generate the output data. A typical value is 0.001. The value of CCCUT will significantly affect the length of the listing of input data for nuclides with large numbers of gamma rays.

The default value for a blank field for any of the above six variables is zero. Bremsstrahlung data should never be computed unless needed because the computing time involved is quite long.

Other than the first two card images just described, we use input data in a format that conforms to that in the ENSDF generated and maintained by the Nuclear Data Project, ORNL. The ENSDF format has been

discussed elsewhere;³³⁻³⁵ we present only a brief discussion of the basic organization of ENSDF as it relates to the specific input needs of our computer program. Because there are many data items available from ENSDF that are not used by our computer program, we describe only those data items needed for our program. Although our discussion is brief, it allows the reader to prepare his own input data if data are not already available in the ENSDF. The reader interested in more complete details is referred to ref. 33.

ENSDF is organized into data sets, each of which consists of a number of 80-column card-image records. (The reader may wish to refer to the example ENSDF data sets shown in Appendix L during the following discussion of these data sets.) For every record except the END record, columns 1 through 5 contain a two-to-five character string consisting of the mass number and, immediately following, the chemical symbol of the nuclide for which nuclear structure information is being given elsewhere on the card image. The END record is blank in every column and simply cues the computer that the end of the data set has been reached. The first record in each data set is always the IDENTIFICATION record and indicates, by means of a key-word label string of characters, the type of data to be found in the data set. For our purposes, we are interested only in the DECAY data sets, that is, those data sets that give information on the radioactive decay of a nuclide. A DECAY data set IDENTIFICATION record contains, among other things, a field (columns 10 through 39) consisting of three parts -- the decaying nucleus, the type of decay, and the word DECAY -- separated by one or more blanks. The decaying nucleus is specified by the mass number followed by the chemical symbol of the parent. The type of decay is specified by any one of the following six two-character mnemonics:

<u>Mnemonic</u>	<u>Type of decay</u>
B-	β^- decay
EC	Electron-capture and/or β^+ decay
B+	
A	Alpha decay
IT	Isomeric-state decay (gamma radiation only)
SF	Spontaneous fission

A half-life may be added in parentheses to specify the decay completely. If a nuclide decays by more than one decay type, separate data sets must be present for each decay type. Our computer program uses the data in this three-part field to assign a mass number, atomic number, and decay type to the parent nuclide. The only other item read from the IDENTIFICATION record (columns 75 through 80) is the date (year/month/day) the data set was entered into ENSDF. For example, 770509 would mean that the data set was entered into ENSDF on May 9, 1977.

Following the IDENTIFICATION record is a NORMALIZATION record, designated by the letter N in column 8, and a PARENT record, designated by the letter P in column 8. There are three data items obtained from the NORMALIZATION record:

1. Columns 10 through 19 give the multiplier for converting relative photon intensities to photons per 100 decays of the parent through this decay branch. If this field is blank, our computer program assigns a default value of 1.0 to this parameter.
2. Columns 22 through 29 give the multiplier for converting relative transition intensity (including conversion electrons) to transitions per 100 decays of the parent through this decay branch. If this field is blank, our computer program assigns a default value to this parameter equal to the value of item 1 described immediately above.
3. Columns 32 through 39 give the branching ratio multiplier for converting intensity per 100 decays through this decay branch to intensity per 100 decays of the parent nucleus. If this field is blank, our computer program assigns a default value of 1.0 to this parameter because the majority of nuclides have only one decay mode.

There are four data items obtained from the PARENT record:

1. Columns 10 through 19 give the energy of the decaying level in kilo-electron volts. This will be 0 or blank, which the computer interprets as 0, except for isomeric-level parents.
2. Columns 22 through 39 give the spin, parity, or both.
3. Columns 40 through 49 give the half-life. Units must be given and are abbreviated as follows:

FS	10^{-15}	sec = femtosecond
PS	10^{-12}	sec = picosecond
NS	10^{-9}	sec = nanosecond
US	10^{-6}	sec = microsecond
MS	10^{-3}	sec = millisecond
S		second
M		minute
H		hour
D		day
Y		year
KY	10^3	year = kiloyear
MY	10^6	year = megayear
GY	10^9	year = gigayear

4. Columns 65 through 74 give the ground-state Q value in kilo-electron volts (total energy available for ground-state to ground-state transition).

For a PARENT record, Columns 1 through 5 are the mass number and chemical symbol of the parent nuclide, whereas, in most other types of records, columns 1 through 5 are the mass number and chemical symbol of the daughter nuclide because the radioactive decay gives information on the level structure, etc., of the daughter nuclide.

In the case of an isomeric-level decay mode (IT DECAY), a PARENT record may be included though it is redundant and, because the same information is available from an associated LEVEL record, not necessary.

Following the NORMALIZATION and PARENT records is the main body of the data set, composed of LEVEL, ALPHA, B-, EC, B+, and GAMMA records, which describe the measured or deduced properties such as spins, gamma-ray energies, etc. These records are associated with the level that decays (for GAMMA records) or the level that is populated (for B-, EC, B+, or ALPHA records). Thus, each LEVEL record is followed by a group of B-, EC, B+, or ALPHA records describing charged-particle decay into the level and GAMMA records describing gamma-ray decay out of the level. If a GAMMA, ALPHA, EC, B+, or B- record properly belongs in a data set but cannot be associated with a particular level, then the record must be placed in the data set prior to any LEVEL records. With this order of the records in mind, we now discuss the data contained in the LEVEL, GAMMA, ALPHA, EC (or B+), and B- records.

Each level of the daughter nuclide involved in the radioactive decay mode must be accompanied by a LEVEL record. A LEVEL record is designated by the letter L in column 8 and contains, for our purposes, four data items:

1. Columns 10 through 19 give the level energy in kilo-electron volts.
2. Columns 22 through 39 give the spin, parity, or both, if known.
3. Columns 40 through 49 give the half-life, if known. Units must be included as discussed above for the PARENT record.
4. Columns 78 through 79 denote a metastable-state level by the characters M or $M1$ for the first isomer, $M2$ for the second, etc.

The GAMMA record is designated by a G in column 8 and contains the following six data items, if known:

1. Columns 10 through 19 give the energy of the gamma-ray photon in kilo-electron volts.
2. Columns 22 through 29 give the relative photon intensity.
3. Columns 32 through 41 denote the multipolarity of the transition.

- Examples would be $E1, M1 + E2, M4$, etc.
4. For a mixed multipole transition, columns 42 through 49 give the mixing ratio, δ .
 5. Columns 56 through 62 give the total conversion coefficient.
 6. Columns 65 through 74 denote the relative total transition intensity (gamma ray + internal conversion electrons).

The B- record, designated by a B in column 8, contains four data items:

1. Columns 10 through 19 give the end-point energy of the β^- transition in kilo-electron volts, if measured. Because the end-point energy can be obtained from the ground-state Q value and the energy of the parent decaying level, this data item is not used unless the B- record is not associated with a particular LEVEL record.
2. Columns 22 through 29 give the intensity of the β^- -decay branch in percentage of the total β^- decay.
3. Columns 42 through 49 give the log(ft) for the β^- transition, if known.
4. Columns 78 through 79 give the uniqueness classification for the β^- decay, if known; e.g., 1U and 2U for first and second unique forbidden

transitions respectively. This field is left blank for allowed transitions.

The EC (or B+) record, designated by a letter E in column 8, contains six data items:

1. Columns 10 through 19 give the energy for electron capture to the level, if measured. As for the B- record, this data item is not used unless the EC (or B+) record is not associated with a particular LEVEL record.
2. Columns 22 through 29 give the intensity of the β^+ -decay branch in percentage of the total electron capture plus β^+ decay.
3. Columns 32 through 39 give the intensity of the electron-capture branch in percentage of the total electron capture plus β^+ decay.
4. Columns 42 through 49 give the log(ft) for the electron capture plus β^+ decay, if known.
5. Columns 65 through 74 give the total electron capture plus β^+ -decay intensity in percentage.
6. Columns 78 through 79 give the uniqueness classification for the EC (or β^+) decay, if known. See the discussion of item 4 on the B- record for details.

When β^+ transitions are energetically forbidden, columns 22 through 29 (item 2) may be left blank; in this case, either item 3, item 5, or both may be given, but only one of these two items is required. If both items 2 and 3 are given, then columns 65 through 74 (item 5) may be left blank.

The ALPHA record, containing the following two data items, is designated by a letter A in column 8:

1. Columns 10 through 19 give the alpha energy in kilo-electron volts. As for the B- and EC (or B+) records, this data item is used only if the ALPHA record is not associated with a particular LEVEL record.
2. Columns 22 through 29 give the intensity of the alpha-decay branch as percentage of the total alpha decay.

There is one minor problem associated with the use of the ENSDF as the source of input data. Although Ewbank et al.³³ indicate that spontaneous fission is one of the allowed decay modes, as of this

writing no decay data sets in which spontaneous fission is the decay mode have been created by the Nuclear Data Project. This is perhaps because there is no specific level in a daughter nucleus with which to associate spontaneous fission radiations such as neutrons, fission gamma rays, and fission fragments. The ENSDF does contain information on the percentage per decay of spontaneous fission for the few high-mass-number nuclides that exhibit spontaneous fission, but this information is not in DECAY data sets. (W. B. Ewbank, director of the Nuclear Data Project, kindly retrieved this information from the ENSDF.) In addition to the percentage per decay of spontaneous fission, we need the number of neutrons emitted per fission, which can be obtained from the data table given by Dillman and Jones.²³ Using these two data items, we can create a spontaneous fission decay data set for use when necessary. Each such data set consists of six records, the IDENTIFICATION, PARENT, NORMALIZATION, LEVEL, and END records discussed above and a record that we shall call the FISSION record, designated by a letter F in column 8. The FISSION record contains, in columns 10 through 19, the number of neutrons emitted per fission and, in columns 22 through 29, the percentage per decay of spontaneous fission. The LEVEL record is actually an unused dummy record in this case and is required for compatibility with other aspects of the EDISTR program; the information on the LEVEL record is not used; the LEVEL record may be blank in columns 10 through 80 if desired.

If output data are to be generated for several radionuclides in a single computer run, then the ENSDF decay data sets are placed consecutively in the input data stream. The first two data cards, which specify option parameters, are not repeated for each ENSDF decay data set; if different options are desired for different nuclides, separate computer runs are required. If a radionuclide decays by more than one decay mode, then there must be a separate ENSDF decay data set for each decay mode. For example, a nuclide may decay partially by alpha emission and partially by electron capture; thus, a decay data set is required for each of these two modes of decay. In these multiple-decay-mode cases the associated ENSDF decay data sets may be placed anywhere within the input stream; they need not be consecutive. Each time a data

set is input by the computer program, all remaining data sets in the input stream are scanned to see if any are associated with the same radioactive nucleus. The net result is that all data sets associated with a given nuclide are used together although they need not be placed consecutively in the input stream.

In addition to these input data, formatted according to the ENSDF scheme as we have explained, there are a number of permanent data sets needed when a computer run of EDISTR is made. These permanent data sets give fluorescence yields, theoretical internal conversion coefficient data, etc., and are stored in random-access disk files. A complete list of all files used by EDISTR is given in Table 10.

3. DETAILED DESCRIPTION OF SUBROUTINES USED BY PROGRAM EDISTR

Program EDISTR is conveniently divided into three functional phases:

(1) the input phase, in which the input data are prepared and put into a suitable format for computational purposes, (2) the computational phase, in which the computations required to implement the theory outlined in Sect. 1 are completed, and (3) an output phase. We shall discuss the various subroutines associated with each phase.

Table 10. Input-output (I/O) channels and associated disk files used by EDISTR

I/O Channel ^a	File name	File Size ^b		Type of data in file
		Maximum No. of records	Record length	
3	CONVER	101	1500	Theoretical internal conversion coefficients
11	BINDIN	104	19	Atomic binding energies
12	FLUORE	104	7	Fluorescence and Coster-Kronig yields
13	RKXRAY	104	6	K-series relative x-ray intensities
14	RLXRAY	104	11	L-series relative x-ray intensities
15	TXRAYER	104	9	Theoretical x-ray emission rates
16	AKLLEN	104	9	KLL Auger-electron energies
17	AKINTE	104	4	K-series relative Auger-electron intensities
18	ALINTE	104	9	L-series relative Auger-electron intensities
19	AKLLIN	28	6	Relative intensities - KLL Auger components for $Z < 28$
21	XALABE	72	7	Output data labels
26	ECOULO	104	15	Electron-capture Coulomb amplitudes; exchange and overlap corrections
40	SEEINP			Newly created output file of decay data in format for dosimetry codes in use at ORNL
41	BREMST			Newly created output file of bremsstrahlung data in format for dosimetry codes in use at ORNL
2	SUBMAS	500	400	
4	TEMP1			
8	MASTER	5000	42	Scratch files for storage of temporary intermediate results
25	COMOUT	2	350	
30	TEMP2			

^aAt ORNL, I/O channel 5 is the default input channel by which ENSDF input data are entered; I/O channel 6 is the default output channel to which most of the output of EDISTR is dumped and subsequently printed.

^bFile size is given only for random-access files. The record length is given in 4-byte units and is appropriate for IBM 360 computer systems.

3.1 Input Phase

The input phase of program EDISTR presents programming problems for two main reasons. First, the ENSDF input-data format, discussed in Sect. 2, may be described as a hybrid between a fixed-field and a free-format type of input. It is fixed field in that specific types of data must appear in specific field locations on the input card images; it is, however, free format in that the data may appear anywhere within the field and are sometimes a mixture of numbers and alphanumeric characters. For example, on every record except an END record, the mass number followed by the chemical symbol appears somewhere in columns 1 through

5. This modified free-format input requires the manipulation of data strings, for which FORTRAN is rather ill equipped. We have written, in FORTRAN, a series of string-manipulating functions similar to those

found in many versions of the BASIC interpreters, which are quite useful in all three phases of EDISTR. The string variables to be operated upon are contained in LOGICAL*1 arrays, and the strings are always terminated by a \ character. The seven string-manipulating functions used by program EDISTR are listed below.

1. FUNCTION INSTR(N, A, B). This function subroutine searches the string variable A (LOGICAL*1 array) for the string variable B (LOGICAL*1 array), starting with the Nth character in array A. The function returns the starting location of B within A. If B is not found, the value zero is returned.

2. FUNCTION LEN(A). This function subroutine finds the length (number of characters) in the string A (LOGICAL*1 array).

3. SUBROUTINE MID(A, N1, N2, B). This subroutine puts into string B (LOGICAL*1 array) the N2 characters of string A (LOGICAL*1 array), beginning with the N1th character of string A. The length of B will be less than N2 if, starting with the N1th character, there are fewer than N2 characters in A. The length of B will be zero if N1 > length of A.

4. SUBROUTINE NUM(X, A). This subroutine takes the real variable X and forms in string A (LOGICAL*1 array) the external representation of X as it would be printed by most BASIC interpreters. The following are several examples of the string A formed by SUBROUTINE NUM:

<u>Value of X</u>	<u>Resulting string A</u>
632.1000	632.1
5.720000E-12	5.72E-12
-4.672000E1	-46.72

5. SUBROUTINE NUM3(X, A, J). This subroutine takes the real variable X of positive value and forms in string A (LOGICAL*1 array) the J characters required to give a three-significant-digit external representation of X. The following are several examples of the string A formed by SUBROUTINE NUM3:

<u>Value of X</u>	<u>Resulting string A</u>	<u>Value of J returned</u>
12.4783	12.5	4
1.29763E-7	1.30E-07	8
0.0562146	0.0562	6
323.725	324.	4
0.000000	0.0	3

6. SUBROUTINE PLUS(A, B). This subroutine concatenates string A (LOGICAL*1 array) and string B (LOGICAL*1 array). The string A returned is the concatenation of original string A and string B. An error condition occurs if the length of resulting string A exceeds 99 characters because this should never occur in program EDISTR.

7. FUNCTION VALL(A). This function subroutine searches for and returns the first valid number in string A. The number is returned as a REAL*4 quantity. If a string contains several embedded numbers, only the first valid number is returned; the search is made from left to right in string A. The following table gives the value of the number returned for several example strings:

<u>String A</u>	<u>Value returned</u>
201TL	201.
316.4D	316.4
DECAY1.EL	1.
DIR7.6XZ5.1Q	7.6
XYZ	0.0

Note from the last line of the table that the value zero is returned if there are no numeric characters in string A. In this case an error message is recorded as a warning of possible trouble.

In addition to the above seven subroutines for handling strings, there are two other general-purpose subroutines that are used extensively in the first phase of program EDISTR. These are:

1. SUBROUTINE ACHEMZ(IA, CHEM, IZ, I). This subroutine obtains the mass number (variable IA), chemical symbol (variable CHEM), and atomic number (variable IZ) from a string of consecutive characters (no imbedded blanks) consisting of the mass number followed by the chemical symbol. The input string is brought into ACHEMZ through a LOGICAL*1 array B, which is in COMMON. The parameter, I, in ACHEMZ is the position in the input string of the first letter of the chemical symbol.

2. FUNCTION NOATOM(CHEM). This subroutine, called by ACHEMZ, returns the value of the atomic number when the chemical symbol (variable CHEM) is provided as input.

Another reason the input phase of EDISTR presented programming problems is that EDISTR was developed over several years and, in its earlier stages, predated the existence of the ENSDF. Although the input data required by EDISTR has not changed significantly over the past few years, the original format for entering that data was considerably different from the format used in the ENSDF. When the ENSDF became available, the easiest way to implement the use of the ENSDF as input was simply to transform the ENSDF into the format formerly used. This leads to some inefficiency in the programming, as is self-evident upon careful examination of the input-phase programming. However, the additional computer time involved is quite small, and because of the man-hours that would be required, streamlining the input phase has not been deemed worth the effort. In the input phase there are, therefore,

a series of subroutines to read the ENSDF data and convert it to a format directly usable by phase 2 of EDISTR. The output data of these subroutines are stored in a random-access file, MASTER.DAT. Because data are input for several nuclides (and perhaps several modes of decay for a single nuclide) a second random-access file, SUBMAS.DAT., is also created by these subroutines. SUBMAS.DAT indexes the records of MASTER.DAT so that records of a particular type and for a particular nuclide may be accessed rapidly. We now briefly describe these programs.

1. SUBROUTINE IDENT. This subroutine reads ENSDF IDENTIFICATION and PARENT records, computes all necessary information about the parent nuclide, and stores the information in a parent record of the MASTER.DAT file. The information stored in the MASTER.DAT file is

Variable	Item stored
IA	Parent mass number
EXC(LOGICAL*1 array)	Isomeric-level indicator
CHEM(INTEGER*2)	Chemical symbol of parent
IZ	Parent atomic number
ITYPE	Decay type
HLIFE(LOGICAL*1 array)	Half-life and units of half-life (abbreviation)
UNITS(REAL*8)	Unabbreviated units of half-life
HLSEC	Half-life value in seconds
NUMD	Total number of decay modes for parent
FDATE(LOGICAL*1 array)	Date data were entered into ENSDF
DECAYE	Total decay energy between parent level and ground state of daughter
ISPI2P	Total angular momentum quantum number of parent level in units of 1/2; i.e., J = 1/2, ISPI2P = 1, J = 1, ISPI2P = 2, etc.
IPARIP	Parity of parent level; +1 = even parity, -1 = odd parity
MULTI(INTEGER*2 array)	Lists the nuclide number in the input stream for each of the decay modes of the parent

Subroutines called by IDENT are JSPIN and HL. The values of ISPI2P and IPARIP are determined in subroutine JSPIN. The values of UNITS and HLSEC are determined in subroutine HL.

2. SUBROUTINE NRECOR. This subroutine reads an ENSDF NORMALIZATION record and, without any additional computation, puts the information into a normalization record in the MASTER.DAT file as follows:

Variable	Item stored
IA	Mass number of daughter nuclide
CHEM(INTEGER*2)	Chemical symbol of daughter
IZ	Atomic number of daughter
PHOMUL	Multiplier for converting relative photon intensity to photons per 100 decays of parent through this decay branch
TRAMUL	Multiplier for converting relative transition intensity (photons + conversion electrons) to transitions per 100 decays of the parent through this decay branch
BRANCH	Branching ratio multiplier for converting intensity per 100 decays through this branch to intensity per 100 decays of parent nucleus
	3. SUBROUTINE LRECOR. This subroutine reads the ENSDF LEVEL records, computes all necessary information about the levels of the daughter nuclide, and stores the information in a level record in the MASTER.DAT file as follows:
Variable	Item stored
E	Level energy in million electron volts (MeV)
IA	Same as corresponding items discussed above for SUBROUTINE IDENT, except these data are for levels in the daughter nucleus, not the parent level
CHEM(INTEGER*2)	
IZ	
ISPI2L	
IPARIL	
HLIFEL(LOGICAL*1 array)	
UNITSL(REAL*8)	
HLSEC	
	4. SUBROUTINE BRECOR. This subroutine reads charged-particle information from the ENSDF ALPHA, B-, B+, EC, and SF records, computes additional required input information about the charged-particle radiations, and stores the information in a charged-particle record in the MASTER.DAT file as follows:
Variable	Item stored
E	Difference in energy in MeV units between parent and daughter nuclear levels. For the spontaneous fission record, this is the number of neutrons produced per fission
IA	Mass number of daughter
CHEM(INTEGER*2)	Chemical symbol of daughter
IZ	Atomic number of daughter
	For spontaneous fission, of parent

Variable	Item stored
ITYPE	Decay type
ICLASS	Forbiddenness of decay (for β decay and electron-capture decay)
PERCEN	Number of α^- , β^- , or β^+ particles for this decay branch per 100 decays of the parent nucleus. For spontaneous fission, this is the number of fissions per 100 decays of the parent nucleus
DECAYE	Energy difference in MeV between parent nuclear level and ground state of daughter (not used for spontaneous fission)
EL	Energy in MeV of daughter level on which transition ends (not used for spontaneous fission)
ISA	Assigned the value 0 unless the transition is not associated with a particular level in the daughter, in which case it is assigned the value 1
PERCE2	Number of electron captures per 100 decays of the parent (used only for electron-capture decay)
ICHECK	Used for β^- , β^+ , and electron-capture decay only. ICHECK = 0 if forbiddenness uniquely determined; ICHECK = 1 if forbiddenness assumed to be allowed; ICHECK = 2 if forbiddenness based on log(ft) value

A subroutine called by BRECOR is FORBID. The values of ICLASS and ICHECK are determined in subroutine FORBID.

5. SUBROUTINE GRECOR. This subroutine reads gamma-ray data from the ENSDF GAMMA record, computes theoretical internal conversion coefficient data, and stores the information in gamma-ray records in the MASTER.DAT file as follows:

Variable	Item stored
E	Gamma-ray energy in MeV
IA	Mass number of daughter (nuclide which emits the gamma ray)
CHEM(INTEGER*2)	Chemical symbol of daughter
IZ	Atomic number of daughter
POLAR(LOGICAL*1 array)	Character string giving the gamma-ray multipolarity; e.g., E1, M1 + E2, etc.
PERCEN	Gamma-ray intensity in number per 100 decays of parent nucleus
EL	Initial energy level in MeV of the gamma-ray transition

Variable	Item stored
ELE	Final energy level in MeV of the gamma-ray transition
ISA	Assigned the value 0 unless the gamma ray is not associated with a particular initial energy level, in which case it is assigned the value 1
RATIO	Mixing ratio for a mixed multiple transition
TCC	Total internal conversion coefficient, if known
ICHECK	ICHECK = 0 if multipolarity can be uniquely determined on basis of experiment or spin changes; ICHECK = 1 otherwise
TTI	Total transition intensity (gamma-rays plus internal conversion electrons) in number per 100 decays of the parent nucleus
CC(REAL*4 array)	Theoretical internal conversion coefficients for K, L1, L2, L3, M, and N+ shells

Subroutines called by GRECOR are GAMEND, ICCOEF, and MULTIP. The value of the parameter ELE, as well as the spin and parity of the ending level of the gamma-ray transition, is determined in GAMEND. The values of POLAR and ICHECK parameters are determined in subroutine MULTIP; the theoretical internal conversion coefficients, in subroutine ICCOEF. By polynomial fit, subroutine ICCOEF determines the theoretical internal conversion coefficients to the four nearest tabulated values in the tables of conversion coefficients as a function of energy. Subroutine ICCOEF calls subroutine MATIN, a matrix inversion subroutine, in making the polynomial fit.

After the MASTER.DAT file of input data has been formed, the next step is to sort the gamma-ray records and the charged-particle records for a given decay type so that the gamma rays and the beta or alpha decays are ordered by increasing energy. This is done by subroutine EORDER. Subroutine BPLUSD searches for data sets in which β^+ decay and electron capture are both energetically possible. In our program, β^+ and electron capture are treated as separate decay modes. For such data sets, subroutine BPLUSD increments the counter of number of decay modes.

The last step in the initial phase of program EDISTR is the calling of subroutine BALAN, an important subroutine that determines the intensity and energy balance of the ENSDF data. The importance of subroutine BALAN

stems from the fact that many ENSDF decay data sets give partial and incomplete decay data. The ENSDF data sets present experimentally measured data, and often the experiments reported are limited in scope. A particular experimental study may have measured relative gamma-ray intensities and nothing else. It would be very tedious and time consuming to manually search through all the ENSDF decay data sets and determine which of them are complete enough to serve as input to EDISTR. The purpose of subroutine BALAN is to compute intensity and energy balances and, in particular, to flag cases in which poor balance conditions exist so that one can tell at a glance whether or not additional or modified input data are required.

The following quantities are checked by subroutine BALAN:

1. For each level of the daughter nucleus, except the ground state, a check is made on the balance between the intensity of charged-particle (alpha and beta), electron-capture, and/or gamma-ray transitions entering a level and gamma-ray transitions leaving a level. If there is more than a 10% imbalance, then the balance data are flagged with a series of asterisks so that the imbalance is readily observed.
2. A check is made to see if the total intensity to the ground and isomeric states of the daughter is approximately 100%. If it differs from 100% by more than 10%, then this fact is flagged with a series of asterisks.
3. The total intensity from the parent is calculated. If it differs from 100% by more than 5%, then this fact is flagged with a series of asterisks.
4. The total energy available in the decay is compared to the total energy of all radiations. If the two values differ by more than 5%, then this fact is flagged by a series of asterisks.
5. If there was no normalization record present in the ENSDF and default values for normalization were used, a warning message is printed so that the results may be carefully checked for validity.

Examples of the output generated by subroutine BALAN are given in Appendix G for the decay of several radionuclides. From Appendix G it will be noted that the normalization record was missing in the ^{35}S decay.

This is of no significance in this particular case because ^{35}S is a pure beta emitter and there are no gamma rays associated with the decay. In the case of ^{144}Ce (Appendix G), there is a 28.5% error in the intensity balance for the 0.09996-MeV level, and this level is flagged with asterisks. The user must decide whether or not this error can be tolerated or whether an attempt should be made to improve the input data. Note that for ^{144}Ce , the overall energy and intensity balance is quite good despite the rather large discrepancy at the 0.09996-MeV level.

3.2 Computational Phase

The bulk of the "number-crunching" calculations are made in the computational phase of EDISTR. All the theoretical methods discussed in Sect. 1 of this report are implemented in the computational phase. We shall discuss briefly each of the subroutines involved. The input data for all parts of the computational phase come from the MASTER.DAT and SUBMAS.DAT random-access files.

1. SUBROUTINE INIT. This subroutine initializes to zero beta spectrum-shape and bremsstrahlung data. It sets up the array of energy values at which beta spectrum-shape data are calculated.
2. SUBROUTINE ALPHA. This is a very simple subroutine that calculates the alpha-particle kinetic energy and recoil-nucleus energy using Eqs. (1) and (2) discussed in Sect. 1. The alpha intensity and the alpha and recoil-nucleus kinetic energies are stored in file TEMP2.DAT by means of a call to subroutine STORE, along with appropriate indices for use in the output phase of EDISTR. The input data used to obtain the alpha and recoil-nucleus energies and intensities are stored in file TEMP1.DAT for eventual printing in the output phase of the program.
3. SUBROUTINE ELECTR. This subroutine implements the beta-decay theory discussed in Sect. 1 and summarized in Eqs. (6) through (22). The numerical integrations required in Eq. (6) are done in subroutine SIMCON, a subroutine called by ELECTR. SIMCON involves numerical integration by quadrature using Simpson's rule. In our work the quadrature is terminated when the estimate of the integral changes by

less than 0.1% of the estimate obtained at the previous quadrature. To improve efficiency and speed of the computations, subroutine SIMCON evaluates both integrals in Eq. (6) simultaneously; that is, both $WP(W)$ and $P(W)$ are summed at the same time. This halves the number of times the complicated function $P(W)$ must be evaluated. SIMCON obtains the integrand $P(W)$ by a call to subroutine F, which in turn calls subroutine GAMMA and HYPER to evaluate the gamma function of complex argument and the hypergeometric function respectively. The GAMMA subroutine is actually a package of four subroutines (GAMMA, GAMMAZ, GAMMAL, GAMMA2) and uses the Pade-power-series approximation for evaluation of the gamma function of complex argument. The hypergeometric function is also evaluated using a power-series approximation, namely,

$${}_1F_1(a; b; z) = \frac{\Gamma(b)}{\Gamma(a)} \sum_{m=0}^{\infty} \frac{\Gamma(a+m)z^m}{\Gamma(b+m)m!} = 1 + \frac{az}{b} + \frac{(a+1)az^2}{2(b+1)b} + \frac{(a+2)(a+1)az^3}{6(b+2)(b+1)b} + \dots$$

In our work this power series is terminated when the absolute value of the contribution of the last term to the sum of the series is less than one part in 10^9 or when thirty terms have been considered, whichever occurs first. Of course, in implementing this power series, TYPE COMPLEX variables are used because a , b , and z are complex numbers in our case.

To speed up the numerical integration, there is a second entry point in subroutine F, SETUP, which calculates all parameters of the integrand that do not vary during the integration. A call to SETUP is made prior to the call to SIMCON.

If bremsstrahlung data are desired, ELECTR makes a call to subroutine BREMS, which evaluates the intensity of bremsstrahlung radiation associated with the β^- or β^+ radiation.

4. SUBROUTINE ECAPT. This subroutine implements the electron-capture decay theory expressed in Eqs. (23) through (26). ECAPT calls function subroutines FACT and DFACT to obtain needed factorial and double

factorial values respectively. After the initial vacancy distribution in the various subshells has been determined, ECAPT makes a call to subroutine GCAL2, which determines the intensities and energies of the resulting x rays and Auger electrons. Essentially, subroutine GCAL2 implements the theory expressed in Eqs. (32) through (61). The only subroutine called by GCAL2 is AUGEE, which in turn calls AUGER. Subroutines AUGEE and AUGER implement Eq. (58) for each of the various components of the LMM Auger-electron transitions. The cumulative intensities of each of the x-ray and Auger-electron transitions are temporarily stored in array variable CFA, and the corresponding energies in array variable EFA. The x-ray and Auger-electron intensity data are not stored directly for use by the output phase of EDISTR because there may be additional x rays and Auger electrons from internal conversion of gamma rays.

5. SUBROUTINE GAMRAY. This subroutine calculates the intensities and energies of gamma-ray transitions and associated internal conversion transitions. The initial vacancy distribution in the various subshells from internal conversion is computed, and a call is made to subroutine GCAL2, by which the intensities and energies of the resulting x rays and Auger electrons are computed. As mentioned previously, GCAL2 is also called by subroutine ECAPT; a brief description of the function of GCAL2 is included with the discussion of subroutine ECAPT. If bremsstrahlung data are desired, GAMRAY makes a call to subroutine BREMSM, which evaluates the intensity of bremsstrahlung radiation associated with the monoenergetic internal conversion electrons. To conserve computer time, the lengthy bremsstrahlung calculations associated with monoenergetic Auger electrons are deferred until the total cumulative Auger intensities are known. The gamma-ray, x-ray, Auger-electron and internal-conversion-electron intensities and energies are stored in file TEMP2.DAT, along with appropriate indices for use in the output phase of EDISTR. The input data used to obtain the data stored in file TEMP2.DAT are stored in file TEMP1.DAT for eventual printing in the output phase of the program. Some of the information stored in TEMP2.DAT are alphanumeric string labels for the input data. GAMRAY makes calls to subroutine EORD to form the appropriate label for an $E0$ multipole transition, to

subroutine PICCD to form the appropriate label for internal conversion coefficients and to form a three-significant-digit value of the internal conversion coefficient, and to subroutine PMULT to form the multipolarity label.

6. SUBROUTINE SPONF. This subroutine calculates data associated with spontaneous fission and is trivial if bremsstrahlung data are not desired. The subroutine simply transfers the spontaneous fission intensity and associated number of neutrons per fission from the MASTER.DAT input file to the TEMP2.DAT file used in the output phase of EDISTR. The calculation of intensities of radiations accompanying spontaneous fission is done in the output phase of EDISTR. If bremsstrahlung data are desired, subroutine SPONF estimates an intensity and average energy of the beta particles accompanying spontaneous fission according to the method summarized in Table 8. Though there will actually be more β^- than β^+ decays, the assumption is that half of the beta particles are β^- particles and half are β^+ particles because the resultant bremsstrahlung spectrum is insensitive to the relative abundance of β^- and β^+ particles. From the average energy of the beta particles and the ratio of average energy to end-point energy of 0.42 for β^- particles and 0.45 for β^+ particles, end-point energies associated with the β^- and β^+ spectra are estimated. The ratios 0.42 and 0.45 are typical for allowed spectra in the mass number range encompassed by fission fragments. Calls to BREMS are then made to estimate the bremsstrahlung data. For purposes of these calculations, the fission process is assumed to be symmetric with the mass and atomic numbers associated with the prompt betas equal to half the corresponding values for the parent nuclide. This is reasonable because beta spectra vary rather slowly with changing mass number.

3.3 Output Phase

The output phase of program EDISTR consists of calls to three subroutines, TABIPU, TABDEC, and TABBRE. Subroutine TABIPU simply takes the input data in file TEMP1.DAT, which is already formatted exactly as desired, and prints it. Subroutine TABIPU makes calls to subroutine

HEADIN to print heading information at the top of each page and to keep track of the number of lines printed so advancement to a new page can be made as needed. A reference to the ENSDF as the input source is printed at the conclusion of the data along with the date the data were entered. Appendix H consists of examples of the output generated by subroutine TABIPU. In these examples, the abbreviation I.C.E. signifies internal conversion electron. The abbreviations AK, ALL, AL2, AL3, AL, AM, and AN+ represent the internal conversion coefficients α_K , α_{L_1} , α_{L_2} , α_{L_3} , α_L , α_M , and α_{N+} respectively. The abbreviation MRS represents δ^2 , the square of the mixing ratio for a mixed multipole gamma-ray transition. All other notations are self-evident.

Subroutine TABDEC analyzes the output data contained in file TEMP2.DAT. Although subroutine TABDEC is quite straightforward, it is also rather lengthy because of a number of desirable output features. First, to shorten the length of the output data without loss of significant data, the contribution to the energy release per transformation of the parent for each radiation is calculated. Then the total energy release per transformation from the three main radiation types is calculated separately. The three radiation types are (1) gamma rays, x rays, and annihilation quanta, (2) beta particles, internal conversion electrons, and Auger electrons, and (3) alpha particles and recoil nuclei. If the contribution of any particular radiation to the energy release per transformation in the appropriate category is less than a predetermined fraction selected by the user, then that radiation is not shown in the printed output.

In the case of spontaneous fission, subroutine TABDEC also calculates the intensities and average energies associated with the radiations concomitant with spontaneous fission and does so according to the methods summarized in Table 8.

Subroutine TABDEC also makes a call to subroutine DAUGHT, by which the percent feeding, if any, of isomeric levels in the daughter nuclide is calculated and an appropriate message printed. In subroutine DAUGHT, a message is also printed indicating whether or not the ground state of the daughter nuclide (or nuclides if there are several decay modes) is

stable. If the daughter nuclide is radioactive, this serves as a notice to the user that decay of the daughter may also need to be considered in dose calculations. Subroutine TABDEC also makes calls to subroutine HEADIN (which in turn calls HEAD2) to print desired heading information and to keep track of the number of lines printed so that advancement to a new page can be facilitated.

Examples of the printed output data of subroutine TABDEC are illustrated for several radionuclides in Appendix I. The effect of changing one of the input parameters, JAM, which was discussed in the early part of Sect. 2, is illustrated for the data of ^{125}I .

Subroutine TABDEC also prints beta spectrum-shape data if input parameter IOP6, discussed early in Sect. 2, equals 1 or 2. Beta spectrum-shape data generated by TABDEC are tabulated in Appendix J and shown graphically in Figs. 1 and 2 for ^{14}C and ^{15}O respectively. Note from the figures (included in Appendix J) that ^{14}C , a β^- emitter, has finite probability of emission at zero kinetic energy, whereas ^{15}O , a β^+ emitter, has zero probability of emission at zero kinetic energy. This difference between β^- and β^+ spectra holds for all β^- decay cases.

If input parameter IOP equals 1, subroutine TABDEC also places the output data into file SEEINP in a format used directly by dosimetry codes at ORNL. This particular output format is well suited for computer retrieval of the output data, regardless of the eventual intended use of the data, and is illustrated for several radionuclides in Appendix K. Referring to Appendix K, note that the data are presented in a series of 80-column card-image records. The first record is an identification record and gives the following data:

1. The mass number of the parent is in columns 1 through 4 (F4.0 format).
2. A parent isomeric level is indicated by an M in Al format in column 5.
3. The chemical element name appears in the field defined by columns 7 through 18, and the element name is left justified in this field.
4. The atomic number of the parent appears in columns 19 through 22 in F4.0 format.
5. The half-life of the parent appears in columns 23 through 33 in 1PE11.3 format.

6. The units of the half-life appear in columns 35 through 42, and the units are left justified in this field.
7. The number of records of individual radiations that follow is given in columns 43 through 46 in I4 format; mnemonics for the decay modes of the parent are given in columns 47 through 58 in 4(1X, A2) format. The mnemonics used are $B^- = \beta^-$ decay, $B^+ = \beta^+$ decay, A = alpha decay, IT = isomeric level decay, EC = electron capture, SF = spontaneous fission.
8. The date the data were run on the computer is given in columns 60 through 68.

The remainder of the card image is a self-evident label so that if the card images are actually punched on cards then the set of cards may easily be kept in order.

Each of the remaining card images in the data set gives intensity and energy information for the individual radiations present in the decay. Each card image consists of two indices in 2I2 format followed by four floating point numbers in 1P4E13.5 format and then by the identifying label for the data set. The first index, which we designate by the symbolic name ICODE, has the following meanings:

Value of ICODE	Type of radiation
1	Gamma rays
2	X rays
3	Annihilation quanta
4	β^+ particles
5	β^- particles
6	Internal conversion electrons
7	Auger electrons
8	Alpha particles
9	Spontaneous-fission radiations

The second index, which we designate by the symbolic name INDEX, has different meanings depending on the value of ICODE:

1. If ICODE = 1, 4, 5, or 8, then INDEX gives the number of the corresponding radiation. That is, if ICODE = 1 and INDEX = 35, then this is the 35th gamma ray associated with the decay (all radiations are ordered according to increasing energy).
2. If ICODE = 3 or 9, INDEX is not used.

3. If ICODE = 2, INDEX gives the code number for x-ray type:

<u>Value of INDEX</u>	<u>X-ray type (Siegbahn notation)</u>
1-3	$K_{\alpha_1} - K_{\alpha_3}$
4-6	$K_{\beta_1} - K_{\beta_3}$
7	K_{β_5}
8	Total K x ray
9-10	$L_{\alpha_1} - L_{\alpha_2}$
11	Total L_{α} x ray
12-17	$L_{\beta_1} - L_{\beta_6}$
18	Total L_{β} x ray
19-21	$L_{\gamma_1} - L_{\gamma_3}$
22	L_{γ_6}
23	Total L_{γ} x ray
24	L_{η}
25	L_i
26	Total L x ray

4. If ICODE = 6, INDEX gives the code number for type of internal conversion electron:

<u>Value of INDEX</u>	<u>Internal-conversion-electron type</u>
1	K shell
2	Total L shell
3	Total M shell
4	Total N^+ shell
5-7	L_1 through L_3 shells

5. If ICODE = 7, INDEX gives the code number for type of Auger electron:

<u>Value of INDEX</u>	<u>Auger-electron type</u>
27-32	$KL_1L_1, KL_1L_2, KL_1L_3, KL_2L_2, KL_2K_3, KL_3L_3$
33	Total KLL
34-36	$KL_1X - KL_3X$
37	Total KLX
38	KXY
39	Total K -series Auger
40-42	L_1MM, L_1MX, L_1XY
43-45	L_2MM, L_2MX, L_2XY
46-48	L_3MM, L_3MX, L_3XY
49-51	Total LMM, LMX, LXY
52	Total L -series Auger
53	MXY
54	Residual low energy, mostly Auger electrons

The meanings of the four floating point numbers in the remainder of each card image are as follows:

1. Columns 5 through 17 contain the percentage per decay intensity of the radiation.

2. Columns 18 through 30 contain the energy of the radiation in million electron volts. In the case of beta particles this column contains the average energy.

3. Columns 31 through 43 contain the end-point kinetic energy in million electron volts of beta radiations. For other types of radiation this column is not used and is arbitrarily set equal to the energy value in columns 18 through 30.

4. Columns 44 through 56 are only used when ICODE = 4 or 5. For beta decay (ICODE = 4 or 5), columns 44 through 56 indicate an allowed or first forbidden nonunique transition by means of the number 0.0; a first forbidden unique or second forbidden nonunique transition is indicated by the number 1.0; a second forbidden unique or third forbidden nonunique transition is indicated by the number 2.0; a third forbidden unique transition is indicated by a 3.0. For ICODE = 2 (x rays) or ICODE = 7 (Auger electrons), columns 44 through 56 were originally used to indicate the grouping or nongrouping of x rays and Auger electrons of similar energy. This feature has since been eliminated and any value in these columns may be ignored; at present only individual x rays and Auger electrons (no groupings of x rays, sum of all x rays, or sums of any kind) are listed in the SEEINP.DAT data file just described (Appendix K). This prevents the inadvertent use of the same information for both individual x rays and Auger-electrons and x-ray and Auger-electron groups.

Finally, subroutine TABBRE prints bremsstrahlung data if input parameter IOPTIO equals 1. Example output bremsstrahlung data for the decay of ^{85}Kr are included in Appendix M and are shown graphically in Fig. 3. If IOPTIO = 1, then bremsstrahlung data for the air medium only are also transferred to file BREMST.DAT. The computer-retrievable format of the card-image records for BREMST.DAT is identical to that described above for file SEEINP.DAT. The reason that data for an air medium are

placed in file BREMST.DAT, rather than data for a tissue medium as might be expected, is because one of the most likely situations in which bremsstrahlung radiation may be of importance is in the case of immersion in a radioactive cloud.

We end this report by briefly discussing the comparison of our calculated results on absolute L x-ray intensities with experimental results. We confine our discussion to the absolute intensities of L x rays because this is one of the parts of the computations for which prior comparisons with experimental data are lacking; also, this is one of the areas of our computer program in which a major effort was made to improve on existing theoretical methods. It has only been in the last few years that extensive experimental data on absolute L x-ray intensities have become available for a number of transuranium nuclides. Table 11 shows a comparison of the L_α , L_β , L_γ , and L_1 x-ray intensities calculated by EDISTR with experimental data of Bemis et al.,³⁶ Toohey,³⁷ and Campbell and McNelles.³⁸ We are gratified that the results from program EDISTR (this work) are generally in good agreement with experimental results. We note that the L_1 intensity tends to be slightly low compared with experimental results. Also, the intensities of all the L x rays in the decay of ^{250}Cf tend to be somewhat low compared with experimental results. However, the decay scheme data of ^{250}Cf have not been well studied and thus are subject to considerable error. The data of Table 11 lead us to believe that our methods are valid and give results that agree well with experimental results for cases in which the decay scheme is well known.

Table 11. Absolute intensities for L -series x rays for selected radionuclides

Parent nuclide	Percentage per disintegration				Source
	L_1	L_α	L_β	L_γ	
^{238}Pu	0.204	4.12	5.62	1.28	^a
	0.26 ± 0.01	4.15 ± 0.07	5.61 ± 0.07	1.36 ± 0.02	^b
	0.24	3.97	5.96	1.24	^c
^{239}Pu	0.0758	1.53	2.11	0.486	^a
	0.113 ± 0.005	1.82 ± 0.04	2.16 ± 0.04	0.53 ± 0.01	^b
	0.08	1.42	2.64	0.46	^c
^{240}Pu	0.193	3.91	5.36	1.22	^a
	0.24 ± 0.01	3.78 ± 0.06	4.84 ± 0.07	1.20 ± 0.03	^b
	0.21	3.51	5.21	1.17	^c
^{242}Pu	0.160	3.24	4.44	1.02	^a
	0.21 ± 0.02	3.10 ± 0.08	4.15 ± 0.10	1.08 ± 0.04	^b
	0.17	3.08	4.28	1.02	^c
^{241}Am		16.5	19.6	4.83	^a
	0.86 ± 0.03	13.2 ± 0.3	19.25 ± 0.60	4.85 ± 0.2	^d
^{244}Cm	0.201	3.91	4.88	1.02	^a
	0.25 ± 0.01	3.86 ± 0.07	4.30 ± 0.07	1.03 ± 0.02	^b
^{246}Cm	0.178	3.47	4.35	0.973	^a
	0.21 ± 0.01	3.33 ± 0.07	3.71 ± 0.07	0.86 ± 0.02	^b
^{250}Cf	0.138	2.60	3.41	0.787	^a
	0.21 ± 0.01	3.27 ± 0.08	3.85 ± 0.08	0.85 ± 0.03	^b

^aProgram EDISTR.

^bC. E. Bemis et al., "Detection of Internally Deposited Actinides," presented at the Ninth Midyear Topical Symposium of the Health Physics Society, Denver, Colo., Feb. 9-12, 1976.

^cR. E. Toohey, "Relative Abundance of Uranium $L_{\alpha,\beta,\gamma}$ Conversion X-rays Following the α -Decay of Plutonium," presented at the Twenty-first Annual Meeting of the Health Physics Society, San Francisco, Calif., June 28-July 2, 1976.

^dJ. L. Campbell and L. A. McNelles, *Nucl. Instrum. Methods* 125: 205 (1975).

REFERENCES

1. *Nuclear Data Sheets*, ed. by Nuclear Data Project, W. B. Ewbank, director, Oak Ridge National Laboratory, Oak Ridge, Tenn.; published serially by Academic Press, New York.
2. C. M. Lederer et al., *Table of Isotopes*, 6th ed., Wiley, New York, 1967.
3. M. J. Martin and P. H. Blichert-Toft, *Nucl. Data Tables* A8: 1-198 (1970).
4. M. J. Martin, ed., ORNL-5114, Oak Ridge National Laboratory, Oak Ridge, Tenn., 1976.
5. D. C. Kocher, ed., ORNL/NUREG/TM-102, Oak Ridge National Laboratory, Oak Ridge, Tenn., 1977.
6. N. B. Gove and M. J. Martin, *Nucl. Data Tables* 10: 205-317 (1971).
7. H. Brysk and M. E. Rose, *Rev. Mod. Phys.* 30: 1-169 (1958).
8. H. Behrens and J. Janecke, *Landolt-Bornstein New Series on Numerical Data and Functional Relationships in Science and Technology*, vol. 4, Springer-Verlag, New York, 1969, pp. 1-315.
9. J. A. Bearden and A. F. Burr, *Rev. Mod. Phys.* 39: 125-42 (1967).
10. F. K. Richtmyer, E. H. Kennard, and J. N. Cooper, *Introduction to Modern Physics*, 6th ed., McGraw-Hill, New York, 1969, pp. 753-54.
11. B. L. Robinson, *Nucl. Phys.* 64: 197-208 (1965).
12. R. S. Hager and E. C. Seltzer, *Nucl. Data Tables* A8: 1-198 (1968).
13. O. Dragoun, Z. Plajner, and F. Schmutzler, *Nucl. Data Tables* A9: 119-35 (1971).
14. M. I. Band, M. B. Trzhaskovskaya, and M. A. Listengarten, *At. Data Nucl. Data Tables* 18: 433-57 (1976).
15. E. L. Church and J. Weneser, *Phys. Rev.* 103: 1035 (1956).
16. J. H. Scofield, *At. Data Nucl. Data Tables* 14: 121-37 (1974).
17. M. I. Babenkov, B. V. Bobykin, and V. K. Petukhov, *Izv. Akad. Nauk SSSR Ser. Fiz.* 36: 2139-42 (1972).
18. M. H. Chen and B. Crasemann, *Phys. Rev.* A8: 7-13 (1973).
19. P. Venugopala Rao, M. H. Chen, and B. Crasemann, *Phys. Rev.* A5: 997-1012 (1972).
20. W. Bambynek et al., *Rev. Mod. Phys.* 44: 716-813 (1972).
21. K. D. Sevier, *Low-Energy Electron Spectrometry*, Wiley-Interscience, New York, 1972.
22. S. K. Haynes, U.S. Atomic Energy Commission CONF-720404, vol. 1 (1972), pp. 559-661.
23. L. T. Dillman and T. D. Jones, *Health Phys.* 29: 111-23 (1975).
24. H. H. Van Tuyl, U.S. Atomic Energy Commission Report HW-83784 (1964), pp. 1-23.
25. K. Liden and N. Starfelt, *Phys. Rev.* 97: 419 (1955).
26. H. W. Koch and J. W. Motz, *Rev. Mod. Phys.* 31: 920-55 (1959).
27. H. Bethe and W. Heitler, *Proc. Roy. Soc. London* A146: 83 (1934).
28. G. Elwert, *Ann. Phys. (Leipzig)* 34: 178 (1939).
29. U. Fano, H. W. Koch, and J. W. Motz, *Phys. Rev.* 112: 1679 (1958).
30. M. J. Berger and S. M. Seltzer, National Aeronautics and Space Administration report NASA SP-3012, 1964.
31. J. K. Knipp and G. E. Uhlenbeck, *Physica* 3: 425 (1936).
32. C. S. Wang Chang and D. L. Falkoff, *Phys. Rev.* 76: 365-71 (1949).
33. W. B. Ewbank et al., ORNL-5054, Oak Ridge National Laboratory, Oak Ridge, Tenn., 1975.
34. W. B. Ewbank, "Evaluated Nuclear Structure Data File (ENSDF) for Basic and Applied Research," presented at the Fifth International CODATA Conference, Boulder, Colo., June 28-July 1, 1976.
35. W. B. Ewbank, "Computer Processing of 'Free-Text' Keyword Strings," presented at the Fifth International CODATA Conference, Boulder, Colo., June 28-July 1, 1976.
36. C. E. Bemis et al., "Detection of Internally Deposited Actinides," presented at the Ninth Midyear Topical Symposium of the Health Physics Society, Denver, Colo., Feb. 9-12, 1976.
37. R. E. Tookey, "Relative Abundances of Uranium α, β, γ Conversion X-rays Following the α -Decay of Plutonium," presented at the Twenty-first Annual Meeting of the Health Physics Society, San Francisco, Calif., June 28-July 2, 1976.

38. J. L. Campbell and L. A. McNelles, *Nucl. Instrum. Methods* 125: 205
(1975).

Appendix A
FLUORESCENCE AND COSTER-KRONIG YIELDS USED IN THIS WORK*

Z	Fluorescence yields				L-shell Coster-Kronig yields		
	ω_K	ω_{L_1}	ω_{L_2}	ω_{L_3}	f_{12}	f_{13}	f_{23}
3	0.000163	0.0	0.0	0.0	0.0	0.0	0.0
4	0.000451	0.0	0.0	0.0	0.0	0.0	0.0
5	0.00101	0.0	0.0	0.0	0.0447	0.0899	0.0887
6	0.00198	0.0	0.0	0.0	0.0894	0.180	0.177
7	0.00351	0.0	0.0	0.0	0.134	0.270	0.266
8	0.00579	0.0	0.0	0.0	0.179	0.359	0.355
9	0.00902	0.0	0.0	0.0	0.224	0.449	0.444
10	0.0140	0.0	0.0	0.0	0.268	0.539	0.532
11	0.0192	0.0	0.0	0.0	0.313	0.629	0.621
12	0.0265	0.0	0.0	0.0	0.313	0.629	0.621
13	0.0357	3.05E-06 ^a	0.0	0.00240 ^a	0.313	0.629	0.621
14	0.0470	9.77E-06 ^a	0.0	0.00108 ^a	0.313	0.629	0.621
15	0.0604	2.12F-05 ^a	0.0	0.000410 ^a	0.313	0.629	0.621
16	0.0761	3.63E-05 ^a	0.0	0.000290 ^a	0.313	0.629	0.621
17	0.0942	5.60E-05 ^a	0.0	0.000230 ^a	0.313	0.629	0.621
18	0.115	8.58E-05 ^a	0.0	0.000190 ^a	0.313	0.629	0.621
19	0.138	0.000115 ^a	0.0	0.000210 ^a	0.313	0.629	0.621
20	0.163	0.000156 ^a	0.0	0.000210 ^a	0.313	0.629	0.621
21	0.190	0.000209	0.0	0.000298	0.313	0.629	0.621
22	0.219	0.000280 ^a	0.0	0.000423	0.313 ^a	0.629 ^a	0.621
23	0.250	0.000288	0.000400 ^f	0.000600 ^f	0.315	0.633	0.621
24	0.282	0.000297 ^a	0.000530 ^f	0.000790 ^f	0.317 ^a	0.636 ^a	0.621
25	0.314	0.000338	0.000880 ^f	0.00126 ^f	0.310	0.644	0.621
26	0.347	0.000384 ^a	0.00118 ^f	0.00149 ^h	0.302 ^a	0.652 ^a	0.621 ⁱ
27	0.381	0.000422	0.00121 ^f	0.00173 ^f	0.314	0.637	0.626
28	0.414	0.000463 ^a	0.00172 ^f	0.00251 ^f	0.325 ^a	0.622 ^a	0.631 ⁱ
29	0.445	0.000492	0.00210 ^f	0.00383 ^h	0.324	0.623	0.639 ⁱ
30	0.479	0.000523 ^a	0.00293 ^f	0.00535 ^f	0.322 ^a	0.624 ^a	0.0157 ⁱ
31	0.510	0.000635	0.00377 ^f	0.00658 ^f	0.294	0.598	0.0244
32	0.540	0.000770 ^a	0.00452 ^f	0.00758	0.266 ^a	0.573	0.0331 ⁱ
33	0.567	0.00100	0.00670	0.00874 ^h	0.284	0.547 ^d	0.0459
34	0.596	0.00130 ^a	0.00994 ^h	0.00979	0.302 ^a	0.560	0.0587
35	0.622	0.00155	0.0139 ^h	0.0110	0.266	0.572	0.0714 ⁱ
36	0.646	0.00185 ^a	0.0193 ⁱ	0.0123	0.230 ^a	0.585 ^d	0.0842 ⁱ
37	0.669	0.00236	0.0211	0.0152	0.240	0.569	0.0904
38	0.691	0.00300 ^a	0.0230	0.0165	0.249 ^a	0.554	0.0966
39	0.711	0.00345	0.0252	0.0196	0.243	0.538	0.103
40	0.730	0.00397 ^a	0.0275 ⁱ	0.0221	0.236 ^a	0.522 ^d	0.109 ⁱ
41	0.748	0.00478	0.0304	0.0242	0.201	0.607	0.115
42	0.764	0.00575 ^a	0.0337 ⁱ	0.0271	0.166 ^a	0.692 ^d	0.121 ⁱ
43	0.779	0.00667	0.0367	0.0318	0.112	0.693	0.125
44	0.793	0.00774 ^a	0.0399	0.0374	0.0570 ^a	0.693	0.130
45	0.807	0.00849	0.0479	0.0383	0.0550	0.694	0.134
46	0.819	0.00930	0.0508	0.0420	0.0540	0.694	0.139
47	0.830	0.0102 ^a	0.0540 ⁱ	0.0449	0.0520 ^a	0.695 ^d	0.143 ⁱ
48	0.840	0.0159	0.0574	0.0453	0.0860	0.694	0.147

Appendix A (continued)
FLUORESCENCE AND COSTER-KRONIG YIELDS USED IN THIS WORK

Z	Fluorescence yields			L-shell Coster-Kronig yields			
	ω_K	ω_{L_1}	ω_{L_2}	ω_{L_3}	f_{12}	f_{13}	f_{23}
49	0.850	0.0249	0.0611	0.0536 ^h	0.120	0.694	0.152
50	0.859	0.0388 ^b	0.0650 ⁱ	0.0579 ^h	0.154 ^b	0.693 ^d	0.156 ⁱ
51	0.867	0.0430	0.0690	0.0633 ^h	0.160	0.316 ^d	0.157
52	0.875	0.0476	0.0738	0.0679	0.167	0.320	0.159
53	0.882	0.0527	0.0789	0.0728	0.173	0.324	0.160
54	0.889	0.0584 ^a	0.0844	0.0781	0.179 ^a	0.328	0.161
55	0.895	0.0592	0.0902	0.0838	0.184	0.332	0.163
56	0.901	0.0600 ^e	0.0965 ⁱ	0.0899 ^h	0.188	0.336 ^d	0.164 ⁱ
57	0.906	0.0634	0.102	0.0966	0.193	0.335	0.163
58	0.911	0.0669	0.109	0.104	0.198	0.334	0.163
59	0.915	0.0706	0.115	0.112	0.202	0.333	0.162
60	0.920	0.0746 ^a	0.122 ⁱ	0.120 ^h	0.207 ^a	0.332 ^d	0.161 ⁱ
61	0.924	0.0791	0.130	0.127	0.206	0.330	0.159
62	0.928	0.0838	0.138	0.135	0.206	0.328	0.157
63	0.931	0.0888	0.146	0.143	0.205	0.326	0.155
64	0.934	0.0941	0.155	0.151	0.204	0.323	0.153
65	0.937	0.0997	0.165 ^c	0.160 ^h	0.203	0.321	0.151
66	0.940	0.106	0.177	0.167	0.203	0.319	0.149
67	0.943	0.112 ^a	0.190 ⁱ	0.175	0.202 ^a	0.317 ^d	0.147 ⁱ
68	0.945	0.112	0.201	0.183	0.201	0.317	0.150
69	0.948	0.112	0.212	0.191	0.200	0.316	0.154
70	0.950	0.112 ^d	0.224 ⁱ	0.200 ^c	0.199	0.316 ^d	0.157 ⁱ
71	0.952	0.113	0.235	0.212	0.198	0.318	0.156
72	0.954	0.113	0.246	0.225	0.197	0.320	0.154
73	0.956	0.114	0.257 ^c	0.239	0.196	0.322	0.153 ^m
74	0.957	0.115 ^a	0.269 ⁱ	0.253 ^h	0.195 ^a	0.324 ^d	0.152
75	0.959	0.113	0.284	0.263	0.194 ^k	0.373	0.151
76	0.961	0.111	0.300 ^c	0.274	0.192 ^k	0.422	0.150
77	0.962	0.109	0.315	0.285	0.188 ^k	0.471	0.150
78	0.963	0.107	0.331 ^j	0.297	0.186 ^k	0.520	0.149
79	0.964	0.105 ^a	0.338	0.309	0.182 ^k	0.569	0.148
80	0.966	0.0983 ^d	0.346 ⁱ	0.321 ^h	0.176 ^k	0.618 ^d	0.147 ⁿ
81	0.967	0.105	0.373 ^c	0.332	0.172 ^k	0.617	0.141 ⁿ
82	0.968	0.112	0.363	0.343	0.167 ^k	0.616	0.158 ^p
83	0.969	0.120 ^a	0.380 ^c	0.355	0.161 ^k	0.614	0.149
84	0.970	0.124	0.396	0.367	0.155 ^k	0.613	0.135
85	0.971	0.129 ^d	0.410 ⁱ	0.380 ^h	0.149 ^k	0.612 ^d	0.120
86	0.972	0.140	0.459 ^g	0.384 ^g	0.140 ^k	0.611	0.105 ^g
87	0.972	0.153	0.476	0.396	0.133 ^k	0.610	0.104
88	0.973	0.166	0.493 ^g	0.408 ^g	0.124 ^k	0.609	0.0998 ^q
89	0.974	0.181	0.511	0.425	0.116 ^k	0.607	0.118
90	0.975	0.197 ^a	0.529 ^a	0.442	0.108 ^k	0.606	0.134
91	0.975	0.199	0.526	0.460 ^c	0.100 ^k	0.605	0.150
92	0.976	0.202 ^e	0.523	0.466	0.0900 ^k	0.604 ^e	0.166 ^r
93	0.976	0.208	0.520	0.472 ^h	0.0800 ^k	0.607	0.198
94	0.977	0.215 ^e	0.517 ^e	0.502 ^e	0.0700 ^k	0.610 ^e	0.229 ^s

Appendix A (continued)
FLUORESCENCE AND COSTER-KRONIG YIELDS USED IN THIS WORK

Z	Fluorescence yields			L-shell Coster-Kronig yields			
	ω_K	ω_{L_1}	ω_{L_2}	ω_{L_3}	f_{12}	f_{13}	f_{23}
95	0.978	0.216	0.530	0.515	0.0570 ^k	0.625	0.209
96	0.978	0.217 ^e	0.544 ^e	0.528 ^e	0.0420 ^k	0.640 ^e	0.188 ^t
97	0.979	0.236	0.523	0.521	0.0320 ^k	0.600	0.206
98	0.979	0.256 ^e	0.503 ^e	0.515 ^e	0.0170 ^e	0.560 ^e	0.223 ^e
99	0.980	0.264	0.510	0.504	0.0170	0.562	0.200
100	0.980	0.273 ^e	0.518 ^e	0.494 ^e	0.0170 ^e	0.564 ^e	0.176 ^e
101	0.980	0.284	0.530	0.513	0.0170	0.540	0.180
102	0.981	0.296	0.542	0.533	0.0180	0.516	0.183
103	0.981	0.308 ^e	0.554 ^e	0.553 ^e	0.0180 ^e	0.492 ^e	0.187 ^e
104	0.981	0.321	0.567	0.574	0.0180	0.468	0.191

*The values of ω_K are based on the least-squares fitted polynomial equation given by Bambynek et al. [W. Bambynek et al., *Rev. Mod. Phys.* 44: 716-813 (1972)],

$$\omega_K/(1 - \omega_K) = A + BZ + CZ^3 ,$$

where $A = 0.015$, $B = 0.0327$, and $C = -0.64 \times 10^{-6}$. The source of values of ω_{L_1} , ω_{L_2} , ω_{L_3} , f_{12} , f_{13} , and f_{23} obtained from the literature are footnoted. Values not footnoted were obtained by extrapolation or interpolation.

^aTheoretical values from E. J. McGuire, *Phys. Rev. A* 3, 587-94 (1971).

^bTheoretical values from E. J. McGuire, *Phys. Rev. A* 5: 2313-17 (1972).

^cExperimental values reported in W. Bambynek et al., *Rev. Mod. Phys.* 44: 716-813 (1972).

^dTheoretical values from B. Crasemann, M. H. Chen, and V. O. Kostroun, *Phys. Rev. A* 4: 2161-64 (1971).

^eTheoretical values from E. J. McGuire, U.S. Atomic Energy Commission CONF-720404, vol. 1 (1972), pp. 662-79.

^fExperimental and semi-theoretical values from P. L. Lee and S. I. Salem, *Phys. Rev. A* 10: 2027-32 (1974).

^gExperimental values from J. C. McGeorge, D. W. Nix, and R. W. Fink, *J. Phys. B* 6: 573-83 (1973).

^hTheoretical values from M. H. Chen, B. Crasemann, and V. O. Kostroun, *Phys. Rev. A* 4: 1-7 (1971).

ⁱTheoretical values from M. H. Chen and B. Crasemann, U.S. Atomic Energy Commission CONF-720404, vol. 1 (1972), pp. 43-58.

^jExperimental values from S. Mohan et al., U.S. Atomic Energy Commission CONF-720404, vol. 1 (1972), pp. 244-50.

^kApproximate fit to a graph of experimental and theoretical values reported in W. Bambynek et al., *Rev. Mod. Phys.* 4

ⁿWeighted average of experimental values reported in W. Bambynek et al., *Rev. Mod. Phys.* 44: 716-813 (1972); and V. R. Veluri et al., *J. Phys. B* 7: 1486-93 (1974).

^pWeighted average of experimental values reported in W. Bambynek et al., *Rev. Mod. Phys.* 44: 716-813 (1972); and R. E. Wood, J. M. Palms, and P. Venugopala Rao, *Phys. Rev. A* 5: 11-13 (1972).

^qWeighted average of experimental values reported in J. C. McGeorge, D. W. Nix, and R. W. Fink, *J. Phys. B* 6: 573-83 (1973); F. B. Gil et al., *Phys. Rev. A* 5: 536-41 (1972); and J. L. Campbell et al., *Can. J. Phys.* 52: 488-98 (1974).

^rWeighted average of experimental values reported in W. Bambynek et al., *Rev. Mod. Phys.* 44: 716-813 (1972); and F. B. Gil et al., *Phys. Rev. A* 5: 536-41 (1972).

^sWeighted average of experimental values reported in W. Bambynek et al., *Rev. Mod. Phys.* 44: 716-813 (1972); J. C. McGeorge, D. W. Nix, and R. W. Fink, *J. Phys. B* 6: 573-83 (1973); J. L. Campbell et al., *Can. J. Phys.* 52: 488-98 (1974); M. R. Zalutsky and E. S. Macias, *Phys. Rev. A* 11: 71-74 (1975); L. Salgueiro et al., *Proc. Phys. Soc.* 77: 657-64 (1961); and J. Byrne et al., *J. Phys. B* 3: 1166-74 (1970).

^tWeighted average of experimental values reported in W. Bambynek et al., *Rev. Mod. Phys.* 44: 716-813 (1972); J. C. McGeorge, D. W. Nix, and R. W. Fink, *J. Phys. B* 6: 573-83 (1973); and M. R. Zalutsky and E. S. Macias, *Phys. Rev. A* 11: 71-74 (1975).

Appendix B
K-SERIES RELATIVE X-RAY INTENSITIES USED IN THIS WORK*

Z	X-ray designation (Siegbahn notation)					
	$K_{\alpha 2}$	$K_{\alpha 3}$	$K_{\beta 1}$	$K_{\beta 2}$	$K_{\beta 3}$	$K_{\beta 5}$
5	0.500	0.0	0.0	0.0	0.0	0.0
6	0.500	0.0	0.0	0.0	0.0	0.0
7	0.500	0.0	0.0	0.0	0.0	0.0
8	0.500	0.0	0.0	0.0	0.0	0.0
9	0.501	0.0	0.0	0.0	0.0	0.0
10	0.501	1.26E-09	0.0	0.0	0.0	0.0
11	0.501	2.93E-09	0.0	0.0	0.0	0.0
12	0.501	4.59E-09	0.0	0.0	0.0	0.0
13	0.501	6.26E-09	0.0140	0.0	0.00660	0.0
14	0.501	1.00E-08	0.0296	0.0	0.0139	0.0
15	0.501	1.54E-08	0.0445	0.0	0.0225	0.0
16	0.501	2.30E-08	0.0618	0.0	0.0311	0.0
17	0.502	3.39E-08	0.0807	0.0	0.0409	0.0
18	0.502	4.96E-08	0.102	0.0	0.0518	0.0
19	0.502	6.97E-08	0.116	0.0	0.0580	0.0
20	0.502	9.62E-08	0.123	0.0	0.0631	0.0
21	0.502	1.36E-07	0.127	0.0	0.0645	4.40E-06
22	0.503	1.75E-07	0.130	0.0	0.0659	1.15E-05
23	0.503	2.32E-07	0.132	0.0	0.0668	2.17E-05
24	0.504	3.03E-07	0.129	0.0	0.0652	3.84E-05
25	0.505	3.92E-07	0.134	0.0	0.0681	5.27E-05
26	0.506	5.03E-07	0.135	0.0	0.0684	7.40E-05
27	0.507	6.37E-07	0.135	0.0	0.0688	0.000101
28	0.508	7.99E-07	0.136	0.0	0.0692	0.000132
29	0.509	1.00E-06	0.134	0.0	0.0685	0.000172
30	0.510	1.24E-06	0.137	0.0	0.0702	0.000210
31	0.512	1.54E-06	0.140	0.0	0.0718	0.000252
32	0.513	1.87E-06	0.144	0.00490	0.0734	0.000299
33	0.514	2.26E-06	0.147	0.00860	0.0751	0.000348
34	0.515	2.73E-06	0.150	0.0131	0.0770	0.000401
35	0.516	3.28E-06	0.153	0.0183	0.0785	0.000457
36	0.517	3.93E-06	0.153	0.0190	0.0786	0.000518
37	0.518	4.68E-06	0.156	0.0245	0.0800	0.000581
38	0.520	5.55E-06	0.160	0.0300	0.0814	0.000650
39	0.521	6.57E-06	0.162	0.0335	0.0829	0.000721
40	0.523	7.73E-06	0.165	0.0370	0.0844	0.000796
41	0.524	9.00E-06	0.167	0.0390	0.0892	0.000874
42	0.525	1.05E-05	0.169	0.0410	0.0939	0.000955
43	0.526	1.22E-05	0.171	0.0430	0.0936	0.00104
44	0.527	1.41E-05	0.173	0.0450	0.0933	0.00113
45	0.528	1.63E-05	0.176	0.0465	0.0929	0.00122
46	0.529	1.88E-05	0.178	0.0480	0.0926	0.00131
47	0.530	2.17E-05	0.180	0.0505	0.0923	0.00141
48	0.532	2.49E-05	0.182	0.0530	0.0934	0.00151

Appendix B (continued)
K-SERIES RELATIVE X-RAY INTENSITIES USED IN THIS WORK

X-ray designation (Siegbahn notation)					
Z	K_{α_2}	K_{α_3}	K_{β_1}	K_{β_2}	K_{β_3}
49	0.533	2.85E-05	0.183	0.0540	0.0945
50	0.534	3.26E-05	0.185	0.0550	0.0956
51	0.535	3.71E-05	0.187	0.0565	0.0965
52	0.537	4.27E-05	0.189	0.0580	0.0972
53	0.538	4.84E-05	0.190	0.0610	0.0980
54	0.539	5.40E-05	0.192	0.0640	0.0987
55	0.541	6.13E-05	0.193	0.0670	0.0995
56	0.543	6.86E-05	0.194	0.0700	0.100
57	0.544	7.90E-05	0.195	0.0730	0.101
58	0.546	8.93E-05	0.197	0.0760	0.102
59	0.548	9.97E-05	0.198	0.0795	0.102
60	0.549	0.000110	0.199	0.0830	0.103
61	0.550	0.000125	0.197	0.0845	0.102
62	0.552	0.000140	0.196	0.0860	0.101
63	0.554	0.000155	0.194	0.0875	0.100
64	0.556	0.000170	0.192	0.0890	0.0993
65	0.558	0.000190	0.195	0.0890	0.101
66	0.560	0.000210	0.198	0.0890	0.102
67	0.562	0.000235	0.200	0.0885	0.104
68	0.564	0.000260	0.202	0.0880	0.105
69	0.566	0.000280	0.205	0.0875	0.106
70	0.567	0.000300	0.207	0.0870	0.107
71	0.570	0.000330	0.209	0.0860	0.108
72	0.572	0.000360	0.212	0.0850	0.110
73	0.574	0.000395	0.214	0.0855	0.111
74	0.576	0.000430	0.216	0.0860	0.112
75	0.578	0.000470	0.219	0.0865	0.113
76	0.580	0.000510	0.222	0.0870	0.115
77	0.581	0.000570	0.224	0.0890	0.116
78	0.583	0.000630	0.226	0.0910	0.118
79	0.586	0.000695	0.227	0.0935	0.118
80	0.588	0.000760	0.228	0.0960	0.119
81	0.590	0.000835	0.228	0.0990	0.119
82	0.593	0.000910	0.228	0.102	0.119
83	0.595	0.00102	0.228	0.105	0.119
84	0.597	0.00112	0.228	0.108	0.119
85	0.600	0.00122	0.228	0.111	0.119
86	0.602	0.00132	0.228	0.113	0.119
87	0.605	0.00145	0.229	0.115	0.120
88	0.608	0.00158	0.230	0.117	0.120
89	0.610	0.00172	0.231	0.119	0.121
90	0.613	0.00185	0.232	0.120	0.122
91	0.616	0.00200	0.233	0.122	0.123
92	0.619	0.00215	0.234	0.123	0.123
					0.00865

Appendix B (continued)
K-SERIES RELATIVE X-RAY INTENSITIES USED IN THIS WORK

X-ray designation (Siegbahn notation)					
Z	K_{α_2}	K_{α_3}	K_{β_1}	K_{β_2}	K_{β_3}
93	0.622	0.00244	0.234	0.124	0.123
94	0.625	0.00273	0.234	0.125	0.124
95	0.628	0.00301	0.234	0.126	0.124
96	0.632	0.00330	0.234	0.128	0.124
97	0.637	0.00361	0.236	0.130	0.125
98	0.642	0.00391	0.238	0.132	0.126
99	0.645	0.00424	0.239	0.133	0.127
100	0.648	0.00457	0.240	0.135	0.128
101	0.652	0.00497	0.241	0.137	0.128
102	0.656	0.00540	0.242	0.138	0.129
103	0.660	0.00587	0.243	0.140	0.129
104	0.664	0.00638	0.244	0.141	0.130

*Data are normalized to K_{α_1} intensity equal 1. Z is the atomic number. The experimental data reported by Salem, Panossian, and Krause [S. I. Salem, S. L. Panossian, and R. A. Krause, At. Data Nucl. Data Tables 14: 91-109 (1974)] have been used as the basis for these data. In the case of atomic numbers for which experimental data are not available, we have used the theoretical calculations of Scofield [J. H. Scofield, Phys. Rev. A 9: 1041-49 (1974) and At. Data Nucl. Data Tables 14: 121-37 (1974)] on x-ray emission rates to obtain a relative intensity.

Appendix C
L-SERIES RELATIVE X-RAY INTENSITIES USED IN THIS WORK*

Z	L1 series			L2 series		
	L_{β_4}	L_{γ_2}	L_{γ_3}	L_{η}	L_{γ_1}	L_{γ_6}
18	0.519	0.0	0.0	0.0	0.0	0.0
19	0.521	0.0	0.0	0.0	0.0	0.0
20	0.523	0.0	0.0	0.0	0.0	0.0
21	0.525	0.0	0.0	0.0	0.0	0.0
22	0.527	0.0	0.0	0.0	0.0	0.0
23	0.528	0.0	0.0	0.0	0.0	0.0
24	0.530	0.0	0.0	0.0	0.0	0.0
25	0.532	0.0	0.0	0.0	0.0	0.0
26	0.534	0.0	0.0	0.0900	0.0	0.0
27	0.537	0.0	0.0	0.0830	0.0	0.0
28	0.540	0.0	0.0	0.0760	0.0	0.0
29	0.543	0.0	0.0	0.0720	0.0	0.0
30	0.546	0.0	0.0	0.0680	0.0	0.0
31	0.548	0.0	0.0	0.0654	0.0	0.0
32	0.551	0.0135	0.173	0.0628	0.0	0.0
33	0.554	0.0256	0.177	0.0604	0.0	0.0
34	0.557	0.0377	0.180	0.0580	0.0	0.0
35	0.559	0.0498	0.181	0.0558	0.0	0.0
36	0.562	0.0619	0.182	0.0535	0.0	0.0
37	0.565	0.0686	0.185	0.0514	0.0	0.0
38	0.569	0.0752	0.188	0.0493	0.0	0.0
39	0.572	0.0819	0.189	0.0477	0.0	0.0
40	0.575	0.0885	0.190	0.0460	0.0330	0.0
41	0.641	0.0924	0.193	0.0445	0.0440	0.0
42	0.706	0.0964	0.196	0.0430	0.0550	0.0
43	0.692	0.100	0.199	0.0415	0.0642	0.0
44	0.678	0.104	0.202	0.0400	0.0733	0.0
45	0.667	0.107	0.204	0.0388	0.0900	0.0
46	0.655	0.110	0.206	0.0375	0.107	0.0
47	0.645	0.113	0.210	0.0365	0.106	0.0
48	0.635	0.116	0.213	0.0355	0.106	0.0
49	0.628	0.120	0.217	0.0345	0.112	0.0
50	0.621	0.125	0.220	0.0335	0.118	0.0
51	0.614	0.128	0.223	0.0328	0.122	0.0
52	0.607	0.132	0.226	0.0320	0.127	0.0
53	0.603	0.136	0.230	0.0310	0.133	0.0
54	0.598	0.140	0.233	0.0300	0.140	0.0
55	0.597	0.144	0.237	0.0293	0.142	0.0
56	0.595	0.148	0.240	0.0285	0.145	0.0
57	0.594	0.151	0.243	0.0278	0.149	0.00130
58	0.592	0.154	0.246	0.0270	0.153	0.00126
59	0.593	0.156	0.250	0.0265	0.156	0.00123
60	0.594	0.159	0.254	0.0260	0.160	0.00119
61	0.597	0.161	0.259	0.0253	0.162	0.00116

Appendix C (continued)
L-SERIES RELATIVE X-RAY INTENSITIES USED IN THIS WORK

Z	L1 series			L2 series		
	L_{β_4}	L_{γ_2}	L_{γ_3}	L_{η}	L_{γ_1}	L_{γ_6}
62	0.600	0.164	0.263	0.0245	0.165	0.00112
63	0.604	0.178	0.267	0.0240	0.167	0.00109
64	0.608	0.192	0.270	0.0235	0.170	0.00105
65	0.613	0.194	0.275	0.0230	0.172	0.00101
66	0.618	0.195	0.280	0.0225	0.174	0.000980
67	0.627	0.197	0.285	0.0221	0.176	0.000940
68	0.635	0.198	0.290	0.0216	0.178	0.000900
69	0.645	0.203	0.294	0.0213	0.180	0.000860
70	0.655	0.207	0.298	0.0210	0.182	0.000830
71	0.667	0.210	0.303	0.0209	0.183	0.000790
72	0.678	0.212	0.307	0.0208	0.184	0.00290
73	0.692	0.215	0.313	0.0209	0.186	0.00500
74	0.705	0.218	0.318	0.0210	0.188	0.00720
75	0.719	0.224	0.323	0.0211	0.191	0.0119
76	0.732	0.230	0.328	0.0212	0.193	0.0165
77	0.749	0.238	0.333	0.0215	0.195	0.0203
78	0.765	0.245	0.338	0.0218	0.197	0.0240
79	0.784	0.254	0.344	0.0222	0.200	0.0275
80	0.803	0.263	0.350	0.0225	0.204	0.0310
81	0.823	0.275	0.355	0.0280	0.206	0.0338
82	0.842	0.286	0.360	0.0230	0.209	0.0365
83	0.864	0.300	0.366	0.0235	0.212	0.0390
84	0.885	0.313	0.372	0.0240	0.215	0.0415
85	0.910	0.328	0.377	0.0243	0.219	0.0435
86	0.934	0.342	0.382	0.0246	0.222	0.0455
87	0.962	0.359	0.389	0.0248	0.225	0.0471
88	0.989	0.375	0.396	0.0250	0.229	0.0487
89	1.02	0.394	0.403	0.0255	0.231	0.0495
90	1.04	0.412	0.410	0.0260	0.234	0.0502
91	1.07	0.431	0.418	0.0263	0.238	0.0507
92	1.10	0.450	0.426	0.0265	0.241	0.0512
93	1.13	0.473	0.433	0.0268	0.242	0.0514
94	1.16	0.495	0.440	0.0270	0.244	0.0516
95	1.20	0.526	0.449	0.0273	0.247	0.0518
96	1.23	0.557	0.457	0.0275	0.251	0.0520
97	1.33	0.564	0.459	0.0288	0.253	0.0532
98	1.38	0.571	0.460	0.0290	0.255	0.0541
99	1.43	0.592	0.465	0.0292	0.257	0.0552
100	1.48	0.615	0.469	0.0294	0.259	0.0563
101	1.54	0.640	0.474	0.0295	0.262	0.0574
102	1.60	0.668	0.479	0.0297	0.264	0.0584
103	1.66	0.698	0.485	0.0299	0.266	0.0597
104	1.74	0.729	0.490	0.0301	0.268	0.0611

Appendix C (continued)
L-SERIES RELATIVE X-RAY INTENSITIES USED IN THIS WORK

L3 series					
Z	L_{β_2}	L_{α_2}	L_{β_5}	L_{β_6}	L_L
21	0.0	0.111	0.0	0.0669	1.02
22	0.0	0.111	0.0	0.0294	0.456
23	0.0	0.111	0.0	0.0175	0.279
24	0.0	0.111	0.0	0.00410	0.177
25	0.0	0.111	0.0	0.00877	0.150
26	0.0	0.111	0.0	0.00674	0.0990
27	0.0	0.111	0.0	0.00538	0.0860
28	0.0	0.111	0.0	0.00442	0.0730
29	0.0	0.111	0.0	0.00136	0.0660
30	0.0	0.111	0.0	0.00315	0.0590
31	0.0	0.111	0.0	0.00382	0.0560
32	0.0	0.111	0.0	0.00417	0.0520
33	0.0	0.111	0.0	0.00443	0.0500
34	0.0	0.111	0.0	0.00463	0.0470
35	0.0	0.111	0.0	0.00481	0.0450
36	0.0	0.111	0.0	0.00496	0.0430
37	0.0	0.111	0.0	0.00529	0.0420
38	0.0	0.111	0.0	0.00561	0.0400
39	0.0	0.111	0.0	0.00581	0.0390
40	0.00700	0.111	0.0	0.00600	0.0380
41	0.0294	0.111	0.0	0.00608	0.0370
42	0.0517	0.111	0.0	0.00623	0.0360
43	0.0724	0.111	0.0	0.00635	0.0360
44	0.0930	0.111	0.0	0.00646	0.0350
45	0.106	0.111	0.0	0.00657	0.0340
46	0.118	0.111	0.0	0.00664	0.0330
47	0.131	0.111	0.0	0.00678	0.0330
48	0.143	0.111	0.0	0.00693	0.0330
49	0.152	0.111	0.0	0.00708	0.0330
50	0.160	0.111	0.0	0.00725	0.0320
51	0.170	0.111	0.0	0.00741	0.0320
52	0.180	0.111	0.0	0.00758	0.0320
53	0.187	0.111	0.0	0.00776	0.0320
54	0.194	0.111	0.0	0.00793	0.0320
55	0.200	0.111	0.0	0.00811	0.0330
56	0.207	0.111	0.0	0.00829	0.0330
57	0.208	0.111	0.00214	0.00847	0.0330
58	0.210	0.111	0.00207	0.00853	0.0330
59	0.212	0.111	0.00201	0.00865	0.0330
60	0.213	0.111	0.00194	0.00875	0.0330
61	0.212	0.111	0.00187	0.00900	0.0340
62	0.211	0.111	0.00180	0.00925	0.0340
63	0.209	0.111	0.00174	0.00960	0.0340
64	0.208	0.111	0.00167	0.00990	0.0340
65	0.207	0.111	0.00160	0.0102	0.0340

Appendix C (continued)
L-SERIES RELATIVE X-RAY INTENSITIES USED IN THIS WORK

L3 series					
Z	L_{β_2}	L_{α_2}	L_{β_5}	L_{β_6}	L_L
66	0.205	0.111	0.00154	0.0105	0.0340
67	0.203	0.111	0.00147	0.0109	0.0350
68	0.200	0.111	0.00140	0.0112	0.0350
69	0.197	0.111	0.00133	0.0115	0.0360
70	0.194	0.111	0.00127	0.0117	0.0360
71	0.204	0.111	0.00120	0.0119	0.0370
72	0.213	0.111	0.00300	0.0121	0.0370
73	0.220	0.112	0.00400	0.0123	0.0380
74	0.227	0.112	0.00500	0.0125	0.0390
75	0.231	0.112	0.00910	0.0131	0.0400
76	0.234	0.112	0.0132	0.0137	0.0400
77	0.237	0.112	0.0165	0.0140	0.0410
78	0.240	0.112	0.0198	0.0143	0.0420
79	0.242	0.112	0.0230	0.0147	0.0430
80	0.245	0.112	0.0262	0.0150	0.0430
81	0.247	0.112	0.0292	0.0153	0.0440
82	0.248	0.112	0.0321	0.0156	0.0450
83	0.250	0.112	0.0347	0.0159	0.0460
84	0.251	0.112	0.0373	0.0162	0.0470
85	0.254	0.112	0.0399	0.0165	0.0480
86	0.256	0.112	0.0425	0.0168	0.0490
87	0.258	0.112	0.0449	0.0172	0.0500
88	0.259	0.112	0.0473	0.0176	0.0510
89	0.260	0.112	0.0496	0.0179	0.0520
90	0.262	0.112	0.0518	0.0182	0.0530
91	0.263	0.112	0.0538	0.0186	0.0540
92	0.264	0.112	0.0558	0.0189	0.0550
93	0.265	0.112	0.0575	0.0192	0.0560
94	0.267	0.112	0.0592	0.0195	0.0570
95	0.268	0.112	0.0609	0.0198	0.0580
96	0.269	0.112	0.0626	0.0201	0.0590
97	0.271	0.112	0.0638	0.0205	0.0600
98	0.273	0.112	0.0646	0.0209	0.0610
99	0.274	0.112	0.0657	0.0212	0.0621
100	0.276	0.112	0.0667	0.0216	0.0631
101	0.277	0.112	0.0677	0.0220	0.0642
102	0.279	0.112	0.0687	0.0224	0.0653
103	0.281	0.112	0.0700	0.0228	0.0664
104	0.282	0.112	0.0713	0.0231	0.0676

*Data for the L1, L2, and L3 series are normalized to L_{β_3} , L_{β_1} , and L_{α_1} intensities equal to 1 respectively. The experimental data reported by Salem, Panossian, and Krause [S. I. Salem, S. L. Panossian, and R. A. Krause, At. Data Nucl. Data Tables 14: 91-109 (1974)] have been used as the basis of these data. In the case of atomic numbers for which experimental data are not available, we have used the theoretical calculations of Scofield [J. H. Scofield, Phys. Rev. A 10: 1507-10 (1974)] on x-ray emission rates to obtain a relative intensity.

Appendix D
K-SERIES RELATIVE AUGER-ELECTRON INTENSITIES USED IN THIS WORK*

Z	KL_1X	KL_2X	KL_3X	KXY
11	0.00460	0.00420	0.00740	0.0
12	0.00920	0.00840	0.0148	0.00107
13	0.0138	0.0126	0.0222	0.00213
14	0.0184	0.0168	0.0296	0.00320
15	0.0230	0.0210	0.0370	0.00427
16	0.0276	0.0252	0.0444	0.00533
17	0.0322	0.0294	0.0518	0.00640
18	0.0368	0.0336	0.0592	0.00747
19	0.0414	0.0378	0.0666	0.00853
20	0.0460	0.0420	0.0740	0.00960
21	0.0500	0.0450	0.0810	0.01116
22	0.0540	0.0480	0.0870	0.01335
23	0.0580	0.0510	0.0930	0.0154
24	0.0620	0.0540	0.0980	0.0173
25	0.0660	0.0570	0.104	0.0192
26	0.0700	0.0600	0.109	0.0210
27	0.0740	0.0630	0.114	0.0228
28	0.0780	0.0650	0.119	0.0246
29	0.0820	0.0680	0.124	0.0263
30	0.0850	0.0710	0.128	0.0280
31	0.0880	0.0730	0.133	0.0297
32	0.0910	0.0750	0.138	0.0314
33	0.0950	0.0780	0.141	0.0331
34	0.0980	0.0810	0.144	0.0347
35	0.102	0.0830	0.148	0.0363
36	0.105	0.0850	0.152	0.0379
37	0.108	0.0870	0.155	0.0395
38	0.111	0.0890	0.158	0.0410
39	0.114	0.0920	0.162	0.0425
40	0.116	0.0940	0.165	0.0440
41	0.119	0.0960	0.168	0.0455
42	0.122	0.0970	0.170	0.0470
43	0.125	0.0990	0.173	0.0484
44	0.127	0.101	0.176	0.0498
45	0.130	0.103	0.178	0.0512
46	0.133	0.104	0.180	0.0526
47	0.136	0.106	0.183	0.0540
48	0.138	0.107	0.185	0.0553
49	0.140	0.109	0.187	0.0566
50	0.142	0.111	0.189	0.0579
51	0.144	0.113	0.191	0.0592
52	0.146	0.114	0.193	0.0604
53	0.149	0.115	0.195	0.0617
54	0.151	0.116	0.196	0.0629
55	0.153	0.118	0.198	0.0641
56	0.154	0.119	0.200	0.0653
57	0.157	0.121	0.201	0.0665
58	0.159	0.122	0.202	0.0677

Appendix D (continued)
K-SERIES RELATIVE AUGER-ELECTRON INTENSITIES USED IN THIS WORK

Z	KL_1X	KL_2X	KL_3X	KXY
59	0.161	0.123	0.204	0.0688
60	0.163	0.124	0.206	0.0699
61	0.165	0.125	0.207	0.0710
62	0.166	0.126	0.208	0.0721
63	0.168	0.127	0.210	0.0732
64	0.170	0.128	0.211	0.0743
65	0.172	0.129	0.212	0.0754
66	0.173	0.130	0.212	0.0764
67	0.175	0.131	0.213	0.0774
68	0.176	0.132	0.214	0.0784
69	0.178	0.133	0.215	0.0794
70	0.179	0.134	0.215	0.0804
71	0.181	0.135	0.217	0.0814
72	0.182	0.135	0.218	0.0923
73	0.184	0.136	0.219	0.0932
74	0.185	0.137	0.219	0.0841
75	0.186	0.138	0.220	0.0850
76	0.187	0.138	0.220	0.0859
77	0.189	0.139	0.221	0.0868
78	0.190	0.140	0.222	0.0877
79	0.191	0.141	0.223	0.0886
80	0.192	0.142	0.223	0.0894
81	0.194	0.142	0.223	0.0903
82	0.195	0.142	0.223	0.0911
83	0.196	0.143	0.224	0.0919
84	0.197	0.143	0.225	0.0927
85	0.198	0.144	0.225	0.0935
86	0.199	0.145	0.225	0.0942
87	0.200	0.145	0.226	0.0958
88	0.201	0.145	0.226	0.0958
89	0.202	0.145	0.226	0.0965
90	0.203	0.145	0.226	0.0972
91	0.204	0.146	0.227	0.0980
92	0.205	0.147	0.227	0.0987
93	0.206	0.147	0.227	0.0994
94	0.207	0.148	0.228	0.100
95	0.208	0.148	0.228	0.100
96	0.209	0.148	0.228	0.101
97	0.210	0.149	0.228	0.102
98	0.211	0.149	0.228	0.102
99	0.212	0.149	0.228	0.103
100	0.213	0.150	0.229	0.103
101	0.214	0.150	0.229	0.104
102	0.215	0.150	0.229	0.104
103	0.216	0.151	0.229	0.105
104	0.217	0.151	0.229	0.105

*These data are based on values reported by Bambynek et al. [W. Bambynek et al., Rev. Mod. Phys. 44: 769 (1972).] Extrapolations and interpolations have been made to obtain data for every atomic number.

Appendix E
KLL AUGER TRANSITION PROBABILITIES (IN MULTIPLES OF
 10^{-3} A.U.) USED IN THIS WORK FOR $Z < 29^*$

Z	KL_1L_1	KL_1L_2	KL_1L_3	KL_2L_2	KL_2L_3	KL_3L_3
6	0.693	0.444	0.138	0.0700	1.08	0.0
7	0.712	0.770	0.226	0.150	1.94	0.0
8	0.731	1.17	0.325	0.270	3.01	0.0
9	0.750	1.63	0.438	0.410	4.29	0.0
10	0.769	2.17	0.562	0.590	5.79	0.0
11	0.788	2.37	0.599	0.690	6.43	0.00500
12	0.807	2.58	0.636	0.780	7.06	0.0100
13	0.826	2.79	0.673	0.877	7.70	0.0200
14	0.845	3.00	0.713	0.986	8.36	0.0390
15	0.864	3.21	0.747	1.07	8.98	0.0610
16	0.890	3.36	0.782	1.13	9.50	0.0900
17	0.917	3.49	0.812	1.17	9.90	0.135
18	0.955	3.63	0.840	1.21	10.3	0.208
19	0.972	3.75	0.864	1.25	10.6	0.285
20	0.992	3.87	0.883	1.29	10.9	0.406
21	1.02	3.96	0.902	1.29	11.1	0.544
22	1.04	4.04	0.919	1.28	11.3	0.695
23	1.07	4.14	0.940	1.27	11.4	0.895
24	1.10	4.20	0.964	1.25	11.5	1.11
25	1.12	4.28	0.996	1.23	11.6	1.33
26	1.15	4.32	1.03	1.19	11.7	1.57
27	1.20	4.37	1.08	1.15	11.7	1.82
28	1.25	4.41	1.12	1.12	11.7	2.03

*These data are based on the theoretical calculations in intermediate coupling of Chen and Crasemann [M. H. Chen and B. Crasemann, *Phys. Rev. A* 8: 7-13 (1973).] at $Z = 13, 15, 18, 20, 23$, and 28 . Data for other atomic numbers were obtained by interpolation and extrapolation. The KL_1L_2 column includes contributions from both the 1P_1 and 3P_0 configurations; the KL_1L_3 column includes contributions from both the 3P_1 and 3P_2 configurations; the KL_3L_3 column includes contributions from both the 3P_0 and 3P_2 configurations.

Appendix F
L-SERIES RELATIVE AUGER-ELECTRON INTENSITIES USED IN THIS WORK*

Z	L1 series		L2 series		L3 series	
	L_1MX	L_1XY	L_2MX	L_2XY	L_3MX	L_3XY
21	0.0	0.0	0.0238	0.0	0.0	0.0
22	0.0	0.0	0.0322	0.0	0.0	0.0
23	0.0	0.0	0.0407	0.0	0.0	0.0
24	0.0	0.0	0.0487	0.0	0.0220	0.0
25	0.0	0.0	0.0565	0.0	0.0435	0.0
26	0.0	0.0	0.0642	0.0	0.0640	0.0
27	0.0	0.0	0.0687	0.0	0.0684	0.0
28	0.0	0.0	0.0731	0.0	0.0729	0.0
29	0.0	0.0	0.0781	0.0	0.0770	0.0
30	0.0	0.0	0.0874	0.0	0.0975	0.0
31	0.0	0.0	0.0965	0.0	0.118	0.0
32	0.0898	0.0	0.106	0.00188	0.137	0.0
33	0.177	0.00710	0.158	0.00550	0.157	0.00566
34	0.244	0.0154	0.207	0.0111	0.214	0.0142
35	0.310	0.0236	0.261	0.0190	0.269	0.0223
36	0.375	0.0317	0.317	0.0292	0.321	0.0301
37	0.404	0.0372	0.361	0.0374	0.346	0.0349
38	0.432	0.0426	0.379	0.0416	0.370	0.0395
39	0.461	0.0479	0.397	0.0455	0.393	0.0437
40	0.489	0.0532	0.414	0.0494	0.415	0.0481
41	0.492	0.0549	0.416	0.0499	0.421	0.0489
42	0.495	0.0566	0.419	0.0505	0.426	0.0496
43	0.498	0.0583	0.422	0.0517	0.429	0.0503
44	0.502	0.0600	0.426	0.0529	0.433	0.0511
45	0.505	0.0617	0.429	0.0541	0.436	0.0519
46	0.508	0.0633	0.433	0.0553	0.439	0.0525
47	0.511	0.0649	0.436	0.0564	0.442	0.0532
48	0.520	0.0662	0.446	0.0577	0.455	0.0568
49	0.528	0.0675	0.456	0.0589	0.467	0.0603
50	0.536	0.0687	0.466	0.0600	0.479	0.0637
51	0.573	0.0763	0.477	0.0645	0.491	0.0670
52	0.597	0.0835	0.487	0.0690	0.513	0.0728
53	0.622	0.0908	0.498	0.0732	0.534	0.0786
54	0.646	0.0981	0.508	0.0776	0.555	0.0843
55	0.671	0.105	0.518	0.0819	0.575	0.0898
56	0.695	0.113	0.529	0.0860	0.596	0.0954
57	0.687	0.110	0.539	0.0860	0.592	0.0941
58	0.679	0.108	0.550	0.0860	0.588	0.0927
59	0.672	0.106	0.560	0.0860	0.584	0.0915
60	0.664	0.104	0.570	0.0861	0.580	0.0901
61	0.668	0.105	0.576	0.0899	0.585	0.0924
62	0.671	0.106	0.582	0.0939	0.589	0.0947
63	0.675	0.107	0.587	0.0977	0.594	0.0971
64	0.678	0.108	0.593	0.102	0.598	0.0993

Appendix F (continued)
L-SERIES RELATIVE AUGER-ELECTRON INTENSITIES USED IN THIS WORK

Z	L1 series		L2 series		L3 series	
	L ₁ MX	L ₁ XY	L ₂ MX	L ₂ XY	L ₃ MX	L ₃ XY
65	0.682	0.110	0.599	0.105	0.602	0.102
66	0.685	0.111	0.600	0.104	0.604	0.102
67	0.689	0.112	0.600	0.103	0.606	0.102
68	0.695	0.113	0.601	0.102	0.608	0.102
69	0.702	0.114	0.602	0.101	0.610	0.102
70	0.708	0.115	0.603	0.1000	0.612	0.102
71	0.708	0.114	0.604	0.0989	0.614	0.102
72	0.709	0.113	0.605	0.0979	0.616	0.102
73	0.709	0.112	0.606	0.0969	0.618	0.102
74	0.709	0.112	0.607	0.0958	0.620	0.102
75	0.710	0.114	0.611	0.0967	0.624	0.103
76	0.711	0.116	0.616	0.0978	0.628	0.104
77	0.712	0.118	0.620	0.0987	0.633	0.105
78	0.714	0.120	0.625	0.0997	0.637	0.106
79	0.715	0.122	0.629	0.101	0.642	0.108
80	0.716	0.124	0.634	0.102	0.646	0.109
81	0.719	0.125	0.638	0.103	0.651	0.110
82	0.723	0.126	0.642	0.105	0.655	0.112
83	0.726	0.126	0.646	0.106	0.660	0.113
84	0.729	0.127	0.650	0.107	0.664	0.115
85	0.733	0.128	0.655	0.109	0.669	0.117
86	0.736	0.129	0.659	0.110	0.673	0.117
87	0.739	0.129	0.664	0.110	0.678	0.117
88	0.740	0.130	0.668	0.111	0.682	0.118
89	0.742	0.131	0.673	0.112	0.687	0.118
90	0.744	0.131	0.677	0.113	0.691	0.118
91	0.747	0.132	0.682	0.114	0.695	0.118
92	0.749	0.133	0.686	0.114	0.699	0.119
93	0.752	0.133	0.691	0.115	0.704	0.119
94	0.754	0.134	0.696	0.116	0.708	0.119
95	0.758	0.135	0.700	0.117	0.712	0.119
96	0.760	0.136	0.705	0.118	0.716	0.119
97	0.763	0.137	0.709	0.119	0.719	0.120
98	0.766	0.137	0.714	0.120	0.723	0.120
99	0.768	0.138	0.719	0.121	0.727	0.120
100	0.771	0.139	0.723	0.122	0.731	0.120
101	0.773	0.140	0.728	0.123	0.735	0.120
102	0.776	0.141	0.733	0.124	0.738	0.121
103	0.780	0.142	0.738	0.125	0.742	0.121
104	0.783	0.142	0.743	0.126	0.746	0.121

*These data are based on the theoretical values calculated in $j-j$ coupling by Rao, Chen, and Crasemann [P. Venugopala Rao, M. H. Chen, and B. Crasemann, *Phys. Rev. A* 5: 997-1012 (1972)]. Each L_i series is normalized to an intensity of 1 for the L_iMM Auger transition. Extrapolations and interpolations have been made to obtain data for every atomic number.

Appendix G
EXAMPLES OF OUTPUT FROM SUBROUTINE BALAN

DECAY of 3 H 1

ENERGY AND INTENSITY BALANCE DATA

LEVEL ENERGY (MEV)	INTENSITY ENTERING LEVEL	INTENSITY LEAVING LEVEL	PERCENT ERROR
--------------------------	--------------------------------	-------------------------------	------------------

INTENSITY TO GROUND AND ISOMERIC STATE(S) OF DAUGHTER(S) = 1.000E+02
TOTAL INTENSITY FROM PARENT = 1.000E+02
PERCENT ERROR = 0.000E-01

TOTAL INTENSITY FROM PARENT = 1.000E+02
VALUE IS WITHIN 0.00E-01% OF 100

TOTAL ENERGY AVAILABLE = 1.860E-02 MEV
TOTAL ENERGY CONTENT OF ALL RADIATIONS = 1.860E-02 MEV
PERCENT ERROR = 0.000E-01

DECAY OF 35 S 16

ENERGY AND INTENSITY BALANCE DATA

LEVEL ENERGY (MEV)	INTENSITY ENTERING LEVEL	INTENSITY LEAVING LEVEL	PERCENT ERROR
--------------------------	--------------------------------	-------------------------------	------------------

WARNING: NORMALIZATION RECORD WAS MISSING!!
PHOTON NORMALIZING FACTOR WAS SET TO DEFAULT VALUE OF 1.

INTENSITY TO GROUND AND ISOMERIC STATE(S) OF DAUGHTER(S) = 1.000E+02
TOTAL INTENSITY FROM PARENT = 1.000E+02
PERCENT ERROR = 0.000E-01

TOTAL INTENSITY FROM PARENT = 1.000E+02
VALUE IS WITHIN 0.00E-01% of 100

TOTAL ENERGY AVAILABLE = 1.675E-01 MEV
TOTAL ENERGY CONTENT OF ALL RADIATIONS = 1.675E-01 MEV
PERCENT ERROR = 0.000E-01

Appendix G (continued)
EXAMPLES OF OUTPUT FROM SUBROUTINE BALAN

DECAY OF 99M TO 43

ENERGY AND INTENSITY BALANCE DATA

LEVEL ENERGY (MEV)	INTENSITY ENTERING LEVEL	INTENSITY LEAVING LEVEL	PERCENT ERROR
1.4047E-01	9.9020E+01	9.9020E+01	0.0000E-01
1.4265E-01	1.0000E+02	1.0000E+02	0.0000E-01

INTENSITY TO GROUND AND ISOMERIC STATE(S) OF DAUGHTER(S) = 1.000E+02

TOTAL INTENSITY FROM PARENT = 1.000E+02

PERCENT ERROR = 0.000E-01

TOTAL INTENSITY FROM PARENT = 1.000E+02

VALUE IS WITHIN 0.00E-01% OF 100

TOTAL ENERGY AVAILABLE = 1.426E-01 MEV

TOTAL ENERGY CONTENT OF ALL RADIATIONS = 1.426E-01 MEV

PERCENT ERROR = 5.359E-03

DECAY OF 144 CE 58

ENERGY AND INTENSITY BALANCE DATA

LEVEL ENERGY (MEV)	INTENSITY ENTERING LEVEL	INTENSITY LEAVING LEVEL	PERCENT ERROR
8.0120E-02	5.6820E+00	5.7251E+00	7.5641E-01
9.9960E-02	1.4311E+00	1.9067E+00	2.8499E+01 *****
1.3353E-01	1.9580E+01	1.9571E+01	4.6437E-02

INTENSITY TO GROUND AND ISOMERIC STATE(S) OF DAUGHTER(S) = 1.005E+02

TOTAL INTENSITY FROM PARENT = 1.000E+02

PERCENT ERROR = 5.071E-01

TOTAL INTENSITY FROM PARENT = 1.000E+02

VALUE IS WITHIN 0.00E-01% OF 100

TOTAL ENERGY AVAILABLE = 3.148E-01 MEV

TOTAL ENERGY CONTENT OF ALL RADIATIONS = 3.154E-01 MEV

PERCENT ERROR = 1.760E-01

Appendix H
EXAMPLES OF OUTPUT FROM SUBROUTINE TABIPU

INPUT DATA
14-CARBON-6 HALFLIFE = 5730 YEARS 26-AUG-78

MODE OF DECAY: BETA MINUS

TYPE OF TRANSITION	MEAN NUMBER/ TRANSFOR- MATION	TRANSITION ENERGY (MEV)	OTHER NUCLEAR PARAMETERS
BETA MINUS	1	1.00E+00	1.565E-01* ALLOWED

* ENDPOINT ENERGY (MEV)

REFERENCE: EVALUATED NUCLEAR STRUCTURE DATA FILE (ENSDF)
NUCLEAR DATA PROJECT, OAK RIDGE NATIONAL LABORATORY
DATE DATA WERE ENTERED INTO ENSDF: 13-OCT-77

INPUT DATA
15-OXYGEN-8 HALFLIFE = 123 SECONDS 26-AUG-78

MODES OF DECAY: ELECTRON CAPTURE, BETA PLUS

TYPE OF TRANSITION	MEAN NUMBER/ TRANSFOR- MATION	TRANSITION ENERGY (MEV)	OTHER NUCLEAR PARAMETERS
ELECT. CAPTURE	1	1.13E-03	2.754E+00 ALLOWED
BETA PLUS	1	9.99E-01	1.732E+00* ALLOWED

* ENDPOINT ENERGY (MEV)

REFERENCE: EVALUATED NUCLEAR STRUCTURE DATA FILE (ENSDF)
NUCLEAR DATA PROJECT, OAK RIDGE NATIONAL LABORATORY
DATE DATA WERE ENTERED INTO ENSDF: 12-JUL-75

Appendix H (continued)
EXAMPLES OF OUTPUT FROM SUBROUTINE TABIPU

INPUT DATA
85-KRYPTON-36 HALFLIFE = 10.72 YEARS 26-AUG-78

MODE OF DECAY: BETA MINUS

TYPE OF TRANSITION	MEAN NUMBER/ TRANSFOR- MATION	TRANSITION ENERGY (MEV)	OTHER NUCLEAR PARAMETERS
BETA MINUS 1	4.30E-03	1.730E-01*	ALLOWED
BETA MINUS 2	9.96E-01	6.870E-01*	UNIQUE FIRST FORBIDDEN
I.C.E. + GAMMA 1	4.33E-03	5.140E-01	M2 MULTIPOLE AK=0.00630

* ENDPOINT ENERGY (MEV)

REFERENCE: EVALUATED NUCLEAR STRUCTURE DATA FILE (ENSDF)
NUCLEAR DATA PROJECT, OAK RIDGE NATIONAL LABORATORY
DATE DATA WERE ENTERED INTO ENSDF: 12-JUL-75

INPUT DATA
99M-TECHNETIUM-43 HALFLIFE = 6.02 HOURS 26-AUG-78

MODE OF DECAY: ISOMERIC LEVEL

TYPE OF TRANSITION	MEAN NUMBER/ TRANSFOR- MATION	TRANSITION ENERGY (MEV)	OTHER NUCLEAR PARAMETERS
I.C.E. + GAMMA 1	9.90E-01	2.174E-03	E3 MULTIPOLE AK= 0.0 AL1=0.0 AL2=0.0 AL3=0.0 AM= 9.23E+10 AN+=7.68E+09
I.C.E. + GAMMA 2	9.90E-01	1.405E-01	M1+E2 MULTIPOLE MRS=0.0139 AK= 0.0988 AL1=0.0109 AM= 0.00216
I.C.E. + GAMMA 3	9.80E-03	1.427E-01	M4 MULTIPOLE AK= 29.5 AL1=4.99 AL2=1.04 AL3=3.16 AM= 1.79 AN+=0.352

REFERENCE: EVALUATED NUCLEAR STRUCTURE DATA FILE (ENSDF)
NUCLEAR DATA PROJECT, OAK RIDGE NATIONAL LABORATORY
DATE DATA WERE ENTERED INTO ENSDF: 29-MAR-78

Appendix H (continued)
EXAMPLES OF OUTPUT FROM SUBROUTINE TABIPU

INPUT DATA
144-CERIUM-58 HALFLIFE = 284.3 DAYS 26-AUG-78

MODE OF DECAY: BETA MINUS

TYPE OF TRANSITION	MEAN NUMBER/ TRANSFOR- MATION	TRANSITION ENERGY (MEV)	OTHER NUCLEAR PARAMETERS
BETA MINUS 1	1.96E-01	1.819E-01*	FIRST FORBIDDEN
BETA MINUS 2	4.60E-02	2.353E-01*	FIRST FORBIDDEN
BETA MINUS 3	7.58E-01	3.154E-01*	FIRST FORBIDDEN
I.C.E. + GAMMA 1	1.43E-02	3.357E-02	M1 MULTIPOLE AK= 0.0 AL1=3.41 AL2=0.292 AL3=0.0605 AM= 0.788 AN+=0.215
I.C.E. + GAMMA 2	1.78E-02	4.093E-02	M1 MULTIPOLE MRS=0.000225 AK= 0.0 AL1=1.90 AL2=0.165 AL3=0.0391 AM= 0.441 AN+=0.120
I.C.E. + GAMMA 3	1.09E-02	5.341E-02	M1 MULTIPOLE MRS=0.00360 AK= 6.88 AL1=0.869 AL2=0.0921 AL3=0.0402 AM= 0.210 AN+=0.0575
I.C.E. + GAMMA 4	2.90E-03	6.600E-02	M1 MULTIPOLE ASSUMED AK= 3.71 AL1=0.469 AL2=0.0380 AL3=0.00771 AM= 0.108 AN+=0.0296
I.C.E. + GAMMA 5	5.73E-02	8.012E-02	M1 MULTIPOLE AK= 2.12 AL1=0.267 AL2=0.0212 AL3=0.00429 AM= 0.0613 AN+=0.0168
I.C.E. + GAMMA 6	1.31E-02	8.650E-02	M1+E2 MULTIPOLE AK= 2.38 AL1=0.300 AL2=0.0237 AL3=0.00477 AM= 0.0690 AN+=0.0189
I.C.E. + GAMMA 7	1.18E-02	9.100E-02	M1+E2 MULTIPOLE AK= 2.04 AL1=0.257 AL2=0.0202 AL3=0.00406 AM= 0.0591 AN+=0.0162
I.C.E. + GAMMA 8	1.25E-03	9.995E-02	E2 MULTIPOLE AK = 1.23 AL1=0.110 AL2=0.291 AL3=0.315 AM= 0.160 AN+=0.0417
I.C.E. + GAMMA 9	1.71E-01	1.335E-01	M1 MULTIPOLE AK= 0.493 AL1=0.0622 AL2=0.00462 AM= 0.0142 AN+=0.00389

* ENDPOINT ENERGY (MEV)

REFERENCE: EVALUATED NUCLEAR STRUCTURE DATA FILE (ENSDF)
NUCLEAR DATA PROJECT, OAK RIDGE NATIONAL LABORATORY
DATE DATA WERE ENTERED INTO ENSDF: 05-MAY-77

Appendix H (continued)
EXAMPLES OF OUTPUT FROM SUBROUTINE TABIPU

INPUT DATA			
252-CALIFORNIUM-98	HALFLIFE = 2.638 YEARS	26-AUG-78	
MODES OF DECAY: SPONT. FISSION, ALPHA			
TYPE OF TRANSITION	MEAN NUMBER/ TRANSFOR- MATION	TRANSITION ENERGY (MEV)	OTHER NUCLEAR PARAMETERS
SPONT. FISSION	3.09E-02		NEUTRONS/FISSION = 3.73
ALPHA 1	5.81E-07	5.707E+00	
ALPHA 2	1.94E-05	5.920E+00	
ALPHA 3	2.32E-03	6.073E+00	
ALPHA 4	1.52E-01	6.174E+00	
ALPHA 5	8.15E-01	6.217E+00	
I.C.E. + GAMMA 1	1.52E-01	4.340E-02	E2 MULTIPOLE AK= 0.0 AL1=14.8 AL2=396. AL3=328. AM= 207. AN+=81.7
I.C.E. + GAMMA 2	1.06E-03	1.002E-01	M1 MULTIPOLE ASSUMED AK= 0.0 AL1=4.92 AL2=0.624 AL3=0.0221 AM= 1.36 AN+=0.522
I.C.E. + GAMMA 3	1.93E-04	1.600E-01	M1 MULTIPOLE ASSUMED AK= 7.02 AL1=1.28 AL2=0.167 AL3=0.00548 AM= 0.356 AN+=0.135

REFERENCE: EVALUATED NUCLEAR STRUCTURE DATA FILE (ENSDF)
NUCLEAR DATA PROJECT, OAK RIDGE NATIONAL LABORATORY
DATE DATA WERE ENTERED INTO ENSDF: 26-AUG-77

Appendix I
EXAMPLES OF THE OUTPUT DECAY SCHEME DATA

OUTPUT DATA			
3-HYDROGEN-1	HALFLIFE = 12.35 YEARS	26-AUG-78	
MODE OF DECAY: BETA MINUS			
TYPE OF RADIATION	MEAN NUMBER/ TRANSFOR- MATION	ENERGY (MEV)	MEV / TRANSFOR- MATION
BETA MINUS	1	1.00E+00	5.683E-03*
ALL LISTED BETAS, INTERNAL CONVERSION AND AUGER ELECTRONS			5.68E-03
ALL LISTED RADIATIONS			5.68E-03
* AVERAGE ENERGY (MEV)			
DAUGHTER NUCLIDE, 3-HELIUM GROUND STATE, IS STABLE.			

INPUT DATA SOURCE: EVALUATED NUCLEAR STRUCTURE DATA FILE (ENSDF)			
NUCLEAR DATA PROJECT, OAK RIDGE NATIONAL LABORATORY.			
DATE INPUT DATA WERE ENTERED INTO ENSDF: 13-OCT-77			
14-CARBON-6	**OUTPUT DATA**	HALFLIFE = 5730 YEARS	26-AUG-78
MODE OF DECAY: BETA MINUS			
TYPE OF RADIATION	MEAN NUMBER/ TRANSFOR- MATION	ENERGY (MEV)	MEV / TRANSFOR- MATION
BETA MINUS	1	1.00E+00	4.945E-02*
ALL LISTED BETAS, INTERNAL CONVERSION AND AUGER ELECTRONS			4.95E-02
ALL LISTED RADIATIONS			4.95E-02
* AVERAGE ENERGY (MEV)			
DAUGHTER NUCLIDE, 14-NITROGEN GROUND STATE, IS STABLE.			

INPUT DATA SOURCE: EVALUATED NUCLEAR STRUCTURE DATA FILE (ENSDF)			
NUCLEAR DATA PROJECT, OAK RIDGE NATIONAL LABORATORY.			
DATE INPUT DATA WERE ENTERED INTO ENSDF: 13-OCT-77			

Appendix I (continued)
EXAMPLES OF THE OUTPUT DECAY SCHEME DATA

OUTPUT DATA						
85-KRYPTON-36		HALFLIFE = 10.72 YEARS		26-AUG-78		
MODE OF DECAY: BETA MINUS						
TYPE OF RADIATION	MEAN NUMBER/ TRANSFOR- MATION	ENERGY (MEV)	MEV/ TRANSFOR- MATION			
BETA MINUS	1	4.30E-03	4.753E-02*	2.04E-04		
BETA MINUS	2	9.96E-01	2.514E-01*	2.50E-01		
GAMMA-RAY	1	4.30E-03	5.140E-01	2.21E-03		
ALL LISTED X-RAYS, GAMMA-RAYS AND ANNIHILATION RADIATION			2.21E-03			
ALL NEGLECTED X-RAYS, GAMMA-RAYS AND ANNIH. RADIATION**			2.48E-07			
ALL LISTED BETAS, INTERNAL CONVERSION AND AUGER ELECTRONS			2.51E-01			
ALL NEGLECTED BETAS, INT. CONVERSION AND AUGER ELECTRONS**			1.55E-05			
ALL LISTED RADIATIONS			2.53E-01			
ALL NEGLECTED RADIATIONS**			1.58E-05			

* AVERAGE ENERGY (MEV)

** EACH NEGLECTED TRANSITION CONTRIBUTES LESS THAN 0.010%
TO THE TOTAL MEV/TRANSFORMATION FOR THIS CATEGORY.

DAUGHTER NUCLIDE, 85-RUBIDIUM GROUND STATE, IS STABLE.

INPUT DATA SOURCE: EVALUATED NUCLEAR STRUCTURE DATA FILE (ENSDF)
NUCLEAR DATA PROJECT, OAK RIDGE NATIONAL LABORATORY.
DATE INPUT DATA WERE ENTERED INTO ENSDF: 12-JUL-75

OUTPUT DATA						
125-IODINE-53		HALFLIFE = 60.14 DAYS		26-AUG-78		
MODE OF DECAY: ELECTRON CAPTURE						
TYPE OF RADIATION	MEAN NUMBER/ TRANSFOR- MATION	ENERGY (MEV)	MEV/ TRANSFOR- MATION			
GAMMA-RAY	1	6.67E-02	3.549E-02	2.37E-03		
K SHELL CONVERSION ELECTRON	8.03E-01	3.678E-03	2.95E-03			
L1 SHELL CONVERSION ELECTRON	9.53E-02	3.055E-02	2.91E-03			
L2 SHELL CONVERSION ELECTRON	7.65E-03	3.088E-02	2.36E-04			
L3 SHELL CONVERSION ELECTRON	1.91E-03	3.115E-02	5.96E-05			
M SHELL CONVERSION ELECTRON	2.09E-02	3.467E-02*	7.25E-04			

Appendix I (continued)
EXAMPLES OF THE OUTPUT DECAY SCHEME DATA

N+ SHELL CONVERSION ELECTRON	4.96E-03	3.549E-02*	1.76E-04
K-ALPHA1 X-RAY	7.41E-01	2.747E-02	2.04E-02
K-ALPHA2 X-RAY	3.98E-01	2.720E-02	1.08E-02
K-BETA1 X-RAY	1.40E-01	3.100E-02	4.34E-03
K-BETA2 X-RAY	4.30E-02	3.171E-02	1.36E-03
K-BETA3 X-RAY	7.20E-02	3.094E-02	2.23E-03
K-BETA5 X-RAY	1.44E-03	3.124E-02	4.51E-05
L-ALPHA X-RAY	6.29E-02	3.768E-03*	2.37E-04
L-BETA X-RAY	5.96E-02	4.093E-03*	2.44E-04
L-GAMMA X-RAY	7.48E-03	4.673E-03*	3.49E-05
KLL AUGER ELECTRON	1.32E-01	2.254E-02*	2.97E-03
KLX AUGER ELECTRON	5.97E-02	2.635E-02*	1.57E-03
KXY AUGER ELECTRON	7.95E-03	3.013E-02*	2.40E-04
LMM AUGER ELECTRON	1.01E+00	3.086E-03*	3.11E-03
LMX AUGER ELECTRON	5.17E-01	3.855E-03*	1.99E-03
LXY AUGER ELECTRON	7.33E-02	4.386E-03*	3.21E-04
MXY AUGER ELECTRON	2.99E+00	6.986E-04*	2.09E-03
RESIDUAL LOW ENERGY	6.22E-01	5.577E-05*	3.47E-05

ALL LISTED X-RAYS, GAMMA-RAYS AND ANNIHILATION RADIATION
ALL NEGLECTED X-RAYS, GAMMA-RAYS AND ANNIH. RADIATION**
ALL LISTED BETAS, INTERNAL CONVERSION AND AUGER ELECTRONS
ALL LISTED RADIATIONS
ALL NEGLECTED RADIATIONS**

* AVERAGE ENERGY (MEV)

** EACH NEGLECTED TRANSITION CONTRIBUTES LESS THAN 0.010%
TO THE TOTAL MEV/TRANSFORMATION FOR THIS CATEGORY.
DAUGHTER NUCLIDE, 125-TELLURIUM GROUND STATE, IS STABLE.

INPUT DATA SOURCE: EVALUATED NUCLEAR STRUCTURE DATA FILE (ENSDF)
NUCLEAR DATA PROJECT, OAK RIDGE NATIONAL LABORATORY.
DATE INPUT DATA WERE ENTERED INTO ENSDF: 17-JUN-78

There are two examples of ^{125}I data. The above uses the option of summing over individual x-ray or Auger-electron components of similar energy.

Appendix I (continued)
EXAMPLES OF THE OUTPUT DECAY SCHEME DATA

OUTPUT DATA			
125-IODINE-53	HALFLIFE = 60.14 DAYS	26-AUG-78	
MODE OF DECAY: ELECTRON CAPTURE			
TYPE OF RADIATION	MEAN NUMBER/ TRANSFOR- MATION	MEV/ ENERGY (MEV)	MEV/ TRANSFOR- MATION
GAMMA-RAY	1	6.67E-02	3.549E-02
K SHELL CONVERSION ELECTRON		8.03E-01	3.678E-03
L1 SHELL CONVERSION ELECTRON		9.53E-02	3.055E-02
L2 SHELL CONVERSION ELECTRON		7.65E-03	3.088E-02
L3 SHELL CONVERSION ELECTRON		1.91E-03	3.115E-02
M SHELL CONVERSION ELECTRON		2.09E-02	3.467E-02*
N+ SHELL CONVERSION ELECTRON		4.96E-03	3.549E-02*
K-ALPHA1 X-RAY		7.41E-01	2.747E-02
K-ALPHA2 X-RAY		3.98E-01	2.720E-02
K-BETA1 X-RAY		1.40E-01	3.100E-02
K-BETA2 X-RAY		4.30E-02	3.171E-02
K-BETA3 X-RAY		7.20E-02	3.094E-02
K-BETA5 X-RAY		1.44E-03	3.124E-02
L-ALPHA1 X-RAY		5.66E-02	3.769E-03
L-ALPHA2 X-RAY		6.30E-03	3.759E-03
L-BETA1 X-RAY		3.58E-02	4.030E-03
L-BETA2 X-RAY		1.02E-02	4.302E-03
L-BETA3 X-RAY		8.18E-03	4.120E-03
L-BETA4 X-RAY		4.96E-03	4.070E-03
L-GAMMA1 X-RAY		4.55E-03	4.572E-03
L-GAMMA2 X-RAY		1.08E-03	4.829E-03
L-GAMMA3 X-RAY		1.85E-03	4.829E-03
KL1L1 AUGER ELECTRON		1.37E-02	2.181E-02
KL1L1 AUGER ELECTRON		2.00E-02	2.215E-02
KL1L3 AUGER ELECTRON		1.78E-02	2.241E-02
KL2L2 AUGER ELECTRON		4.14E-03	2.244E-02
KL2L3 AUGER ELECTRON		5.32E-02	2.272E-02
KL3L3 AUGER ELECTRON		2.29E-02	2.300E-02
KL1X AUGER ELECTRON		1.92E-02	2.601E-02*
KL2X AUGER ELECTRON		1.50E-02	2.634E-02*
KL3X AUGER ELECTRON		2.54E-02	2.661E-02*
KXY AUGER ELECTRON		7.95E-03	3.013E-02*
L1MM AUGER ELECTRON		9.35E-02	3.553E-03*
L1MX AUGER ELECTRON		5.58E-02	4.318E-03*
L1XY AUGER ELECTRON		7.80E-03	4.850E-03*
L2MM AUGER ELECTRON		2.77E-01	3.226E-03*
L2MX AUGER ELECTRON		1.35E-01	3.990E-03*
L2XY AUGER ELECTRON		1.91E-02	4.523E-03*

Appendix I (continued)
EXAMPLES OF THE OUTPUT DECAY SCHEME DATA

L3MM AUGER ELECTRON	6.36E-01	2.956E-03*	1.88E-03
L3MX AUGER ELECTRON	3.26E-01	3.720E-03*	1.21E-03
L3XY AUGER ELECTRON	4.63E-02	4.252E-03*	1.97E-04
MXY AUGER ELECTRON	2.99E+00	6.986E-04*	2.09E-03
RESIDUAL LOW ENERGY	6.22E-01	5.577E-05*	3.47E-05

ALL LISTED X-RAYS, GAMMA-RAYS AND ANNIHILATION RADIATION	4.20E-02
ALL NEGLECTED X-RAYS, GAMMA-RAYS AND ANNIH. RADIATION**	6.83E-06
ALL LISTED BETAS, INTERNAL CONVERSION AND AUGER ELECTRONS	1.94E-02
ALL LISTED RADIATIONS	6.14E-02
ALL NEGLECTED RADIATIONS**	6.83E-06

* AVERAGE ENERGY (MEV)

** EACH NEGLECTED TRANSITION CONTRIBUTES LESS THAN 0.010%
TO THE TOTAL MEV/TRANSFORMATION FOR THIS CATEGORY.
DAUGHTER NUCLIDE, 125-TELLURIUM GROUND STATE, IS STABLE.

INPUT DATA SOURCE: EVALUATED NUCLEAR STRUCTURE DATA FILE (ENSDF)
NUCLEAR DATA PROJECT, OAK RIDGE NATIONAL LABORATORY.
DATE INPUT DATA WERE ENTERED INTO ENSDF: 17-JUN-78

There are two examples of ^{125}I data. The above uses the option of showing separately every individual x-ray or Auger-electron component.

OUTPUT DATA

252-CALIFORNIUM-98	HALFLIFE = 2.638 YEARS	26-AUG-78
--------------------	------------------------	-----------

MODES OF DECAY: SPONT. FISSION, ALPHA

TYPE OF RADIATION	MEAN NUMBER/ TRANSFOR- MATION	MEV/ ENERGY (MEV)	MEV/ TRANSFOR- MATION
SPONTANEOUS FISSION NEUTRON	1.15E-01	2.164E+00*	2.50E-01
SPONTANEOUS FISSION FRAGMENT	6.18E-02	9.514E+01*	5.88E+00
SPONT. FISSION PROMPT GAMMA	2.67E-01	8.847E-01*	2.36E-01
SPONT. FISSION DELAYED GAMMA	2.51E-01	9.578E-01*	2.41E-01
SPONTANEOUS FISSION BETA	1.92E-01	1.280E+00*	2.46E-01
ALPHA	3	2.32E-03	5.977E+00
RECOIL ATOM		2.32E-03	9.646E-02
ALPHA	4	1.52E-01	6.076E+00
RECOIL ATOM		1.52E-01	9.806E-02
ALPHA	5	8.15E-01	6.118E+00
RECOIL ATOM		8.15E-01	9.875E-02
GAMMA-RAY	1	1.48E-04	4.340E-02

Appendix I (continued)
EXAMPLES OF THE OUTPUT DECAY SCHEME DATA

L1 SHELL CONVERSION ELECTRON	2.19E-03	1.894E-02	4.15E-05
L2 SHELL CONVERSION ELECTRON	5.87E-02	1.962E-02	1.15E-03
L3 SHELL CONVERSION ELECTRON	4.86E-02	2.447E-02	1.19E-03
M SHELL CONVERSION ELECTRON	3.07E-02	3.860E-02*	1.19E-03
N+ SHELL CONVERSION ELECTRON	1.21E-02	4.340E-02*	5.26E-04
GAMMA-RAY	2	1.26E-04	1.002E-01
L1 SHELL CONVERSION ELECTRON	6.20E-04	7.574E-02	4.69E-05
L2 SHELL CONVERSION ELECTRON	7.86E-05	7.642E-02	6.01E-06
M SHELL CONVERSION ELECTRON	1.72E-04	9.540E-02*	1.64E-05
N+ SHELL CONVERSION ELECTRON	6.58E-05	1.002E-01*	6.59E-06
GAMMA-RAY	3	1.94E-05	1.600E-01
K SHELL CONVERSION ELECTRON	1.36E-04	3.178E-02	4.32E-06
L1 SHELL CONVERSION ELECTRON	2.48E-05	1.355E-01	3.36E-06
M SHELL CONVERSION ELECTRON	6.89E-06	1.552E-01*	1.07E-06
K-ALPHA1 X-RAY	6.25E-05	1.093E-01	6.83E-06
K-ALPHA2 X-RAY	3.95E-05	1.044E-01	4.12E-06
K-BETA1 X-RAY	1.46E-05	1.234E-01	1.80E-06
K-BETA2 X-RAY	7.99E-06	1.272E-01	1.02E-06
K-BETA3 X-RAY	7.73E-06	1.223E-01	9.46E-07
L-ALPHA X-RAY	2.47E-02	1.493E-02*	3.69E-04
L-BETA X-RAY	3.23E-02	1.921E-02*	6.21E-04
L-GAMMA X-RAY	7.49E-03	2.300E-02*	1.72E-04
L-ETA X-RAY	6.63E-04	1.749E-02	1.16E-05
L-L X-RAY	1.31E-05	1.264E-02	1.66E-07
LMM AUGER ELECTRON	2.47E-02	1.173E-02*	2.89E-04
LMX AUGER ELECTRON	1.76E-02	1.572E-02*	2.76E-04
LXY AUGER ELECTRON	2.93E-03	1.884E-02*	5.53E-05
MXY AUGER ELECTRON	1.48E-01	4.371E-03*	6.45E-04
RESIDUAL LOW ENERGY	4.80E-02	1.006E-03*	4.83E-05
ALL LISTED X-RAYS, GAMMA-RAYS AND ANNIHILATION RADIATION	1.21E-03		
ALL NEGLECTED X-RAYS, GAMMA-RAYS AND ANNIH. RADIATION**	9.45E-08		
ALL LISTED BETAS, INTERNAL CONVERSION AND AUGER ELECTRONS	5.49E-03		
ALL NEGLECTED BETAS, INT. CONVERSION AND AUGER ELECTRONS**	1.37E-06		
ALL LISTED ALPHA PARTICLES AND RECOIL NUCLEI	5.92E+00		
ALL NEGLECTED ALPHA PARTICLES AND RECOIL NUCLEI**	1.18E-04		
ALL LISTED RADIATIONS	1.25E+01		
ALL NEGLECTED RADIATIONS**	1.19E-04		

* AVERAGE ENERGY (MEV)

** EACH NEGLECTED TRANSITION CONTRIBUTES LESS THAN 0.010%
TO THE TOTAL MEV/TRANSFORMATION FOR THIS CATEGORY.

DAUGHTER NUCLIDE, 248-CURIUM GROUND STATE, IS RADIOACTIVE
AND WILL CONTRIBUTE ADDITIONALLY TO DOSE.

INPUT DATA SOURCE: EVALUATED NUCLEAR STRUCTURE DATA FILE (ENSDF)
NUCLEAR DATA PROJECT, OAK RIDGE NATIONAL LABORATORY.
DATE INPUT DATA WERE ENTERED INTO ENSDF: 26-AUG-77

Appendix J
EXAMPLES OF BETA SPECTRA GENERATED BY PROGRAM EDISTR

14-CARBON-6		HALFLIFE = 5730 YEARS		26-AUG-78	
BETA SPECTRUM DATA FOR ALL DECAY BRANCHES					
ENERGY (MEV)	BETAS PER PER DECAY	ENERGY (MEV)	BETAS PER PER DECAY	ENERGY (MEV)	BETAS PER PER DECAY
0.00000	9.910E+00	0.00120	9.816E+00	0.01500	1.145E+01
0.00010	9.900E+00	0.00130	9.817E+00	0.01600	1.150E+01
0.00011	9.898E+00	0.00140	9.821E+00	0.01800	1.158E+01
0.00012	9.897E+00	0.00150	9.826E+00	0.02000	1.163E+01
0.00013	9.896E+00	0.00160	9.832E+00	0.02200	1.166E+01
0.00014	9.895E+00	0.00180	9.850E+00	0.02400	1.166E+01
0.00015	9.894E+00	0.00200	9.871E+00	0.02600	1.164E+01
0.00016	9.893E+00	0.00220	9.897E+00	0.02800	1.159E+01
0.00018	9.891E+00	0.00240	9.925E+00	0.03000	1.153E+01
0.00020	9.889E+00	0.00260	9.955E+00	0.03200	1.146E+01
0.00022	9.887E+00	0.00280	9.986E+00	0.03600	1.125E+01
0.00024	9.885E+00	0.00300	1.002E+01	0.04000	1.099E+01
0.00026	9.882E+00	0.00320	1.005E+01	0.04500	1.060E+01
0.00028	9.880E+00	0.00360	1.012E+01	0.05000	1.015E+01
0.00030	9.878E+00	0.00400	1.019E+01	0.05500	9.648E+00
0.00032	9.876E+00	0.00450	1.028E+01	0.06000	9.102E+00
0.00036	9.872E+00	0.00500	1.036E+01	0.06500	8.522E+00
0.00040	9.867E+00	0.00550	1.044E+01	0.07000	7.917E+00
0.00045	9.862E+00	0.00600	1.052E+01	0.07500	7.293E+00
0.00050	9.857E+00	0.00650	1.060E+01	0.08000	6.658E+00
0.00055	9.852E+00	0.00700	1.067E+01	0.08500	6.019E+00
0.00060	9.848E+00	0.00750	1.074E+01	0.09000	5.381E+00
0.00065	9.843E+00	0.00800	1.081E+01	0.10000	4.135E+00
0.00070	9.839E+00	0.00850	1.087E+01	0.11000	2.971E+00
0.00075	9.835E+00	0.00900	1.093E+01	0.12000	1.935E+00
0.00080	9.831E+00	0.01000	1.105E+01	0.13000	1.075E+00
0.00085	9.827E+00	0.01100	1.115E+01	0.14000	4.380E-01
0.00090	9.824E+00	0.01200	1.124E+01	0.15000	7.106E-02
0.00100	9.819E+00	0.01300	1.132E+01	0.15648	0.000E-01
0.00110	9.816E+00	0.01400	1.139E+01		

AVERAGE BETA ENERGY = 4.945E-02

TOTAL BETAS PER DECAY FOR ALL BRANCHES = 1.000E+00

Appendix J (continued)
EXAMPLES OF BETA SPECTRA GENERATED BY PROGRAM EDISTR

15-OXYGEN-8

HALFLIFE = 123 SECONDS

26-AUG-78

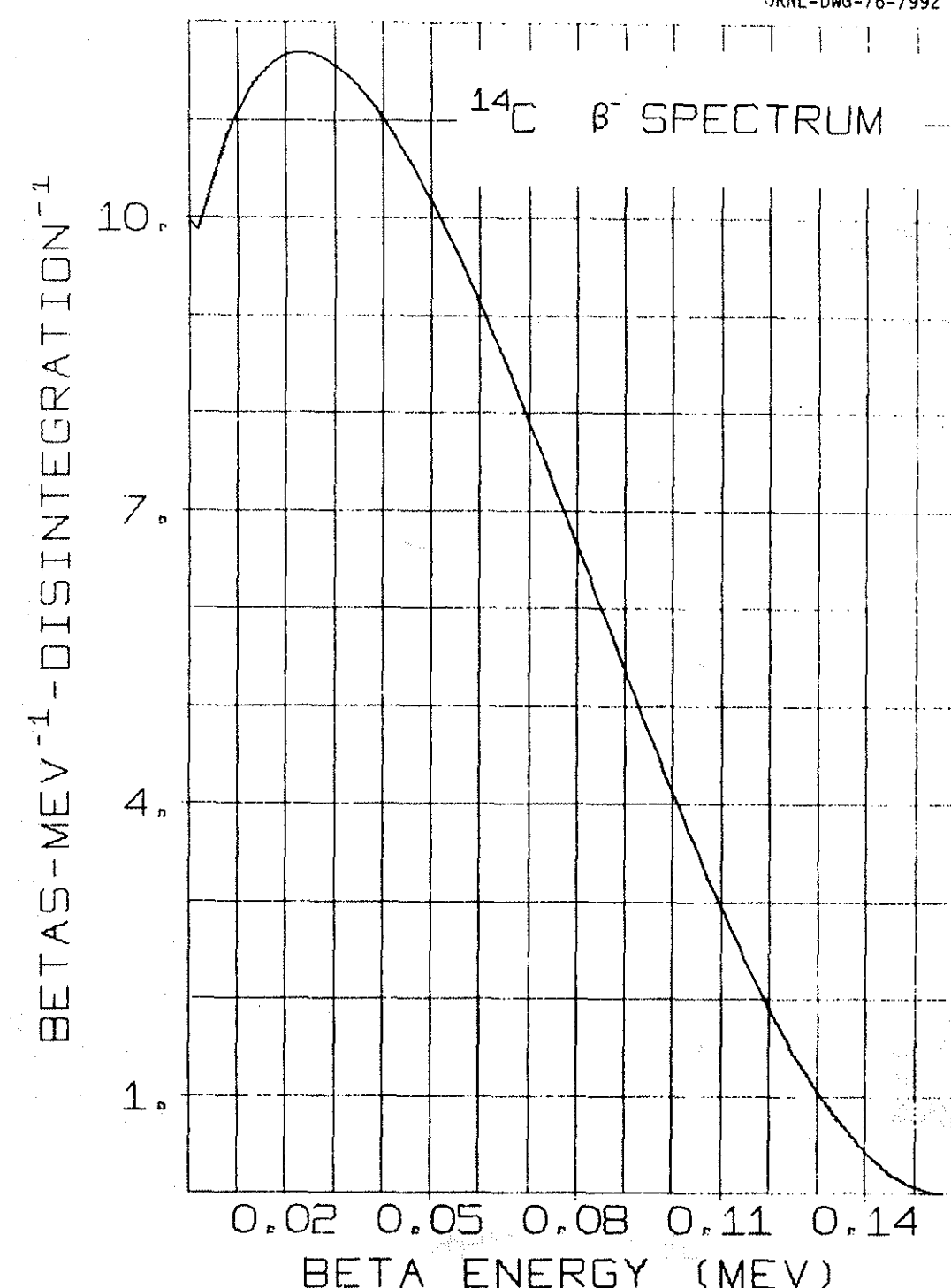
BETA SPECTRUM DATA FOR ALL DECAY BRANCHES

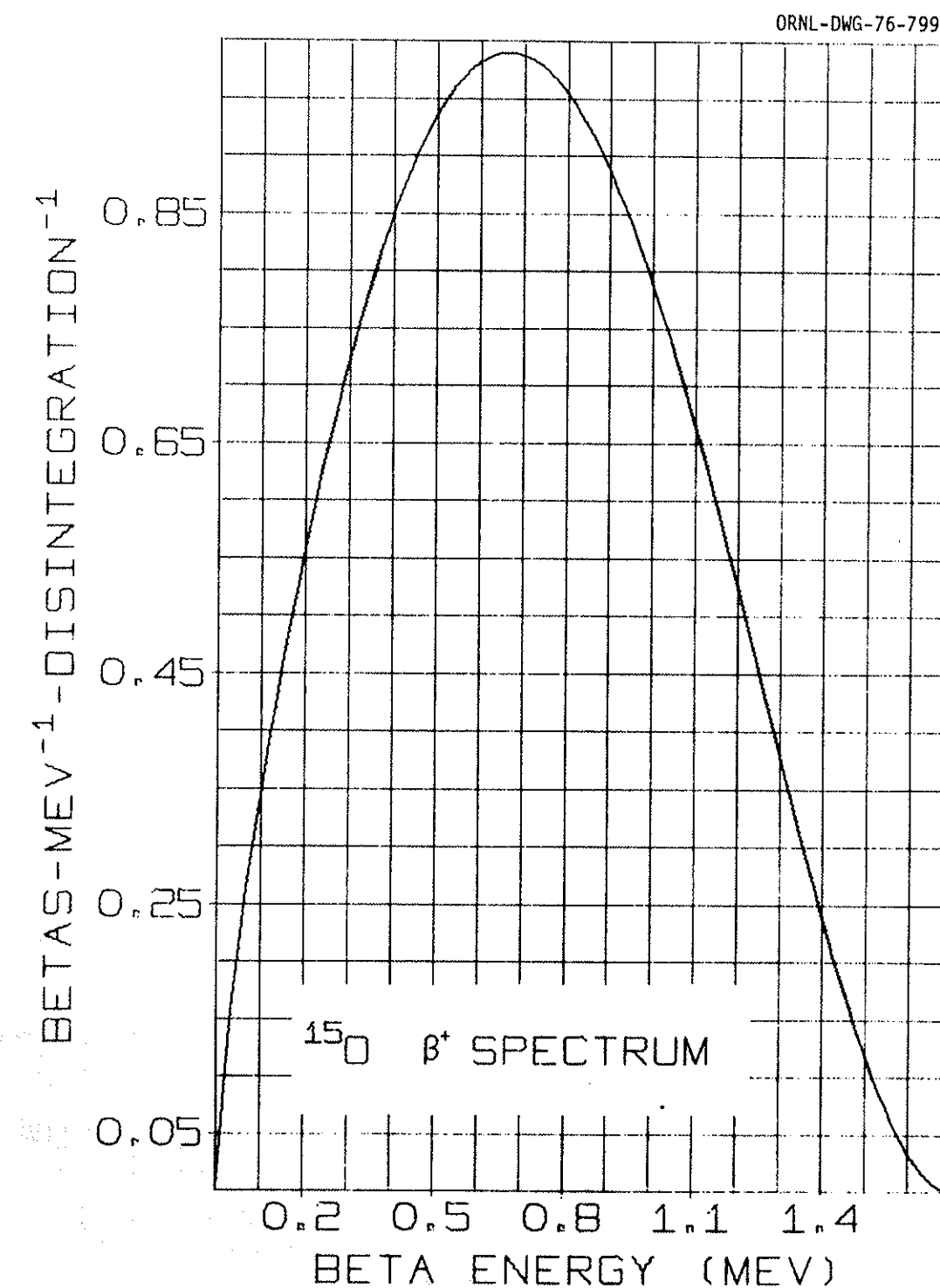
ENERGY (MEV)	BETAS PER MEV PER DECAY	ENERGY (MEV)	BETAS PER MEV PER DECAY	ENERGY (MEV)	BETAS PER MEV PER DECAY
0.00000	0.0000E-01	0.00260	1.042E-02	0.07500	2.706E-01
0.00010	1.873E-08	0.00280	1.171E-02	0.08000	2.834E-01
0.00011	3.981E-08	0.00300	1.300E-02	0.08500	2.958E-01
0.00012	7.685E-08	0.00320	1.429E-02	0.09000	3.080E-01
0.00013	1.373E-07	0.00360	1.686E-02	0.10000	3.317E-01
0.00014	2.303E-07	0.00400	1.940E-02	0.11000	3.546E-01
0.00015	3.664E-07	0.00450	2.253E-02	0.12000	3.769E-01
0.00016	5.592E-07	0.00500	2.561E-02	0.13000	3.985E-01
0.00018	1.163E-06	0.00550	2.863E-02	0.14000	4.195E-01
0.00020	2.162E-06	0.00600	3.160E-02	0.15000	4.400E-01
0.00022	3.691E-06	0.00650	3.452E-02	0.16000	4.600E-01
0.00024	5.876E-06	0.00700	3.738E-02	0.18000	4.985E-01
0.00026	8.858E-06	0.00750	4.019E-02	0.20000	5.354E-01
0.00028	1.277E-05	0.00800	4.296E-02	0.22000	5.707E-01
0.00030	1.775E-05	0.00850	4.568E-02	0.24000	6.044E-01
0.00032	2.390E-05	0.00900	4.836E-02	0.26000	6.366E-01
0.00036	4.018E-05	0.01000	5.359E-02	0.28000	6.674E-01
0.00040	6.237E-05	0.01100	5.867E-02	0.30000	6.967E-01
0.00045	9.950E-05	0.01200	6.362E-02	0.32000	7.246E-01
0.00050	1.480E-04	0.01300	6.843E-02	0.36000	7.759E-01
0.00055	2.088E-04	0.01400	7.313E-02	0.40000	8.215E-01
0.00060	2.825E-04	0.01500	7.773E-02	0.45000	8.700E-01
0.00065	3.695E-04	0.01600	8.222E-02	0.50000	9.092E-01
0.00070	4.703E-04	0.01800	9.093E-02	0.55000	9.388E-01
0.00075	5.850E-04	0.02000	9.931E-02	0.60000	9.588E-01
0.00080	7.133E-04	0.02200	1.074E-01	0.65000	9.692E-01
0.00085	8.553E-04	0.02400	1.152E-01	0.70000	9.702E-01
0.00090	1.010E-03	0.02600	1.228E-01	0.75000	9.618E-01
0.00100	1.359E-03	0.02800	1.302E-01	0.80000	9.444E-01
0.00110	1.753E-03	0.03000	1.374E-01	0.85000	9.184E-01
0.00120	2.190E-03	0.03200	1.445E-01	0.90000	8.842E-01
0.00130	2.663E-03	0.03600	1.581E-01	1.00000	7.936E-01
0.00140	3.167E-03	0.04000	1.712E-01	1.10000	6.784E-01
0.00150	3.697E-03	0.04500	1.869E-01	1.20000	5.462E-01
0.00160	4.251E-03	0.05000	2.020E-01	1.30000	4.058E-01
0.00180	5.411E-03	0.05500	2.165E-01	1.40000	2.682E-01
0.00200	6.622E-03	0.06000	2.306E-01	1.50000	1.456E-01
0.00220	7.869E-03	0.06500	2.443E-01	1.60000	5.205E-02
0.00240	9.137E-03	0.07000	2.576E-01	1.73180	0.0000E-01

AVERAGE BETA ENERGY = 7.353E-01

TOTAL BETAS PER DECAY FOR ALL BRANCHES = 9.989E-01

ORNL-DWG-76-7992





Appendix K
EXAMPLES OF DECAY SCHEME DATA IN COMPUTER
RETRIEVABLE FORMAT

125.	IODINE	53.	6.014E+01 DAYS	47 EC	26-AUG-78	125.I 53.	0
1 1	6.67142E+00	3.54919E-02	3.54919E-02	0.00000E-01		125.I 53.	1
6 1	8.02591E+01	3.67810E-03	3.67810E-03	0.00000E-01		125.I 53.	2
6 5	9.52601E+00	3.05527E-02	3.05527E-02	0.00000E-01		125.I 53.	3
6 6	7.64725E-01	3.08799E-02	3.08799E-02	0.00000E-01		125.I 53.	4
6 7	1.91444E-01	3.11505E-02	3.11505E-02	0.00000E-01		125.I 53.	5
6 3	2.09118E+00	3.46732E-02	3.46732E-02	0.00000E-01		125.I 53.	6
6 4	4.96142E-01	3.54919E-02	3.54919E-02	0.00000E-01		125.I 53.	7
2 1	7.40800E+01	2.74724E-02	2.74724E-02	0.00000E-01		125.I 53.	8
2 2	3.97809E+01	2.72018E-02	2.72018E-02	0.00000E-01		125.I 53.	9
2 3	3.16322E-03	2.68746E-02	2.68746E-02	0.00000E-01		125.I 53.	10
2 4	1.40011E+01	3.09951E-02	3.09951E-02	0.00000E-01		125.I 53.	11
2 5	4.29664E+00	3.17101E-02	3.17101E-02	0.00000E-01		125.I 53.	12
2 6	7.20057E+00	3.09441E-02	3.09441E-02	0.00000E-01		125.I 53.	13
2 7	1.44456E-01	3.12373E-02	3.12373E-02	0.00000E-01		125.I 53.	14
2 9	5.65657E+00	3.76930E-03	3.76930E-03	2.00000E+00		125.I 53.	15
210	6.29577E-01	3.75890E-03	3.75890E-03	2.00000E+00		125.I 53.	16
212	3.58233E+00	4.02950E-03	4.02950E-03	2.00000E+00		125.I 53.	17
213	1.01818E+00	4.30160E-03	4.30160E-03	2.00000E+00		125.I 53.	18
214	8.17864E-01	4.12050E-03	4.12050E-03	2.00000E+00		125.I 53.	19
215	4.96444E-01	4.06950E-03	4.06950E-03	2.00000E+00		125.I 53.	20
217	4.28768E-02	4.17310E-03	4.17310E-03	2.00000E+00		125.I 53.	21
219	4.54956E-01	4.57220E-03	4.57220E-03	2.00000E+00		125.I 53.	22
220	1.07958E-01	4.82900E-03	4.82900E-03	2.00000E+00		125.I 53.	23
221	1.84837E-01	4.82900E-03	4.82900E-03	2.00000E+00		125.I 53.	24
224	1.14635E-01	3.60600E-03	3.60600E-03	0.00000E-01		125.I 53.	25
225	1.81010E-03	3.33540E-03	3.33540E-03	0.00000E-01		125.I 53.	26
727	1.36751E+00	2.18130E-02	2.18130E-02	2.00000E+00		125.I 53.	27
728	2.00157E+00	2.21478E-02	2.21478E-02	2.00000E+00		125.I 53.	28
729	1.78062E+00	2.24080E-02	2.24080E-02	2.00000E+00		125.I 53.	29
730	4.14493E-01	2.24440E-02	2.24440E-02	2.00000E+00		125.I 53.	30
731	5.31897E+00	2.27220E-02	2.27220E-02	2.00000E+00		125.I 53.	31
732	2.28557E+00	2.29984E-02	2.29984E-02	2.00000E+00		125.I 53.	32
734	1.92263E+00	2.60140E-02	2.60140E-02	2.00000E+00		125.I 53.	33
735	1.50124E+00	2.63412E-02	2.63412E-02	2.00000E+00		125.I 53.	34
736	2.54156E+00	2.66118E-02	2.66118E-02	2.00000E+00		125.I 53.	35
738	7.95391E-01	3.01345E-02	3.01345E-02	0.00000E-01		125.I 53.	36
740	9.34830E+00	3.55330E-03	3.55330E-03	2.00000E+00		125.I 53.	37
741	5.58470E+00	4.31750E-03	4.31750E-03	2.00000E+00		125.I 53.	38
742	7.80149E-01	4.84980E-03	4.84980E-03	2.00000E+00		125.I 53.	39
743	2.77333E+01	3.22610E-03	3.22610E-03	2.00000E+00		125.I 53.	40
744	1.35158E+01	3.99030E-03	3.99030E-03	2.00000E+00		125.I 53.	41
745	1.91295E+00	4.52260E-03	4.52260E-03	2.00000E+00		125.I 53.	42
746	6.36234E+01	2.95550E-03	2.95550E-03	2.00000E+00		125.I 53.	43
747	3.26257E+01	3.71970E-03	3.71970E-03	2.00000E+00		125.I 53.	44
748	4.63482E+00	4.25200E-03	4.25200E-03	2.00000E+00		125.I 53.	45
753	2.99148E+02	6.98609E-04	6.98609E-04	0.00000E-01		125.I 53.	46
754	6.22443E+01	5.57654E-05	5.57654E-05	0.00000E-01		125.I 53.	47

Appendix K (continued)
 EXAMPLES OF DECAY SCHEME DATA OUTPUT IN COMPUTER
 RETRIEvable FORMAT

3.	HYDROGEN	1. 1.235E+01	YEARS	1 B-	26-AUG-78	3.H 1. 0
5 1	1.00000E+02	5.68295E-03	1.86000E-02	0.00000E-01		3.H 1. 1
14.	CARBON	6. 5.730E+03	YEARS	1 B-	26-AUG-78	14.C 6. 0
5 1	1.00000E+02	4.94543E-02	1.56478E-01	0.00000E-01		14.C 6. 1
15.	OXYGEN	8. 1.230E+02	SECONDS	9 EC B+	26-AUG-78	15.0 8. 0
4 1	9.98870E+01	7.35330E-01	1.73180E+00	0.00000E-01		15.0 8. 1
3 3	1.99774E+02	5.11000E-01	5.11000E-01	0.00000E-01		15.0 8. 2
2 1	2.64721E-04	3.92400E-04	3.92400E-04	0.00000E-01		15.0 8. 3
2 2	1.32361E-04	3.92400E-04	3.92400E-04	0.00000E-01		15.0 8. 4
727	2.11093E-02	3.56000E-04	3.56000E-04	2.00000E+00		15.0 8. 5
728	2.28289E-02	3.62000E-04	3.62000E-04	2.00000E+00		15.0 8. 6
729	6.70044E-03	3.69000E-04	3.69000E-04	2.00000E+00		15.0 8. 7
730	4.44719E-03	3.73000E-04	3.73000E-04	2.00000E+00		15.0 8. 8
731	5.75170E-02	3.75000E-04	3.75000E-04	2.00000E+00		15.0 8. 9
35.	SULPHUR	16. 8.744E+01	DAYS	1 B-	26-AUG-78	35.S 16. 0
5 1	1.00000E+02	4.88318E-02	1.67470E-01	0.00000E-01		35.S 16. 1
252.	CALIFORNIUM	98. 2.638E+00	YEARS	67 SF A	26-AUG-78	252.CF98. 0
9 1	3.09200E+00	3.73000E+00	3.73000E+00	0.00000E-01		252.CF98. 1
8 1	5.80623E-05	5.61645E+00	9.06468E-02	0.00000E-01		252.CF98. 2
8 2	1.93541E-03	5.82607E+00	9.40300E-02	0.00000E-01		252.CF98. 3
8 3	2.32249E-01	5.97664E+00	9.64601E-02	0.00000E-01		252.CF98. 4
8 4	1.51930E+01	6.07564E+00	9.80579E-02	0.00000E-01		252.CF98. 5
8 5	8.14808E+01	6.11835E+00	9.87473E-02	0.00000E-01		252.CF98. 6
1 1	1.48269E-02	4.33990E-02	4.33990E-02	0.00000E-01		252.CF98. 7
6 5	2.19182E-01	1.89390E-02	1.89390E-02	0.00000E-01		252.CF98. 8
6 6	5.87101E+00	1.96200E-02	1.96200E-02	0.00000E-01		252.CF98. 9
6 7	4.85996E+00	2.44690E-02	2.44690E-02	0.00000E-01		252.CF98. 10
6 3	3.07134E+00	3.86020E-02	3.86020E-02	0.00000E-01		252.CF98. 11
6 4	1.21194E+00	4.33990E-02	4.33990E-02	0.00000E-01		252.CF98. 12
1 2	1.25980E-02	1.00200E-01	1.00200E-01	0.00000E-01		252.CF98. 13
6 5	6.19845E-02	7.57400E-02	7.57400E-02	0.00000E-01		252.CF98. 14
6 6	7.86103E-03	7.64210E-02	7.64210E-02	0.00000E-01		252.CF98. 15
6 7	2.78926E-04	8.12700E-02	8.12700E-02	0.00000E-01		252.CF98. 16
6 3	1.71830E-02	9.54030E-02	9.54030E-02	0.00000E-01		252.CF98. 17
6 4	6.57589E-03	1.00200E-01	1.00200E-01	0.00000E-01		252.CF98. 18
1 3	1.93816E-03	1.60000E-01	1.60000E-01	0.00000E-01		252.CF98. 19
6 1	1.36057E-02	3.17800E-02	3.17800E-02	0.00000E-01		252.CF98. 20
6 5	2.47797E-03	1.35540E-01	1.35540E-01	0.00000E-01		252.CF98. 21
6 6	3.22766E-04	1.36221E-01	1.36221E-01	0.00000E-01		252.CF98. 22
6 7	1.06230E-05	1.41070E-01	1.41070E-01	0.00000E-01		252.CF98. 23
6 3	6.89091E-04	1.55203E-01	1.55203E-01	0.00000E-01		252.CF98. 24
6 4	2.62441E-04	1.60000E-01	1.60000E-01	0.00000E-01		252.CF98. 25
2 1	6.24558E-03	1.09290E-01	1.09290E-01	0.00000E-01		252.CF98. 26
2 2	3.94721E-03	1.04441E-01	1.04441E-01	0.00000E-01		252.CF98. 27
2 3	2.06104E-05	1.03760E-01	1.03760E-01	0.00000E-01		252.CF98. 28
2 4	1.46147E-03	1.23423E-01	1.23423E-01	0.00000E-01		252.CF98. 29

Appendix K (continued)
 EXAMPLES OF DECAY SCHEME DATA OUTPUT IN COMPUTER
 RETRIEvable FORMAT

2 5	7.99434E-04	1.27193E-01	1.27193E-01	0.00000E-01	252.CF98. 30
2 6	7.73203E-04	1.22325E-01	1.22325E-01	0.00000E-01	252.CF98. 31
2 7	5.88958E-05	1.24128E-01	1.24128E-01	0.00000E-01	252.CF98. 32
2 9	2.21982E+00	1.49590E-02	1.49590E-02	2.00000E+00	252.CF98. 33
210	2.48176E-01	1.47030E-02	1.47030E-02	2.00000E+00	252.CF98. 34
212	2.41091E+00	1.95520E-02	1.95520E-02	2.00000E+00	252.CF98. 35
213	5.97797E-01	1.80601E-02	1.80601E-02	2.00000E+00	252.CF98. 36
214	1.89881E-02	1.96630E-02	1.96630E-02	2.00000E+00	252.CF98. 37
215	2.33554E-02	1.85650E-02	1.85650E-02	2.00000E+00	252.CF98. 38
216	1.38961E-01	1.88156E-02	1.88156E-02	2.00000E+00	252.CF98. 39
217	4.46183E-02	1.72870E-02	1.72870E-02	2.00000E+00	252.CF98. 40
219	6.04415E-01	2.28606E-02	2.28606E-02	2.00000E+00	252.CF98. 41
220	1.05764E-02	2.30200E-02	2.30200E-02	2.00000E+00	252.CF98. 42
221	8.67756E-03	2.33060E-02	2.33060E-02	2.00000E+00	252.CF98. 43
222	1.25367E-01	2.36580E-02	2.36580E-02	2.00000E+00	252.CF98. 44
224	6.63000E-02	1.74910E-02	1.74910E-02	0.00000E-01	252.CF98. 45
225	1.30969E-03	1.26420E-02	1.26420E-02	0.00000E-01	252.CF98. 46
727	3.52638E-05	7.87300E-02	7.87300E-02	2.00000E+00	252.CF98. 47
728	6.73327E-05	7.96524E-02	7.96524E-02	2.00000E+00	252.CF98. 48
729	1.92444E-05	8.42837E-02	8.42837E-02	2.00000E+00	252.CF98. 49
730	4.76675E-06	8.04800E-02	8.04800E-02	2.00000E+00	252.CF98. 50
731	3.82565E-05	8.51300E-02	8.51300E-02	2.00000E+00	252.CF98. 51
732	1.26510E-05	8.98013E-02	8.98013E-02	2.00000E+00	252.CF98. 52
734	3.71007E-05	9.88280E-02	9.88280E-02	2.00000E+00	252.CF98. 53
735	2.62723E-05	9.95090E-02	9.95090E-02	2.00000E+00	252.CF98. 54
736	4.04735E-05	1.04358E-01	1.04358E-01	2.00000E+00	252.CF98. 55
738	1.79645E-05	1.18491E-01	1.18491E-01	0.00000E-01	252.CF98. 56
740	1.51190E-02	1.55252E-02	1.55252E-02	2.00000E+00	252.CF98. 57
741	1.14968E-02	1.95302E-02	1.95302E-02	2.00000E+00	252.CF98. 58

Appendix L
EXAMPLES OF INPUT DECAY SCHEME DATA FOR EDISTR
FORMATTED ACCORDING TO THE ENSDF SYSTEM

14N	14C B- DECAY	NBS-MJM	771013
14N	N 0.0	0+	1.0
14C	P 0.0	0+	5730 Y 40
14N	L 0.0	1+	STABLE
14N	B	100	9.040 3
15N	15O B+ DECAY	NBS-MJM	780329
15O	P 0.0	1/2-	122.24 S 16
15N	L 0.0	1/2-	STABLE
15N	E 2753.8	7 99.887	6 0.113
			6 8.640 1
35CL	35S B- DECAY	NBS-MJM	771227
35S	P 0.0	3/2+	87.44 D 7
35CL	L 0.0	3/2+	STABLE
35CL	B	100	5.010 2
3HE	3H B- DECAY	NBS-MJM	771013
3HE	N	1.0	
3H	P 0.0	1/2+	12.35 Y 1
3HE	L 0.0	1/2+	STABLE
3HE	B 18.60	2 100.0	3.05
85RB	85KR B- DECAY (10.72 Y)	NBS-MJM	750712
85RB	N 1.00		
85KR	P 0.0	9/2+	10.72 Y 1
85RB	L 0.0	5/2-	STABLE
85RB	B 687	2 99.57	1
85RB	L 513.99	1 9/2+	9.445 7
85RB	B 173	2 0.43	1
85RB	G 513.99	1 0.43	9.51 2
99TC	99TC IT DECAY (6.02 H)	NBS-MJM	780329
99TC	N 1.0		
99TC	L 0.0	9/2+	STABLE
99TC	L 140.474	11 (7/2)+	
99TC	G 140.466	15 88.97	24 M1+F2
99TC	L 142.648	11 (1/2)-	-0.118 6
99TC	G 142.674	4 0.0	0.113 3 99.02
99TC	G 142.675	25 0.0241	14 M4
125TE	125I EC DECAY	NBS-MJM	780617
125TE	N 1.0	1.0	1.0
125I	P 0.0	5/2+	60.14 D 11
125TE	L 0.0	1/2+	STABLE
125TE	L 35.4919	5 3/2+	
125TE	E 142.5	20	100
125TE	G 35.4919	5 6.67	22 M1(+E2) C.003 LT

Appendix L (continued)
EXAMPLES OF INPUT DECAY SCHEME DATA FOR EDISTR
FORMATTED ACCORDING TO THE ENSDF SYSTEM

144PR	144CE R- DECAY	75NDS, FSD-DCK	770505
144PR	N 0.108	7	
144CE	P 0.0	0+	284.3 D 3
144PR	G 43.		315.4 15
144PR	G 66.	0.5	C?
144PR	G 86.5	3.2	?
144PR	G 91.	23.2	C?
144PR	G 146.		?
144PR	L 0.0	0-	17.28 M 3
144PR	B	75.9	7.41510
144PR	L 59.03	33-	7.2 M 2
144PR	G 59.03	3	M3
144PR	L 80.12	3 1-	136 PS 9
144PR	B	4.6	8.22 5
144PR	G 80.12	315.2	2.49
144PR	L 99.96	3 2-	0.66 NS 5
144PR	G 40.93	3 4.5	0.015 LE 2.68
144PR	G 99.95	5 0.367	2.15
144PR	L 133.530	221-	7 PS 4
144PR	B	19.6	7.24 4
144PR	G 33.57	3 2.3	4.81
144PR	G 53.41	5 1.10	CC
144PR	G 133.53	3 100	0.06 LT 8.10
144PR			0.579
248CM	252CF A DECAY	55AS42, 70BA18, 71WA28, 64AS10	76NDS 780205
248CM	N 1.0	0.96908	8
252CF	P 0.0	0+	2.638 Y 10
248CM	L 0		6217.1 5
248CM	A 6118.3	5 84.2	3 1.0
248CM	L 43.40		126 PS 10
248CM	A 6075.7	5 15.7	3 3.24
248CM	G 43.399	25 0.0153	9 E2 6
248CM	L 144		
248CM	A 5976.6	0.24	4 65
248CM	G 100.2	0.013	AP
248CM	L 297		
248CM	A 5826.3	0.002	AP1200 AP
248CM	G 160	15 0.002	
248CM	L 510	8+	
248CM	A 5616	6E-5	AP2600 AP
148CE	252CF SF DECAY		780620
252CF	P 0.0	0+	
252CF	N	0.3092	
252CF	F 3.73	3 3.092	
252CF	L		

Appendix M
EXAMPLE OF BREMSSTRAHLUNG DATA GENERATED BY EDISTR

85-KRYPTON-36

HALFLIFE = 10.72 YEARS

26-AUG-78

BREMSSTRAHLUNG PHOTONS PER DISINTEGRATION

AIR, TISSUE, BONE AND FAT COLUMNS INCLUDE INTERNAL BREMS.

ENERGY INTERVAL

(MEV)

FROM

TO

INTERNAL

AIR

TISSUE

BONE

FAT

0.0045	0.0055	2.4813E-04	1.7220E-03	1.6241E-03	2.0337E-03	1.4427E-03
0.0055	0.0065	2.0551E-04	1.3766E-03	1.2988E-03	1.6248E-03	1.1546E-03
0.0065	0.0075	1.7508E-04	1.1372E-03	1.0733E-03	1.3416E-03	9.5470E-04
0.0075	0.0085	1.5227E-04	9.6240E-04	9.0861E-04	1.1348E-03	8.0862E-04
0.0085	0.0095	1.3453E-04	8.2963E-04	7.8348E-04	9.7784E-04	6.9761E-04
0.0095	0.0105	1.2034E-04	7.2570E-04	6.8552E-04	8.5503E-04	6.1067E-04
0.0105	0.0115	1.0874E-04	6.4236E-04	6.0694E-04	7.5657E-04	5.4090E-04
0.0115	0.0125	9.9081E-05	5.7419E-04	5.4266E-04	6.7607E-04	4.8381E-04
0.0125	0.0135	9.0909E-05	5.1750E-04	4.8920E-04	6.0915E-04	4.3632E-04
0.0135	0.0145	8.3908E-05	4.6971E-04	4.4412E-04	5.5274E-04	3.9626E-04
0.0145	0.0155	7.7844E-05	4.2893E-04	4.0564E-04	5.0462E-04	3.6206E-04
0.0155	0.0165	7.2542E-05	3.9378E-04	3.7247E-04	4.6314E-04	3.3256E-04
0.0165	0.0175	6.7866E-05	3.6319E-04	3.4361E-04	4.2707E-04	3.0689E-04
0.0175	0.0185	6.3713E-05	3.3637E-04	3.1829E-04	3.9544E-04	2.8437E-04
0.0185	0.0195	5.9999E-05	3.1269E-04	2.9594E-04	3.6752E-04	2.6448E-04
0.0195	0.0210	8.4989E-05	4.3746E-04	4.1409E-04	5.1406E-04	3.7019E-04
0.0210	0.0230	1.0179E-04	5.1185E-04	4.8467E-04	6.0122E-04	3.8458E-04
0.0230	0.0250	9.2207E-05	4.5366E-04	4.2971E-04	5.3267E-04	3.8458E-04
0.0250	0.0270	8.4108E-05	4.0549E-04	3.8419E-04	4.7592E-04	3.4402E-04
0.0270	0.0290	7.7178E-05	3.6503E-04	3.4596E-04	4.2829E-04	3.0994E-04
0.0290	0.0320	1.0678E-04	4.9598E-04	4.7020E-04	5.8173E-04	4.2145E-04
0.0320	0.0360	1.2268E-04	5.5111E-04	5.2274E-04	6.4596E-04	4.6897E-04
0.0360	0.0400	1.0721E-04	4.6713E-04	4.4330E-04	5.4718E-04	3.9805E-04

Appendix M (continued)

EXAMPLE OF BREMSSTRAHLUNG DATA GENERATED BY EDISTR

85-KRYPTON-36

HALFLIFE = 10.72 YEARS

26-AUG-78

BREMSSTRAHLUNG PHOTONS PER DISINTEGRATION

AIR, TISSUE, BONE AND FAT COLUMNS INCLUDE INTERNAL BREMS.

ENERGY INTERVAL

(MEV)

FROM

TO

INTERNAL

AIR

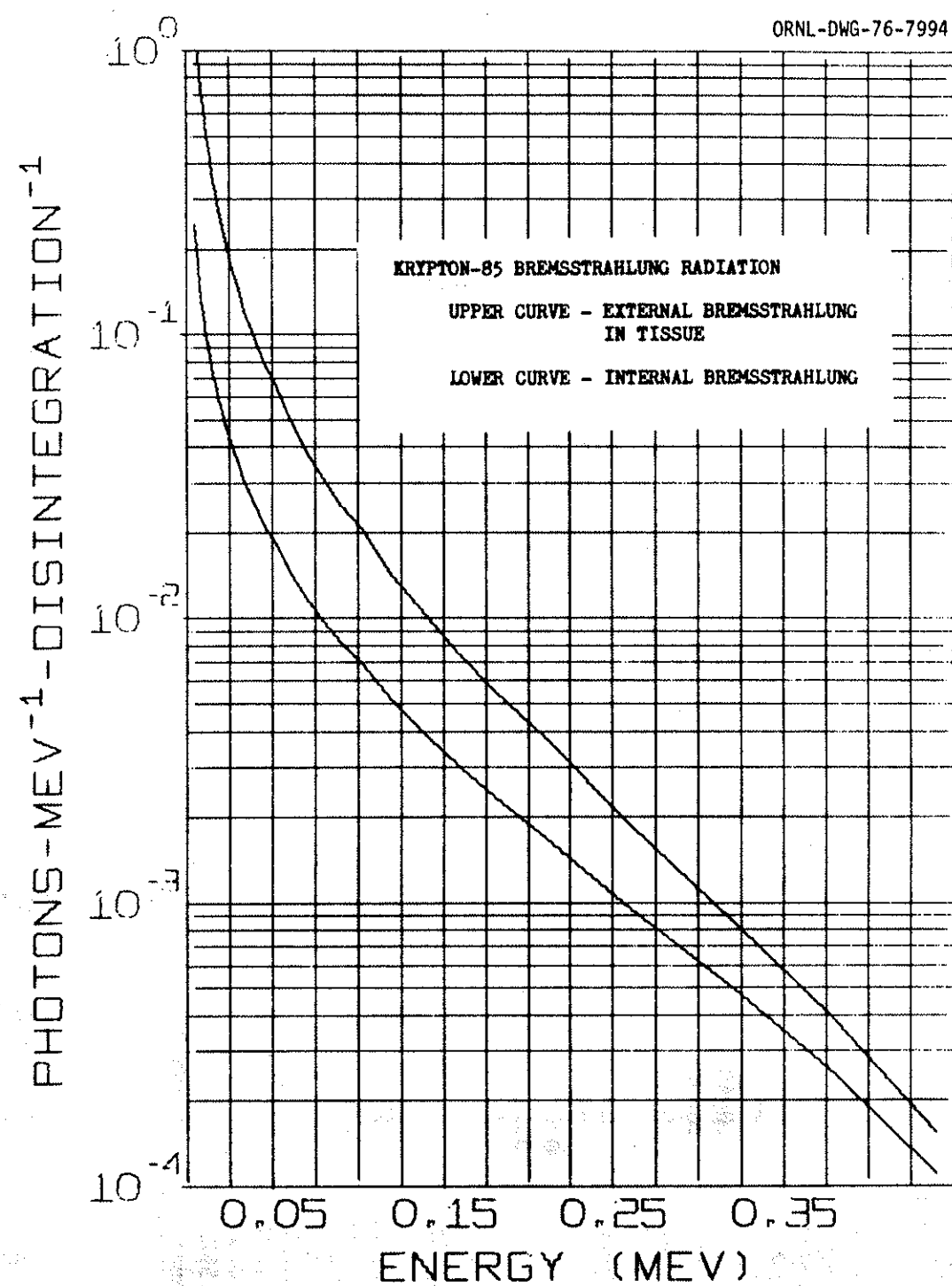
TISSUE

BONE

FAT

0.0400	0.0440	9.4743E-05	4.0136E-04	3.8106E-04	4.6985E-04	3.4245E-04
0.0440	0.0480	8.4496E-05	3.4871E-04	3.3122E-04	4.0797E-04	2.9790E-04
0.0480	0.0550	1.3288E-04	5.3514E-04	5.0853E-04	6.2572E-04	4.5771E-04
0.0550	0.0650	1.4920E-04	5.6848E-04	5.4075E-04	6.6376E-04	4.8760E-04
0.0650	0.0750	1.2063E-04	4.3761E-04	4.1666E-04	5.1026E-04	3.7635E-04
0.0750	0.0850	9.9562E-05	3.4552E-04	3.2927E-04	4.0233E-04	2.9790E-04
0.0850	0.0950	8.3476E-05	2.7814E-04	2.6528E-04	3.2343E-04	2.4038E-04
0.0950	0.1100	1.0629E-04	3.4099E-04	3.2549E-04	3.9598E-04	2.9539E-04
0.1100	0.1300	1.0500E-04	3.1435E-04	3.0053E-04	3.6406E-04	2.7354E-04
0.1300	0.1500	7.9935E-05	2.2478E-04	2.1522E-04	2.5961E-04	1.9646E-04
0.1500	0.1700	6.2035E-05	1.6461E-04	1.5785E-04	1.8959E-04	1.4450E-04
0.1700	0.1900	4.8819E-05	1.2267E-04	1.1780E-04	1.4087E-04	1.0815E-04
0.1900	0.2300	7.7620E-05	1.8520E-04	1.7811E-04	2.1204E-04	1.6897E-04
0.2300	0.2900	6.0558E-05	1.2515E-04	1.2089E-04	1.4190E-04	1.1227E-04
0.2900	0.3500	3.1856E-05	5.7737E-05	5.6035E-05	6.4748E-05	5.2518E-05
0.3500	0.4100	1.6179E-05	2.5986E-05	2.342E-05	2.8780E-05	2.3980E-05
0.4100	0.4700	7.5043E-06	1.0796E-05	1.0580E-05	1.1799E-05	1.0110E-05
0.4700	0.5500	3.8840E-06	5.0621E-06	4.9846E-06	5.4501E-06	4.8104E-06
0.5500	0.6500	3.6756E-07	4.1713E-07	4.1378E-07	4.3777E-07	4.0555E-07

III



ORNL/TM-6689
Dist. Category - UC-41

INTERNAL DISTRIBUTION

1. S. R. Bernard
2. R. O. Chester
3. Mark Cristy
4. D. E. Dunning, Jr.
- 5-14. K. F. Eckerman
15. W. B. Ewbank
- 16-17. M. R. Ford
18. N. B. Gove
19. S. V. Kaye
20. G. G. Killough
21. F. F. Knapp, Jr.
22. D. C. Kocher
23. M. J. Martin
24. D. C. Parzyck
25. C. R. Richmond
26. P. S. Rohwer
27. K. M. Samuels
28. S. B. Watson
29. J. P. Witherspoon
- 30-39. Internal Dosimetry Information Center, ORNL
- 40-41. Central Research Library
42. Document Reference Section, ORNL, Y-12 Technical Library
- 43-44. Laboratory Records Department
45. Laboratory Records, ORNL-RC
46. ORNL-Patent Office
47. RSIC Library

EXTERNAL DISTRIBUTION

48. S. Acharya, U.S. Nuclear Regulatory Commission, Washington, DC 20555
49. W. J. Bair, Manager, Biology Department, Battelle-Pacific Northwest Laboratories, Battelle Boulevard, Richland, Washington 99352
50. Dr. W. T. Bell, Department of Physics, Australian National University, Box 4, P.O., Canberra, A.C.T. 2600, Australia
51. A. Brodsky, Office of Standards Development, U.S. Nuclear Regulatory Commission, Washington, DC 20555
52. R. J. Cloutier, Manpower, Education Research Training, Oak Ridge Associated Universities, Oak Ridge, TN 37830
53. S. F. Deus, CPRD, Instituto de Energia Atomica, CP 11049, Pinheiros, CEP 05508, San Paulo, S.P., Brazil
- 54-68. L. Thomas Dillman, Department of Physics, Ohio Wesleyan University, Delaware, OH 43015
69. L. E. Feinendegen, Director of Institute of Medicine, U.F.A., Institut fur Medizion, Kernforschungsanlage Julich, Postfach 1913, 517, Julich, Federal Republic of Germany
70. Dr. Luigi Frittelli, Comitato Nazionale, Per L'energia Nucleare, Casella Postale 2358, 00100 Roma A.S., Italy
71. Lou Garcia, Environmental Protection Agency, Washington, DC
72. Dr. Kenneth Goodrich, Provost, Ohio Wesleyan University, Delaware, OH 43015
73. J. H. Harley, Director, Environmental Measurements Laboratory, U.S. Department of Energy, 376 Hudson Avenue, New York, NY 10014

74. Mr. Rodney I. Heathcott, Division of Occupational Health and Radiation Control, Texas Department of Health Resources, 1100 West 49th Street, Austin, TX 78756
75. K. Henrichs, Klinikum Steglitz, AloHg. Hukkarmediziu Biophysik, Hindenburgdamm 30, D-100 Berlin 45, West Germany
76. Dr. F. R. Hudson, Department of Physics, Mount Vernon Hospital, Northwood-Middx. HA6 2RN, United Kingdom
77. Dr. V. Husak, Department of Nuclear Medicine, University Hospital, 775 20 Olomouc, Czechoslovakia
78. R. E. Johnston, Department of Radiology, Division of Nuclear Medicine, University of North Carolina, Chapel Hill, NC 27514
79. A. Kaul, Klinikum Steglitz der Freien Universitat, Department Physik und Strahlenschutz (Biophysik) Hindenburgdamm 30, D-100 Berlin 45, Federal Republic of Germany
80. Kathrine A. Lathrop, University of Chicago, Chicago, IL
81. R. Loevinger, Radiation Physics Division, National Bureau of Standards, Washington, DC 20235
82. C. W. Mays, Radiobiology Laboratory, University of Utah Medical Center, salt Lake City, UT 84132
83. K. Z. Morgan, School of Nuclear Engineering, Georgia Institute of Technology, Atlanta, GA 30332
84. J. C. Nenot, Vice-President, Electricite de France, Comite de Radioprotection, 71 rue de Miromesnil, 75384 Paris Cedex 08, France
85. Bertil Nosslin, Allmanna Sjukhuset, Diagnostiska isotop-laboratoriet, S-214 01 Malmo, Sweden
86. Mr. M. E. Noz, Department of Nuclear Medicine, N.Y.U. Medical Center, Building UH, Room HC 106, 550 Fifth Avenue, New York, NY 10016
87. J. W. Poston, School of Nuclear Engineering, Georgia Institute of Technology, Atlanta, GA 30332
88. P. V. Ramzaev, Institute of Radiation Hygiene, 8 Mira ul, Leningrad 197101, U.S.S.R.
89. H. D. Roedler, Bundesgesundheitsamt, Ingolstadter Landstrasse 1, 8042 Neuherberg
90. Dr. Trevia Schlesinger, School of Pharmacy, University of Southern California, 1985 Zonal Avenue, Los Angeles, California 90033
91. Robert Simpson, Bureau of Radiological Health, Food and Drug Administration, 12720 Twinbrook Parkway, Rockville, MD 20852
92. Robert E. Sullivan, Bioeffects Analysis Branch, Criteria and Standards Division, Office of Radiation Programs, U.S. Environmental Protection Agency, Washington, DC 20460
93. Frank Swanberg, Chief, Branch of Health and Environmental Research, U.S. Nuclear Regulatory Commission, Washington, DC 20555
94. Mr. T. N. Tan, Radiation Protection Officer, Monash University, Clayton, Victoria, Australia 3168
95. R. C. Thompson, Senior Staff Scientist, Biology Department, Battelle-Pacific Northwest Laboratories, Battelle Boulevard, Richland, Washington 99352

96. N. Veall, Clinical Research Centre, Radioisotope Division, Watford Road, Harrow, Middlesex HA1 3UJ, England
97. J. Vennart, MRC Radiobiology Unit, Harwell, Didcot, Oxon, OX11 ORD, England
98. Dr. Lauren R. Wilson, Dean of Academic Affairs, Ohio Wesleyan University, Delaware, OH 53015
99. R. W. Wood, Pollutant Characterization and Safety, Office of Health and Environmental Research, U.S. Department of Energy, Washington, DC 20545
100. Office of Assistant Manager, Energy Research and Development, DOE-ORO, Oak Ridge, TN 37830
- 101-356. Given distribution as shown in DOE/TIC-4500 (Rev. 67), April 1979, category UC-41, Health and Safety